TECHNISCHE UNIVERSITÄT MÜNCHEN
FAKULTÄT FÜR MEDIZIN

Klinik und Poliklinik für Plastische und Handchirurgie
Klinikum rechts der Isar

Electrospun curcumin gelatin blended nanofibrous mats accelerate wound healing by Dkk-1 mediated fibroblast mobilization and MCP-1 mediated anti-inflammation

Xinyi Dai

Vollständiger Abdruck der von der Fakultät für Medizin der Technischen Universität München zur Erlangung des akademischen Grades eines

Doctor of Philosophy (Ph.D.)

genehmigten Dissertation.

Betreuer: Univ.-Prof. Dr. A. F. Schilling

Vorsitzender: Univ.-Prof. Dr. C. Zimmer

Prüfer der Dissertation:

1. Univ.-Prof. Dr. H.-G. Machens

2. Priv.-Doz. Dr. R. H. H. Burgkart

Die Dissertation wurde am 26.09.2016 bei der Fakultät für Medizin der Technischen Universität München eingereicht und durch die Fakultät für Medizin am 14.12.2016 angenommen.

ABSTRACT

Background: Acute wounds occur as a result of trauma as well as surgery. It is estimated that 300 million acute wounds are treated globally each year [1]. In the United States alone, approximately 11 million people are affected and 3 million are hospitalized annually. These numbers continue to rise, making wound management a great challenge to society and medical professionals, especially plastic surgeons [2,3]. Traditional reconstructive surgical intervention such as skin flap transplantation still faces the problem of donor tissue insufficiency, post-operative flap compromise, host immunological rejection or even loss of function [4,5,6,7]. Therefore, wound therapy via noninvasive approaches is of major importance and a variety of compounds have been discussed to improve it [8].

Turmeric, the product of Curcuma longa, is one of these compounds and has a very long history of being used for treatment of wounds in many Asian countries. Curcumin, the principal curcuminoid of turmeric, has been recently identified as a powerful modulator of processes involved in healing. However, the inherent limitations of the compound itself, such as hydrophobicity, instability, poor absorption and rapid systemic elimination, pose big hurdles for translation to wider clinical application. Accumulating evidence indicates that nano-formulation is capable of improving solubility of previously unsoluble compounds. Electrospinning, known for many years in the textile industry and organic polymer science, has recently emerged as a novel technique for

generating nanoscale biomimetic scaffolds for tissue engineering. The simplicity of the electrospinning process itself and the possibility to incorporate therapeutic compounds into the nonwoven nanofiber meshes during spinning allow the development of controlled drug delivery systems with this method.

For wound healing applications, such a system should ideally be able to mimick the structure and biological function of extracellular matrix (ECM) proteins, to provide structural and mechanical integrity as well as support for cellular processes.

The aim of the present PhD thesis was it to engineer curcumin/gelatin blended nanofibrous mats by electrospinning to adequately enhance the bioavailability of the hydrophobic curcumin for wound treatment. For this purpose these electrospun curcumin/gelatin blended nanofibrous mats were evaluated as both drug-release system and biomimetic scaffold/dressing for topical application. The potential mechanisms being involved were also scrutinized.

Materials and methods: We prepared curcumin/gelatin blended nanofibrous mats by electrospinning and scrutinized their properties including material characterization (SEM, XRD, FITR), curcumin release profile, tensile mechanical properties, cytotoxicity/biocompatibility (LDH, WST, LIVE/DEAD). To further explore curcumin action through such nanoformulation, fibroblast cell based cytokine paracrine profile and subsequent fibroblast migration and monocyte/macrophage cell chemotaxis assays were performed. The healing capacity of the medicated nanofibrous mats was assessed both *in vitro* and *in*

vivo.

Principle findings: 1) curcumin was successfully formulated into gelatin based nanofibers as amorphous nanosolid dispersion and could be control-released to enhance its bioavailability. 2) The resulting medicated nanofibrous mats showed agreeable biocompatibility without cytotoxic effects that facilitated cell-based dermal regeneration *in vitro* and accelerated wound healing *in vivo*. 3) The underlying mechanisms of the accelerated wound healing by topically applied curcumin/gelatin nanofibrous mats were found to be a combination of curcumin's ability of *in situ* fibroblasts mobilization, which is partially mediated by Dkk-1 regulated Wnt/β-catenin signaling, and of its immunomodulatory action, specifically, the persistent inhibition of the inflammatory chemotaxis through decreased expression of MCP-1 by fibroblasts.

Conclusions: These results demonstrate the feasibility and effectiveness of bioactive curcumin in a biomimetic nanofibrous structure on accelerated wound healing. These results open an avenue to translate this ancient medicine for modern wound therapy, which is promising for future non-invasive approaches to cure wounds faster through medicated wound dressings.

TABLE OF CONTENTS

1. INTRODUCTION 1
   1.1. The human skin 1
      1.1.1. Anatomy 1
      1.1.2. Function 6
   1.2. Acute wound 13
      1.2.1. Acute wound classification 13
      1.2.2. Skin regeneration and wound healing 17
   1.3. Curcumin from turmeric: a promising candidate for wound therapy 26
   1.4. Electrospinning: an encouraging approach for regenerative medicine 32
      1.4.1. Electrospinning history and fundamentals 32
      1.4.2. Electrospinning for advanced wound dressing 37
      1.4.3. Electrospinning for drug delivery 38
2. HYPOTHESIS 38
3. MATERIALS AND METHODS 39
   3.1. Materials 39
      3.1.1. Reagents 39
      3.1.2. Cell culture mediums 40
      3.1.3. Buffers 40
      3.1.4. Cell lines 40
      3.1.5. Commercial kits 40
      3.1.6. Antibodies 40
      3.1.7. Devices 41
   3.2. Methods 41
      3.2.1. Electrospinning of Curcumin/Gelatin blended nanofibrous mat 41
      3.2.2. Scanning electron microscopy (SEM) 42
      3.2.3. X-ray diffraction (XRD) spectroscopy 42
      3.2.4. Fourier transform infrared (FTIR) spectrometer 42
      3.2.5. Curcumin release profile 43
      3.2.6. Tensile mechanical properties 43
      3.2.7. Cell isolation and culture 44
      3.2.8. LDH and WST-1 assay 45
      3.2.9. Live and dead assay 45
      3.2.10. Cell visualization on the scaffold 46
      3.2.11. Fibroblasts in vitro wound healing assay 46
      3.2.12. Fibroblasts cytokine profile array 46
      3.2.13. Quantified ELISA assay for Dkk-1, SDF-1 α, MCP-1 and TSP-1 47
      3.2.14. β-catenin immunofluorescence and fibroblast migration 47

3.2.15. Dkk-1 mediated fibroblast migration 48
3.2.16. MCP-1 mediated PBMC and macrophage chemotaxis.... 49
3.2.17. Animal housing conditions 49
3.2.18. Surgical procedure for acute wound animal model 49
3.2.19. Wound closure analysis 50
3.2.20. Histological analysis 50
3.2.21. Collagen content analysis 50
3.2.22. Macrophage immunohistochemistry 51
3.2.23. Statistical analysis 51
4. RESULTS 52
4.1. Material characterization 52
4.1.1. Morphology of electrospun nanofibrous mat 52
4.1.2. Electrospinning nanoformulates curcumin 53
4.1.3. Curcumin incorporation in nanofiber 54
4.1.4. Curcumin release profile 55
4.1.5. Tensile mechanical properties of Cc/Glt NM 56
4.2. Biocompatibility and cytotoxicity 57
4.2.1. Cytotoxicity of electrospun NM *in vitro* 57
4.2.2. Fluorescence-based cytotoxicity *in vitro* 58
4.2.3. Cell visualization on the nanofibrous mat 60
4.3. Curcumin activates fibroblasts 61
4.3.1. Fibroblasts *in vitro* wound healing 61
4.3.2. Fibroblasts cytokine paracrine profile array 62
4.3.3. Quantified cytokine expression of Dkk-1, SDF-1α, MCP-1 and TSP-1 63
4.4. Dkk-1 mediates curcumin induced fibroblasts mobilization . 64
4.4.1. β-catenin signaling in migrated fibroblasts 64
4.4.2. Dkk-1 mediates fibroblast migration 65
4.5. MCP-1 mediates curcumin induced anti-inflammation 67
4.5.1. Curcumin inhibits PBMC chemotaxis 67
4.5.2. Curcumin inhibited macrophage (MV-4-11) chemotaxis is mediated by MCP-1 68
4.6. Wound healing *in vivo* 69
4.6.1. Cc/Glt NM accelerates wound closure *in vivo* 69
4.6.2. Cc/Glt NM enhances dermal regeneration 70
4.6.3. Cc/Glt NM enhances collagen deposition 72
4.6.4. Cc/Glt NM inhibits macrophage infiltration *in vivo* 74
5. DISCUSSION 75
5.1. Electrospun Cc/Glt NM successfully nano-formulates crucmumin and enhances its bioavailability for wound therapy 77
5.2. Electrospun Cc/Glt NM is ideal for topical wound treatment 89
5.3. Delivered curcumin exterts synergistic signalling to accelerate wound healing 98
5.4. Electrospun Cc/Glt NM could be a benificial complement to

current wound therapy 108
6. GENERAL CONCLUSIONS AND PERSPECTIVES 115
7. APPENDIX 116
8. ACKNOWLEDGEMENTS 118
9. REFERENCES 126

LIST OF FIGURES AND TABLES

Figure 1: Structure of the human skin .....错误！未定义书签。
Figure 2: "Brick and Motar" pattern of the stratum corneum 8
Figure 3: Acute wounds 14
Figure 4: Molecular structures of turmeric-derived curcuminoids.....28
Figure 5: Electrospinning process.....33
Figure 6: Bending instability.....34
Figure 7: Morphology.....52
Figure 8: Curcumin nanoformulation.....53
Figure 9: Curcumin incorporation in gelatin nanofiber.....54
Figure 10: Curcumin release *in vitro*.....55
Figure 11: Mechanical property of Cc/Glt NM.....57
Figure 12: Cytotoxicity of electrospun NM *in vitro*.....58
Figure 13: Fluorescence-based cytotoxicity *in vitro* 59
Figure 14: Cell visualization on the nanofibrous mat.....61
Figure 15: Fibroblast *in vitro* wound healing 62
Figure 16: Paracrine profile of fibroblasts.....63
Figure 17: Quantified cytokine expression.....64
Figure 18: β-catenin signaling in migrated cell.....65
Figure 19: Dkk-1 mediates fibroblast migration.....66
Figure 20: Curcumin inhibits PBMC chemotaxis.....67
Figure 21: Curcumin inhibited macrophage (MV-4-11) chemotaxis is mediated by MCP-1.....68
Figure 22: Topical application of Cc/Glt NM accelerates wound closure *in vivo* 69
Figure 23: Topical application of Cc/Glt NM enhances dermal regeneration.....71
Figure 24: Topical application of Cc/Glt NM enhances collagen deposition 73
Figure 25: Topical application of Cc/Glt NM inhibits macrophage infiltration *in vivo*.....74
Figure 26: Scheme of curcumin nanoformulation through electrospinning.....87
Figure 27: Scheme of potential mechanism of curcumin induced accelerated wound healing.....104

LIST OF ABBREVIATIONS

AKT or PKB	Protein kinase B
Bcl-2	B-cell lymphoma 2
bFGF /FGF-2	Basic fibroblast growth factor
BSA	Bovine serum albumin
CAT	Catalase
Cc/Glt NM	Curcumin/Gelatin nanofibrous mats
CCL5	Chemokine (C-C motif) ligand 5
CE	Collision energy
CM-Cc/Glt NM	Conditioned medium of curcumin/gelatin nanofibrous mat
CM-Glt NM	Conditioned medium of gelatin nanofibrous mat
CXP	Collision cell exit potential
Dkk-1	Dickkopf-related protein-1
DMEM	Dulbecco's Modified Eagle's Medium
DMSO	Dimethyl sulfoxide
DNA	Deoxyribonucleic acid
Dox	Doxorubicin hydrochloride
DP	Declustering potential
E. *coli*	Escherichia coli
ECM	Extracellular matrix
EEP	Ethyl ethylene phosphate
EGF	Epidermal growth factor
EHD	Electrohydrodynamic
FDA	US Food and Drug Administrationthe
FTIR	Fourier transform infrared
Glt NM	Gelatin nanofibrous mats
GPx	Glutathione peroxidase

GRAS	Generally recognized as safe
HB-EGF	Heparin binding epidermal growth factor
HBO	Hyperbaric oxygen
HGF	Hepatocyte growth factor
HHC	Hexahydrocurcumin
HO	Heme oxygenase
HPLC	High-performance liquid chromatography
HS-27	Human fibroblast cell line
I.P.	Intraperitoneal injection
IGF	Insulin-like growth factor
IKK	I kappa B kinase
IL-1	Interleukin-1
IL-6	Interleukin-6
IL-8	Interleukin-8
KGF	Keratinocyte growth factor
LD50	Lethal 50% dose values
LDH	Lactate dehydrogenase
LPS	Lipopolysaccharide
MCP-1	Monocyte chemoattractant protein 1
MMPs	Matrix metalloproteinases
MNPs	Magnetic nanoparticles
MRSA	Methicillin-resistant Staphylococcus aureus
MV-4-11	Human Macrophage cell line
NAC	N-acetyl-l-cysteine
NFDs	Nanofiber-based wound dressings
NF-κB	Nuclear factor kappa-light-chain-enhancer of activated B cells
NGF	Nerve growth factor
NM	Nanofibrous mat
NO	Nitric oxide

NPWT	Negative-pressure wound therapy
OHC	Octahydrocurcumin
PBMC	Peripheral blood mononuclear cells
PBS	Phosphate-buffered saline
PCL	Polycaprolactone
PCU	Poly carbonate urethane
PDGF	Platelet-derived growth factor
PEG	Poly ethylene glycol
PI3K	Phosphoinositide 3-kinase
PLA	Polylactic acid
PLGA	Poly(lactic-co-glycolic acid)
PLLA	Poly (L-lactic acid)
PSR	Picro-sirius red
PU	Polyurethane
PVA	Poly(vinyl alcohol)
PVP K90	Polyvinylpyrrolidone K 90
RGD	Arg-Gly-Asp
ROS	Reactive oxygen species
S1P	Sphingosine-1-phosphate
SD	Standard deviation
SDF-1α	Stromal cell derived factor 1α
SEM	Scanning electron microscopy
SOD	Superoxide dismutase
TCH	Tetracycline hydrochloride
TGF-β1	Transforming growth factor beta 1
THC	Tetrahydrocurcumin
TIMPs	Inhibitors of metalloproteinases
TNF-α	Tumor necrosis factor alpha
TSP-1	Thrombospondin-1

USFDA	US Food Drug Administration
UV	Ultraviolet (UV)
VAC	Vacuum assisted closure
VEGF	Vascular endothelial growth factor
VRE	Vancomycin-resistant enterococci
WST-1	Water-soluble tetrazolium-1
XRD	X-ray diffraction

1. INTRODUCTION

1.1. The human skin

1.1.1. Anatomy

Human skin, the largest organ of human body, accounts for about 16% of the total body weight and covers its entire external surface. For the average adult human, the skin has a surface area of between 1.5-2.0 square meters (16.1-21.5 sq ft.), most of it between 2-3 mm (0.10 inch) thick [9]. It is rich in blood vessels, lymph-vessels, nerves, muscles and various kinds of cutaneous appendages, for example, the average square inch (6.5 cm^2) of skin holds 650 sweat glands, 20 blood vessels, 60,000 melanocytes, and more than 1,000 nerve endings [10]. It is composed of three primary layers: the **epidermis**, the **dermis** and **subcutis** (Figure 1).

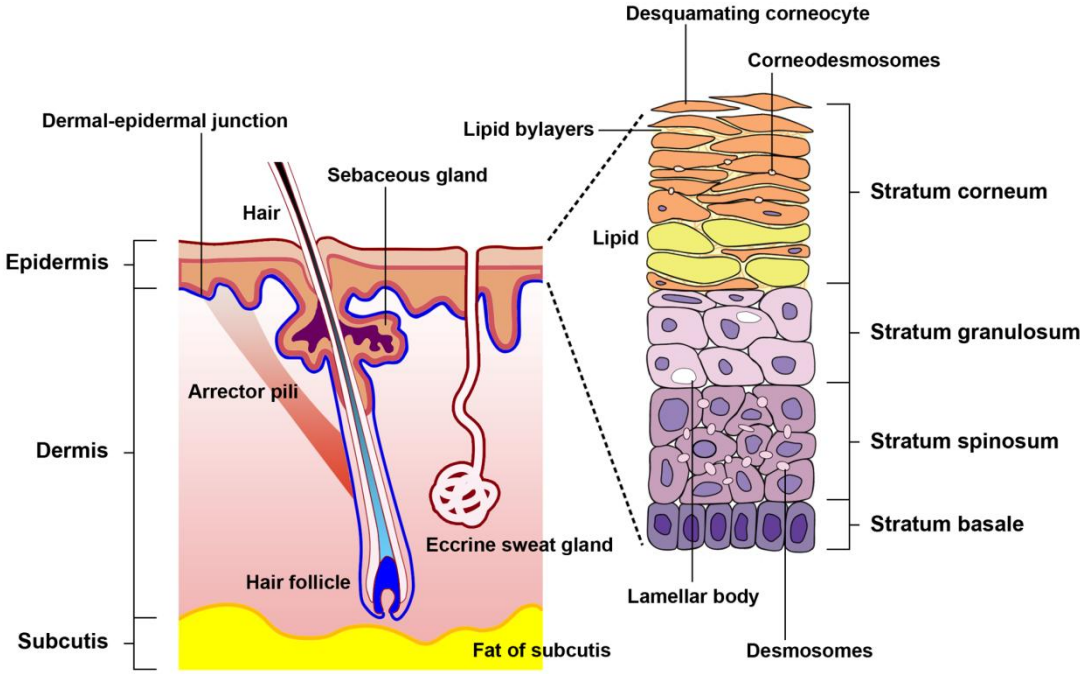

Figure 1: Structure of the human skin. Human skin can be divided into three layers: epidermis, dermis and subcutis. Epidermis is composed of 4 or 5 layers depending on the region of skin being considered.

The stratified, cellular epidermis is the outer layer, being the outermost physical and chemical barrier between the interior body and exterior environment; the underlying dermis is the deeper layer that provides structural support of the skin; beneath lies a layer of loose connective tissue known as the subcutis, or hypodermis, which is an important depot of fat that is separated from the rest of the body by a vestigial layer of striated muscle called the panniculus carnosus. Between dermis and epidermis is the sectional, undulating dermal-epidermal junction with dermal papillae from the papillary dermis projecting perpendicular to the skin surface. It provides mechanical support for the epidermis and acts as a partial barrier against exchange of cells and large molecules through which the epidermis obtains nutrients and disposes of waste.

Epidermis

The epidermis is the relatively thin and toughly stratified squamous epithelium mainly composed of keratinocytes that originate from cells in the deepest layer of the epidermis known as the basal layer. They slowly migrate up toward the surface of the epidermis and then are gradually shed and are replaced by new keratinocytes from below. These cells synthesise the protein keratin, whose differing stages of maturation form the four separate layers of the epidermis, that is, **stratum basale** (basal or germinativum cell layer), **stratum spinosum** (spinous or prickle cell layer), **stratum granulosum** (granular cell layer) and **stratum corneum** (horny layer)[11]. The epidermis varies in thickness from 0.05 mm on the eyelids to 0.8-1.5 mm on the soles of the feet and palms of the hand[12]. In some thick epidermis, there lies a thin layer of translucent cells called **stratum lucidum**. It is just a transition between the stratum granulosum and stratum corneum which is not usually seen in thin epidermis.

Stratum basale

The stratum basale (basal layer, sometimes termed as stratum **germinativum**) is the deepest and innermost layer of the five epidermis layers, which is the outer covering of skin in mammals and lies adjacent to the dermis. It is primarily made up of dividing and non-dividing keratinocytes[13]. Non-dividing keratinocytes are attached to the basement membrane via hemidesmosomes while dividing keratinocytes, being considered as the basal keratinocyte stem cells (stem cells of the epidermis), divide and differentiate from this deeper layer toward the surface to form the keratinocytes of the stratum spinosum, which also migrate superficially. Other types of cells found within the stratum basale include melanocytes, Langerhans cells (immune cells), and Merkel cells (touch receptors)[14]. The pigment (melanin) producing melanocytes, with dendritic processes stretching between relatively large numbers of neighbouring keratinocytes, compose only a small proportion of the basal cell population. The melanin pigment accumulates in melanosomes that are transferred to the adjacent keratinocytes and remains as granules. It is vital to provide protection against ultraviolet (UV) radiation[15]. Merkel cells are oval receptor cells found in the basal layer with large numbers in touchsensitive sites such as the fingertips and lips. They are closely associated with cutaneous nerves and are associated with the sense of light touch discrimination of shapes and textures[16]. Langerhans cells are dendritic cells (antigen-presenting immune cells) that are present in all layers of the epidermis, but are most prominent in the stratum spinosum[17].

Stratum spinosum

The stratum spinosum is initially formed by mature basal cells moving towards the outer layer of the skin. Desmosomes connect cells in the stratum spinosum as intercellular bridges. Langerhans cells, with a stellate appearance, represent 3-6% of all cells in the epidermis[18]. Being derived from the bone

marrow and having similar morphology and function as macrophages, they are immunulogically active cells mainly located in the middle of this layer and are in close contact with keratinocytes. They play a significant role in immune reactions of the skin, for example, in skin infections. The local Langerhans cells take up and process microbial antigens to become fully functional antigen-presenting cells[19].

Stratum granulosum

The stratum granulosum (or granular layer) is a thin layer of granular cells that come from the keratinocytes migrating from underlying stratum spinosum while flattening and losing their nuclei and cytoplasm that appears granular at this level. At the transition between this layer and the stratum corneum, granular cells secrete lamellar bodies (containing lipids and proteins) into the extracellular space, leading to the formation of the hydrophobic lipid envelope responsible for the skin's barrier properties[20].

Stratum corneum

The outermost portion of the epidermis where the final outcome of keratinocyte maturation is found to be layers of hexagonal-shaped, non-viable cornified cells (corneocytes) is the stratum corneum. It provides the natural physical and water-retaining barrier of the skin against most bacteria, viruses and other foreign substances. In most areas of the skin, there are 10-30 layers of stacked corneocytes in the stratum corneum with the palms and soles having the most[21]. Within this layer, each corneocyte is surrounded by a protein envelope and is filled with water-retaining keratin proteins whose orientation together with the shape of the corneocyte is responsible for the strength of the stratum corneum. In the extracellular space around the corneocyte also lies a stacked layer of lipid (inter cellular lipid matrix), serving as barrier for water, drugs or other substances. Specially, the corneocyte can absorb three times its weight in water whereas if water content drops below 10%, it becomes

rough, less pliable with possible scaling and cracking[22]. In a clinical point or view, the structural complexity of the stratum corneum is of great importance to influence the transdermal drug delivery[23].

Dermis

The dermis is a thick layer of fibrous and elastic tissue (made mostly of collagen, elastin, and fibrillin) that gives the skin its flexibility and strength. It varies in thickness, ranging from 0.6 mm on the eyelids to 3 mm on the back, palms and soles[24]. Two layers, namely the thin **papillary layer** and the thicker **reticular layer** form the dermis. The papillary dermis connects with the epidermis which contains thin loosely arranged collagen fibers while in the deeper reticular layer run thicker bundles of collagen that are parallel to the skin surface and extend to the subcutis tissue[25]. The dermis is mainly made up of fibroblasts, immunocompetent mast cells and macrophages. Collagen fibers secreted by fibroblasts compose 70% of the dermis and contribute to its strength and toughness[26]. Elastin and proteoglycans are also produced by fibroblast and respectively exert the function of maintaining normal elasticity and flexibility as well as providing viscosity and hydration[27]. In addition, there are dermal vasculature, nerve endings, sweat glands and oil (sebaceous) glands, hair follicles embedded within the fibrous tissue of the dermis with different functions: The dermal vasculature provides nutrients to the skin and helps regulate the body temperature; the nerve endings sense pain, touch, pressure, and temperature; the sweat glands produce sweat in response to heat and stress; the sebaceous glands secrete oily sebum into hair follicles that keeps the skin moist and soft and acts as a barrier against foreign substances while the hair follicles produce the various types of hair and contain stem cells capable of regenerating damaged epidermis[28]. It should be noted that over different parts of the body, their number varies.

Subcutis

The subcutis, also called the hypodermis or superficial fascia, is the lowermost layer of the skin. It consists primarily of loose connective tissue and fat which helps insulate the body from heat and cold and serves as an energy storage area. The types of cells in the hypodermis are fibroblasts, adipose cells, and macrophages[29]. Compared to the dermis, larger blood vessels and nerves are found in this layer.

1.1.2. Function

Human skin is a complex metabolically active organ, which has important physiological functions. Basically, it is the principal site of interaction with the surrounding world and serves as a protective barrier that prevents underlying muscles, bones, ligaments, and other internal organs from exposure to hazardous environmental factors, such as ultraviolet (UV) radiation, temperature extremes, toxins, bacteria and trauma, so as to sustain the organism's homeostasis. In the mean time, it allows and limits the inward and outward passage of water, electrolytes and various substances. Additionally, it also has other important duties including sensory perception, immunologic surveillance, thermoregulation, excretion, resorption, metabolism and control of insensible fluid loss.

Barrier function

The primary function of the epidermis is to produce the protective, semi-permeable stratum corneum that permits terrestrial life. In this way, healthy skin is able to provide the body a strong protection against numerous harmful environmental factors including physical (mechanical trauma, thermal injury, and radiation), chemical (destructive agents, surface active substances, xenobiotics, allergens) and biological (bacteria, viruses) threats. Since the concept of the skin barrier was first introduced by Marchionini and Schade[30] as they applied scientific evidence for the protective function of the water-lipid mantle of the skin, numerous studies have been performed concerning the

barrier function in detail. Currently, the stratum corneum is considered to account for 90% of the skin barrier function due to its main constituents, the corneocytes and lipid bilayers that embed these cells. They are found to form the 'brick and mortar mosaic' structure[31], with which the barrier function is established. It consists of a patterned lipid lamellae localized in the extracellular spaces between anucleate corneocytes that contains keratin filaments bound to a peripheral cornified envelope, a 15-20 nm thick structure composed of defined structural, cross-linked proteins such as filaggrin [32,33]. The many layers of these specialized cells in the stratum corneum provide a tough and resilient framework, which determines the speed of the transcutaneous exchange of substances and performs the multiple defensive functions. Therefore, in addition to the cells, the main biochemical components of the skin barrier are lipids and proteins: the mechanical resistance of the epidermal barrier mainly comes from in the cornified envelope embedded corneocytes. The water permeability and the substances exchange with the external environment are largely determined by the surrounding lipid layers, identified as the cornified lipid envelope[34]. Through such physical and mechanical barriers, skin is able to withstand pressure, stress or trauma. Certainly, when the mechanical impact is stronger than the skin, a wound will occur and such a breakage through skin leads to loss of one or more of the skin functions. Likewise, through the penetration barrier, skin helps retain necessary body fluids and moisture, avoiding excessive water loss and protects the human body from absorption of external fluids or liquids. It is worth mentioning that the stratum corneum was recently found to be a dynamic system with metabolic activity, not merely an inert layer of dead cells as previously accepted. It responds to external influences through the process of regulating DNA and structural protein synthesis, proteolysis and ion transport (Figure 2)[35], a mechanism that needs more elucidation.

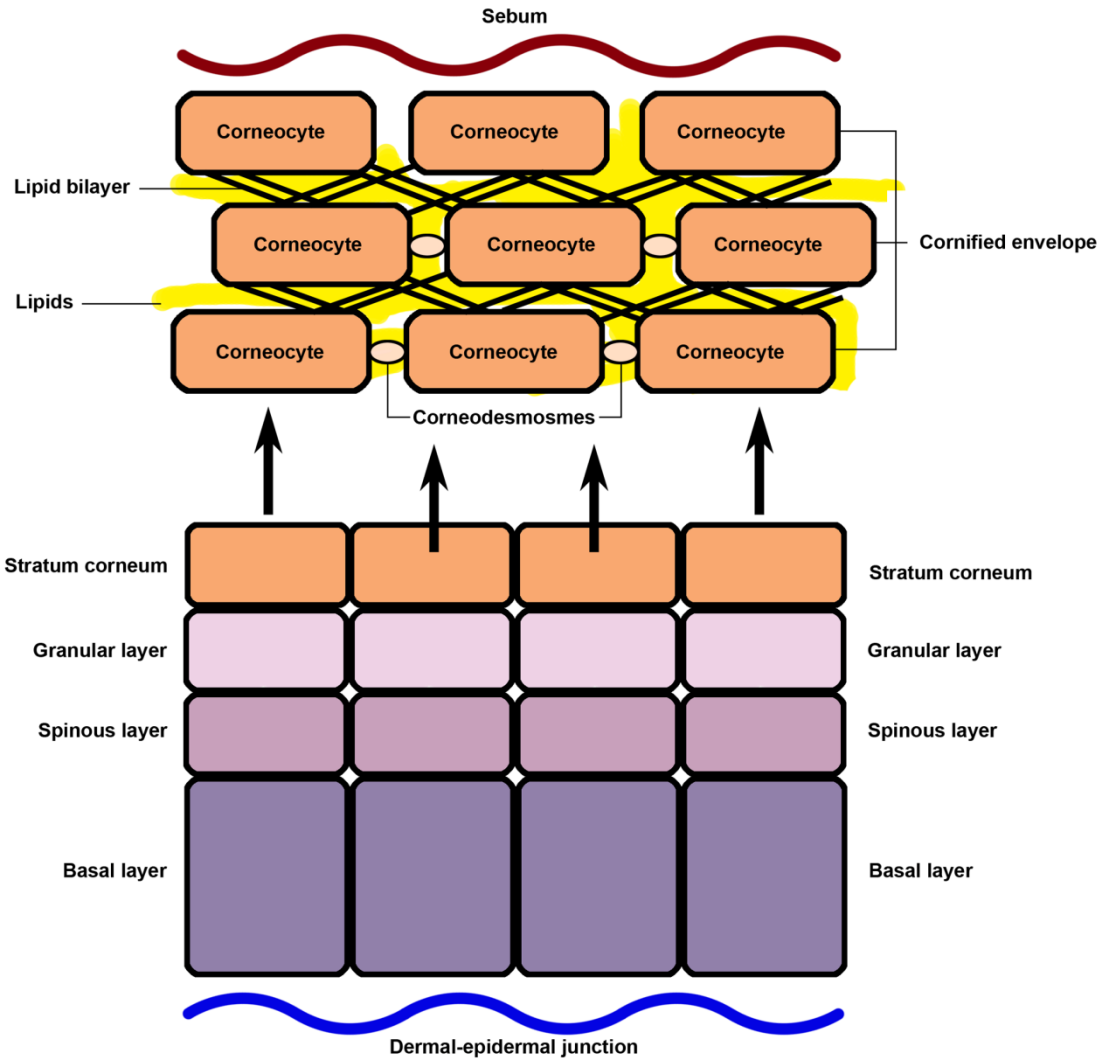

Figure 2: "Brick and Motar" pattern of the stratum corneum. As keratinocytes differentiate into corneocytes from the basal layer (Stratum basale) to the outermost layer (Stratum corneum), the lipid envelope and the cornified envelope are formed with the maturation of desmosomes to corneodesmosomes. Thus, the epidermal barrier is formed by corneocytes (bricks) and surrounding lipids (motar).

The second skin barrier comes from the melanocytes that produce Melanin - a dark-coloured light-sensitive pigment. If it weren't for the melanin pigmentation in the epidermis, the ultraviolet light (UV light) radiating from sun would damage the underlying tissue in our bodies. The skin and its pigmentation also helps protect against many medical illnesses like skin cancers.

Last but not least, the top layer of skin is covered with a thin, oily coat of moisture that passively prevents most foreign substances or organisms (such as bacteria, viruses and fungi) from entering the skin.

Thermal regulation

Humans maintain their core temperature within a small range, between 36 and 38°C. The skin is the major organ that controls heat and moisture flow to and from the surrounding environment so as to maintain a normal body temperature upon challenges to the thermal homeostasis. Under normal conditions, the inner body heat generated by deep organs is transported to the surface of the skin via the blood and released into the environment via conduction, convection, radiation or the evaporation of sweat. The cooled blood then returns to the body core, thus reducing the core temperature. Human beings can perceive different levels of cold and warmth through sensory receptors in the skin[36]. Studies showed that cold receptors are located more superficially in the dermis at an average depth of 0.15 to 0.17 mm than warmth receptors (0.3 to 0.6 mm), whose number is far lower [37,38]. So the skin is more dedicated to the rapid detection of cold than of warmth, which is reasonably the result of long-term evolution of human beings. These thermal sensors, together with the cold- and warm-sensitive nerve endings, the sympathetic nerve system and the posterior hypothalamus, which acts a controller of body temperature, play a crucial role in thermal regulation[39]. By sensing the thermal disturbances occurring at the border between the inner body and the exterior environment, a defense responses or thermal regulatory response can be triggered[40]. In heat conditions, blood flow increases, and heat transferred from the interior body to the skin is conducted and convected. Also, the hypothalamus sends nerve signals to the sweat-producing skin glands, causing them to release about 1-2 liters of water per hour, thus, through evaporation of sweat, heat is carried away. In the cold situation, however, decreased conductance due to decreased blood flow, as result from

vasoconstriction (contracting small blood vessels), is able to keep the heat from escaping and thus the dermis retains more of the internal body temperature[41]. Besides, the fatty subcutaneous layer of the skin also acts as an insulation barrier, helping to prevent the loss of heat from the body and decreasing the effect of cold temperature. It is through this combination of heat loss and heat gain mechanisms that the skin can help maintain human body core temperature within a very small range.

Sensation

An important function of the skin is to detect principal sensations: heat, cold, touch, pressure and pain, which is detected through a variety of sensory nerve endings in the skin. For example, in the finger tips and lips deeper within the skin there lie Meissner's corpuscles[42] and Pacinian corpuscles[43], both being major types of mechanoreceptors sensitive to either light touch or vibration and pressure. The skin is supplied by both myelinated and unmyelinated branches of spinal nerves, which form both a superficial and a deep nerve plexus in the dermis as they enter from the subcutaneous fat. Unmyelinated branches from either plexus terminate in nerve endings. Terminals from a single axon may serve an area around 1 cm^2 and overlap with nerve endings from other axons. In certain sensory neurons (pseudounipolar neurons), such as those for touch and warmth, the electrical impulse travels along an axon from the periphery to the neuron (cell body), and from the neuron to the spinal cord along another branch of the same axon. Such an inflow of cutaneous sensory information is firmly controlled and regulated by the cerebral cortex. Therefore, the skin is highly sensitive to rapid mechanical stimulation, with reportedly detectable positional movements of less than 1 μm[44,45].

In the mammalian peripheral nervous system, warmth receptors are thought to be unmyelinated C-fibres (low conduction velocity), while those responding to cold have both C-fibers and thinly myelinated A delta fibers (faster conduction

velocity)[46]. The perception of innocuously cool temperatures occurs when the skin is cooled as little as 1 °C from a basal temperature of 32 °C, and studies of thermal acuity in humans finds the thermal thresholds for warm and cold detection near around 34 and 31 °C, respectively[47]. Changes in temperature of 0.03 °C can be detected, especially if the skin temperature changes faster than 0.007 °C /sec. The most sensitive part of skin for thermal variation is found to be on the face, as pain will be caused when temperatures fall below 18°C or rise above 45°C[48].

Pain is a distressing feeling often induced by intense or damaging stimuli, such as a pressure greater than 55 g/mm^2 or by disruption of skin [49]. Likewise, skin contact to a number of chemicals may also elicit pain.

Studies indicate that there are specific sensors, called nociceptors[50], that respond only to noxious, high intensity stimuli by sending signals along the nerve fiber to the spinal cord if the currents generated by the stimuli are above a given threshold. The thermal, chemical or mechanical "specificity" of a nociceptor is determined by ion channels it expresses at its peripheral end. So far Dozens of different types of nociceptor ion channels have been identified[51]. There are two different types of nerve sensory fibers, A-delta or C fiber, along which pain signals are transfed from the periphery to the spinal cord. A-delta fiber is not only thicker than the C fiber but also being sheathed in an electrically insulating material, the myelin, so that it has a higher conductive velocity (5–30 m/s) for pain signals than that of the unmyelinated C fiber (0.5–2 m/s)[52]. Pain evoked by the (faster) A-delta fibers is felt first as sharp pain and is followed by a duller pain, often described as burning, carried by the C fibers.

Itch is a sensation related to pain, which was first defined more than 340 years ago by the German physician Samuel Hafenreffer[53] as an "unpleasant sensation that elicits the desire or reflex to scratch". Recent data suggest that there is a broad overlap between pain and itch related peripheral mediators

and/or receptors, and there are astonishingly similar mechanisms of neuronal sensitization possibly due to the fact that unmyelinated nerve fibers for itch and pain both originate in the skin and the information is conveyed centrally, though in two distinct systems, by the same nerve bundle and spinothalamic tract[54]. Within the last decade understanding of the neural and molecular structures inducing the sensation of itch during normal and pathophysiological conditions has been greatly enhanced [55]. For example, histamine is considered to be the most important mediator of itch[56], and has been regarded as a main target for antipruritic therapies. Studies indicate that histamine H1 receptor inhibition lead to almost complete suppression of histamine inducecd itch[57]. However, other mediators, such as interleukins, protease-activated receptors, transient receptor potential receptors, opioids and cannabinoids, are also capable of mediating this sensation[58].

Endocrine

Skin itself possesses the capacity to generate several hormones and substances with hormone-like activity through paracrine, autocrine, intracrine and endocrine mechanisms[59]. They are released in the circulation and are important for functions of the entire human organism.

Skin is one of our main sources of vitamin D, because it is the unique site of Cholecalciferol (D3) synthesis, specifically, in the two lowermost layers of the epidermis (the stratum basale and stratum spinosum), where keratinocytes contain both the machinery needed to produce calcitriol and vitamin D receptor[60]. In addition, insulin-like growth factor-1, sexual steroids, glucocorticoids, neuropeptides, retinoids, peroxisome and eicosanoids are also major examples of hormones active in the skin[61].

1.2. Acute wound

1.2.1. Acute wound classification

An acute wound is an injury to the skin that occurs suddenly rather than over time. There are principally two types of acute wounds, namely, traumatic wounds and surgical wounds[62]. Regrettably, every individual in the world is at risk for traumatic injury. Regarding mortality, traumatic injury globally is the sixth leading cause of death and the fifth ranking cause of moderate and severe disability. Especially, it accounts as the first cause of death and disability for younger people. For example, nearly 40% of the injured in the German trauma registry were aged between 20 and 39 years [63]. A more recent report of Global Burden of Disease Study (GBD) auspiced by the World Health Organization (WHO) indicated that traumatisms accounted for 11.2% of the global burden of disease (278.6 million of disability-adjusted life years) [64]. Except for trauma, millions of surgical wounds are created annually in the course of routine medical care in the United States and Europe. For example, data from the National Center for Health Statistics (NIH's Research Portfolio Online Reporting Tool, RePORT; http://report.nih.gov/), 40 million inpatient surgical procedures were performed in the United States in 2000, followed closely by 31.5 million outpatient surgeries. Unfortunately, the need for post-surgical wound care is still sharply on the rise [65]. According to a new global industry analysts report (Wound prevalence and wound management 2012-2020)[66], surgical wounds account for the even vast majority of skin injuries, with an estimated global rate of 100 million surgical incisions each year, and growing at 3.1% CAGR (Compound Average Growth Rate).

Pre-hospital acute wounds are often precipitated by accidental injury or trauma, such as burns, lacerations, or abrasions[67](Figure 3). Technically, it is mainly caused when the external forces exceeds the strength of the skin or its underlying tissues,which may vary from minor cut, abrasion through to

extensive tissue injuries.

Figure 3: Acute wounds. Acute wounds are caused by trauma (including burn) or surgery. Traumatic wounds demonstrated here are as (A), finger tip injury left wound with only skin and soft tissue defect and (B), crush injury of the hand with both skin defect and deep tissue damage or (C): Hot press injury (burn wound). Surgical wounds are as (D), excisional wound at anterior tibial area and (E), wound secondary to dorsopedal free skin flap harvesting. Wound infection (F) is one of the most common complications of acute wounds mainly due to contamination or insufficient debridement of the wound.[68,69,70,71]

Normally, a traumatic wound is classified by whether it is tidy or not. Specific examples for different types of traumatic wounds are: ***Abrasion*** - a rough surface scrapes or rubs the skin, causing trauma and tearing the tissue, such as the knee scraping against asphalt; ***Puncture*** - a pointed object pokes into the tissue, sometimes causing deep multi-layered trauma, such as the foot stepping on a nail; ***Laceration*** - A sharp object delivers a hard blow to the tissue, resulting in a tear that can be jagged and irregular, such as bumping a leg on a table, causing a break in the skin or ***Incision*** - a straight edged cut to the skin caused by a sharp blade such as cutting a finger with a knife. As the historical and clinical features surrounding the cutaneous injury process differ, it is necessary to evaluate and treat acute wounds individually.

Surgical wounds, on the other hand, are purposefully incised or laid open by a

surgeon (Figure 3). Although they usually appear to be much more tidy than those wounds caused by trauma or injury, the integrity of the skin at different levels of epidermis, dermis or subcutaneous tissue are inevitably broken as well. It's classification, mainly in relation to potential infection, was first introduced by the National Academy of Sciences in 1964[72], which has been the foundation for infectious risk assessment, perioperative protocol development, and surgical decision-making. In an updated 1985 guideline issued by the Center for Disease Control's (CDC), estimated postoperative rates of surgical site infections was provided[73]. Most recently, the American College of Surgeons-National Surgical Quality Improvement Program (ACS-NSQIP) database provided a tool to assess surgical outcomes drawing from the records of hundreds of hospitals, including the defined Surgical Wound Classifications[73]:

Wound class	Definition	Example	Infection rate
Class I	Clean wounds	Mastectomy, Hernias	⩽2%
Class II	Clean contaminated wounds	Gastrectomy, Hysterectomy	5% -15%
Class III	Contaminated wounds	Rupture appy, Emergent bowl resect	>15%
Class IV	Dirty or infected wounds	Intestinal fistular resection	>30%

Table 1: Wound classification. Class I / Clean Wounds: These are uninfected operative wounds in which no inflammation is encountered and the respiratory, alimentary, genital, or uninfected urinary tracts are not entered. **Class II / Clean-Contaminated Wounds:** These are

operative wounds in which the respiratory, alimentary, genital, or urinary tract is entered under controlled conditions and without unusual contamination. **Class III / Contaminated Wounds:** These include open, fresh, accidental wounds, operations with major breaks in sterile technique or gross spillage from the gastrointestinal tract, and incisions in which acute, non-purulent inflammation is encountered (including necrotic tissue without evidence of purulent drainage, such as dry gangrene). **Class IV / Dirty or Infected Wounds:** These include old traumatic wounds with retained devitalized tissue and those that involve existing clinical infection (purulence already present in wound) or perforated viscera.

According to this category, wounds in ***Class I*** run 2% or lower risk of infection. They are primarily closed with a drain (if needed) connected to a closed system and are usually included in clean surgical procedures; ***Class II*** wounds run 5% to 15% risk of infection and are usually included in clean/contaminated surgical procedures; ***Class III*** wounds run more than 15% risk of infection, which are usually included in contaminated surgical procedures whereas wounds in ***Class IV*** run more than 30% risk of infection and are usually included in dirty/infected surgical procedures or conditions (incision and drainage of perirectal abscess, perforated bowel repair, peritonitis, appendectomy with perforation and/or pus noted, perforated gastric ulcer, ruptured appendectomy, open fracture with prolonged time in the field before treatment, dental extractions with abscess) [74]. This scheme is considered the gold standard by which wounds are classified. With this in mind, it is easy to identify and describe the degree of bacterial contamination of surgical wounds at the time of surgery, which provides guidance for appropriate interventions that lead to different types of wound closure, namely, **primary closure** (closure by primary intent), **delayed primary closure** or **secondary closure** (closure by secondary intent)[75].

1.2.2. Skin regeneration and wound healing

Acute wounds are a common health problem and clinical burden that has posed great challenges to our healthcare system. Facilitating the healing of these unintended or deliberate injuries with maximal restoration of tissue function while minimizing aesthetic impact on the patient remains to be a central concern of clinical care. Healing without complications is critical for survival, as restoration of the skin integrity guarantees homeostasis to protect the individual. Numerous studies have been made in discovering the cellular and molecular pathways responsible for natural (acute) wound healing, and tremendous progress has been made till recently. However, the complete mechanisms underpinning wound healing and skin regeneration are still poorly understood, and current therapies are therefore limited. Undoubtedly, an appropriate plan of therapeutic interventions for acute wounds could be improved by a thorough understanding of the relationship between clinical, cellular, and subcellular events occurring during the normal healing process. This is a well-organized physiological process leading to predictable tissue repair, where platelets, keratinocytes, immune surveillance cells, microvascular cells and fibroblasts play key roles in the restoration of tissue integrity.

The normal mammalian response to a break in cutaneous defect integrity occurs in four overlapping, but biologically distinct phases. Although a time-scale compartmentalization of the healing process risks oversimplification and inaccuracies, such modeling is useful in making a comprehensible outline of wound repair. **Hemostasis** (coagulation) occurs immediately upon injury, leading to fibrin clot formation initiated by platelets, which also release numerous mediators to attract other functional cells to the site of injury[76]. The **inflammatory phase** begins with the arrival of neutrophils and followed by macrophages and lymphocytes, whose purpose is to remove devitalized tissue and prevent invasive infection. Next, there is a **proliferative phase** in which

new blood vessel formation (angiogenesis), extracellular matrix (ECM) components synthesis and re-epithelialization is achieved[77]. In this phase, balance between scar formation and tissue regenerations occurs, because it is found that in adult wounds, scar formation usually predominates whereas in fetal wound healing, an impressive amount of regeneration is possible[78]. Finally, comes the longest phase of wound healing which typically lasts 6-24 months from the time of injury, the **remodeling phase**, the purpose of which is to maximize the strength and structural integrity of the wound. In this phase, collagen remodeling along with vascular maturity and regression take place. Interruption of any of these phases may arrest the wound-healing cascade and lead to delayed wound healing or even non-healing wounds. The alteration in one or more mediators such as those inflammatory cells, growth factors, proteases like the matrix metalloproteinases (MMPs), cellular and extracellular elements impair the normal healing [79]; also, in the presence of some negatively exogenous factors, such as concurrent diabetes, malnutrition, or the exposure of smoking, radiation, inmmunuocompromise, adequate healing of wounds tends to fail [80].

Hemostasis

An acute wound upon injury directly leads to vascular damage and bleeding, and the immediate priority is to prevent blood loss by vasoconstriction and blood clot formation to seal the broken vessel. Therefore, hemostasis begins immediately following tissue injury by the exposure of blood components together with the injured tissue to the subendothelial layers of the vessel wall, activating both intrinsic and extrinsic clotting cascade. In brief, pro-thrombin is activated to form thrombin, which then cleaves fibrinogen to generate fibrin which later forms the clot along with platelets and the plasma fibronectin. Disrupted blood vessels also bring about the extravastion of blood constituents into the wound, through which platelets adhere, clump and aggregate to form the initial hemostatic plug (blood coagulation) that plug the disrupted vessels.

Suzuki et al. shown that the adhesiveness of these platelets results from the activation of intergrin receptors on their surface [81]. The blood clot, mainly made up of cross-linked fibrin, erythrocytes, platelets and other ECM proteins such as fibronectin, vitronectin and thrombospondin[82], acts as a first defense against mirobial invasion.

In the mean time, platelets in the clot undergo degranulation, releasing a cadre of biologically active substances mainly consisting of chemoattractants for inflammatory cells, activation factors for local fibroblasts and endothelial cells and vasoconstrictors. They include chemokine (C-C motif) ligand 5 (CCL5), thrombin, platelet-derived growth factor (PDGF), transforming growth factor-β (TGF-β), vascular endothelial growth factor (VEGF)[5], basic fibroblast growth factor (FGF-2), hepatocyte growth factor (HGF), Insulin-like growth factor (IGF), epidermal growth factor (EGF), sphingosine-1-phosphate (S1P), which promote cell migration and growth into the site of injury. Besides, as a result of the intrinsic and extrinsic coagulation cascades, fibrin monomers are cross-linked and polymerized. They turn into a gel and serve as a provisional lattice (fibrin matrix) for incoming cells during the later phases of wound healing.

Inflammation phase

Almost immediately after injury, inflammatory cells are also recruited to the wound site. They are attracted by the activated complement cascade, TGF-β, and products of bacterial degradation such as lipopolysaccharide (LPS). For example, when hemostasis is completed, local vessels dilate and increase their permeability under the effect of Bradykinin (developed the by coagulation cascade) as well as C3a and C5a anaphylatoxins (developed by the complement cascade), to allow inflammatory cells to migrate toward the wound site[83]. Master cell participants in this process, as it can release histamine and leukotrienes under the stimulation of C3a and C5a anaphylatoxin, and finally cause the local endothelial cells to disconnect their

cellular contact[84]. Chemotaxis of inflammatory cells into the wound is then induced in this phase, which is of crucial importance. CCL5, released by platelets, is one of the most potent monocyte chemoattractants; thrombin, in addition to its role as an early mediator of clot formation, also promotes monocyte chemotaxis through the release of pro-inflammatory cytokines such as CCL2, interleukin-6 (IL-6) and IL-8 by endothelial cells [85]. These chemokines largely facilitate the infiltration of inflammatory cells, principally, neutrophils, macrophages and lymphocytes.

In the first 2 days, the wound cavity is filled as neutrophils first infiltrate into the fibrin matrix. They employ various strategies to kill bacteria and actively decontaminate the wound, including the secretion of proteases and antimicrobial peptides, removing dead tissue through phagocytosis and the generation of oxygen-dependent and independent killing mechanisms to prevent infection[86]. Next, they release a variety of proteases to degrade remaining extracellular matrix to prepare the wound for further healing. Peters et al. reported that without neutrophils, macrophages lack guidance in conducting the healing process [87]. Although neutrophils help decrease infection during cutaneous wound healing, studies indicates that their absence does not prevent the overall progress of wound healing[88]. Their prolonged persistence in the wound, on the contrary, has been proposed to be able to convert acute wounds into nonhealing wounds.

48 to 72 hours after injury, monocytes attracted by monocyte chemoattractant protein 1 (MCP-1) are recruited into the wound after neutrophils. This chemokine (also known as CCL2), with PDGF as its major inducer[89,90], can be released by many types of cells at different stage of wound healing such as neutrophils, keratinocytes and even monocytes themselves[91,92]. When circulation monocytes egress into the tissue, they alter their phenotype and differentiate into macrophages, which are the predominant cell type at the

wound site by the third day after injury. Macrophages have been considered as "central" players in wound healing. Accumulated evidence indicates their protective immunologic role in organizing the activity of other cell types at the following stages of healing[93]. Specifically, they phagocytose debris like apoptotic neutrophils and other dead cells and remove bacteria; they act as antigen-presenting cells, and most importantly, produce cytokines and multiple peptide growth factors such as TGF-β, TGF-α, basic FGF (bFGF), VEGF and PDGF that activate and attract local endothelial cells, fibroblasts and keratinocytes. Thus they enable wound healing by inducing cell proliferation, new blood vessel formation as well as synthesizing extracellular matrix in the healing wound[94]. As a matter of fact, macrophages play such a pivotal role in enabling wound healing, that their absence has been observed to lead to severe consequences. Leibovich and Ross pointed out in their landmark study that antimacrophage serum together with hydrocortisone significantly diminished macrophage accumulation in a geinea pig model of skin wounds[95], which markedly impaired wound healing[95,96]. This implies a vital role for macrophages during normal wound healing and more in-depth studies are needed to fully understand their function.

Interestingly however, although timely and transient inflammatory responses after injury are found helpful to the healing process, the inflammation seems not to be not essential for skin wound healing. In a recent study, Martin et al. found that there are no differences of healing rates for both incisional and excisional wounds between PU.1 null mice (depletion of macrophages and neutrophils) and their wild-type siblings. Furthremore the repair from these “macrophageless” mice appears to be scar-free in the embryo. These results suggest that inflammation is not an essential prerequisite for efficient tissue repair, as long as microbial infection is controlled. Furthermore, local modulation of the cellular inflammatory response at the site of wounding might be a beneficial therapeutic strategy for management of tissue repair in the

clinic, which is very inspiring for translational studies [97].

As the macrophage inflammation resolves around 5 to 7 days after injury, CCL3, 4, and 5 are then produced in the granulation tissue, which then chemoattract the last cell type entering the wound, the lymphocyte. They are considered to exert a specific response against microbes and other foreign material in the wound, for example, B-lymphocytes via antibodies in response to antigen binding to the B-cell receptor and T-lymphocytes through production of cytokines and stimulation of cytolytic activity in response to the interactions between the TCR and major histocompatibility complex bound antigen on antigen-presenting cells. Finally, lymphocyte-induced inflammation is resolved by IFN-c and TNF-a mediated apoptosis[98]. Mast cells also appear during the later part of the inflammatory phase, but their function remains unclear. Accumulating evidence showed that the activated mast cell participates in a variety of events of the healing phases, such as triggering and modulating the inflammatory stage, proliferation of connective cellular elements and remodelling the newly formed connective tissue matrix[99]. Shiota N et al. found that wound healing after skin scald injury was partially impaired in mast cell-deficient mice, indicating they may contribute to the healing process, especially in the proliferative and remodeling phases after injury[44]. More work is needed to identify its mechanisms and potential roles in wound healing.

Proliferative phase

The proliferative phase occurs approximately from days 4 to 21 following injury and overlaps with the inflammatory phase. Briefly, major events involved in this phase are fibroblasts influx, ECM deposition, new blood vessels formation and re-epithelialization. It starts with the degradation of the initial fibrin-platelet matrix and the invasion of fibroblasts and endothelial cells. Proteases of serine, cysteine and those from MMP families are secreted through the fibrin clot and

provisional matrix to facilitate this process[100].

In this phase, fibroblasts, macrophages and endothelial cells are the major types of cells that account for the formation of granulation tissue, a dense conglomeration of blood vessels, macrophages and fibroblasts embedded within a loose matrix of fibronectin, hyaluronic acid and collagen. It appears approximately four days post injury, as the embedding cells play independent roles to form extracellular matrix and new blood vessels. For example, fibroblasts produce most collagen types in the ECM whereas keratinocytes can also synthesize some types[101]; new blood vessels, on the other hand, are developed from preexisting vessels stimulated by angiogenic factors released by macrophages (VEGF, bFGF, angiopoietin1 and thrombospondin), keratinocytes (CXCL8 and VEGF) and endothelial cells themselves (CXCL8 and VEGF)[102,103,104,105].

Fibroblasts become the predominant cell type by three to five days after injury. They are activated by a series of factors such as PDGF and TGF-β secreted by macrophages and mast cells[106,107], and then proliferate and produce matrix proteins like fibronectin, hyaluronic acid, collagen and proteoglycans. All of these proteins help construct granulation tissue, a new ECM that gradually replaces the previously formed provisional fibrin matrix for keratinocyte migration[108]. When fibroblasts produce extracellular matrix to replace the provisional fibrin matrix for keratinocyte migration, macrophages also release certain proangiogenic factors to induce new blood vessel formation from endothelial cells as described above. Michaels et al. observed impaired wound healing when angiogenesis inhibitor endostatin was applied, and topical vascular endothelial growth factor is effective in counteracting this effect[109]. Needless to say, new blood vessels formation and granulation tissue survival is of great importance for wound healing during this phase.

Approximately four days after injury, myofibroblasts appear in the wound. They become most abundant in the proliferation phase of wound healing, and progressively disappear in the later stage of healing, possibly by an apoptotic mechanism[110]. They differentiate from fibroblasts in a complex process, regulated by at least a cytokine (TGF-β1), an extracellular matrix component (the ED-A splice variant of cellular fibronectin), as well as the presence of mechanical tension[111]. Kato et al. found the inhibition of either fibronectin or the corresponding integrin receptors prevents TGF-β1-mediated myofibroblast differentiation [112]. Myofibroblasts correlate with contraction and closure of the wound through focal adhesions between myofibroblasts and the extracellular matrix[113].

The timeframe of the re-epithelialization process is slightly different from that of the other events in the proliferative phase, which probably begin almost immediately upon injury. Platelets in the early wound release epidermal growth factor (EGF) which stimulates the keratinocytes adjacent to the wound. Other key factors found to be able to stimulate the proliferation of kerationcytes in healing wounds include TGF-α, heparin binding epidermal growth factor (HB-EGF), hepatocyte growth factor (HGF) and keratinocyte growth factor (KGF)[114]. Stimulated through specific integrin mediators, keratinocytes alter their phenotype and migrate laterally toward the wound, interacting with extracellular matrix proteins such as fibronectin and proceeding to move beneath the provisional ECM [115]. Matrix metalloproteinase also helps promote the re-epithelialization process by releasing keratinocytes from their substratum and facilitating their migration through the matrix[116]. Mirastschijski et al. found that through systemic administration of the synthetic broad-spectrum MMP inhibitor (GM 6001), the re-epitheliaization process was significantly delayed. This study suggested that keratinocyte resurfacing, wound contraction, and granulation tissue organization are highly MMP-dependent processes [117]. The migrating keratinocytes do not divide

until the new epithelial layer is established. Then, keratinocytes and fibroblasts secrete laminin and type IV collagen to form the basement membrane and the keratinocytes then become columnar and divide to restore the epidermal layer[118].

The dysregulation of the proliferative phase impairs wound healing and underlies the pathophysiology of chronic wounds and fibrotic disorders such as hypertrophic scarring and keloids. Therefore, understanding the signals that mediate the proliferative phase would help developing new therapeutics for acute wound healing[119].

Remodeling phase

The last stage of wound healing characterized by ECM turnover coupled with a significant decrease in cellularity is the remodeling phase which is also the longest part. It usually presents itself from 21 days up to 1 year. The process of wound remodeling occurs once granulation tissue entirely covers the wound and re-epithelialization has been completed by keratinocytes. Again, this processes overlaps with the others. The decline in cellularity is mainly due to the apoptosis of residual inflammatory cells, myofibroblasts and the regression of the neovasculature[111]. The word "remodeling" refers to both the processes of wound contraction produced by wound myofibroblasts and collagen remodeling, in which the initial type III collagen laid down by fibroblasts (proliferative phase) is gradually replaced by type I collagen over time[120]. This process is mediated by matrix metalloproteinases (MMP) produced by all three major cell types formed in the proliferative phase: macrophages, fibroblasts, and endothelial cells. The activity of MMP is important for collagen metabolism[121]. The turnover of collagen subtypes and crosslinking of the collagen gradually strengthen the wound. Tensile strength increases from 1 to 8 weeks after wounding[122] and reaches at best around 80% that of unwounded skin.

In conclusion, skin wound healing is a complex and dynamic biological process requiring the interaction and coordination of many different cell types and molecules, including growth factors and cytokines. Tremendous strides have been made in illustrating the potential pathways involved in normal and impaired healing. However, this increased understanding has not led to complete success in patient care. Administration of growth factors and cytokines as well as exogenous pro-healing drugs from both natural or synthesized molecules and compounds, has been reported to improve the wound healing process. However, as wound healing involves multiple molecular mechanisms at the same time, no single agent therapy is likely to be fully successful, and more work is still needed before full understanding of the wound healing process can be reached.

1.3. Curcumin from turmeric: a promising candidate for wound therapy

Natural plant products have long been used for various purposes including medicine, since many of them have pharmacological or biological activity. As a matter of fact, medicines derived from plants have played a pivotal role in the health care of many cultures, both ancient and modern. For example, botanical supplements have been used for centuries in traditional medicine, including Ayurveda (science of long life), Chinese medicine as well as Kampo (Japanese medicine), many of which have exhibited vigorous healing activity[123].

Turmeric is one such herb known as the “golden spice” or “spice of life”. Being a product of *Curcuma longa*, a rhizomatous herbaceous perennial plant belonging to the ginger family *Zingiberaceae*, it has at least 6000 years of documented history of medicinal use for wound healing, rheumatoid arthritis, chronic anterior uveitis, conjunctivitis, skin cancer, small pox, chicken pox, urinary tract infections, and liver ailments[124]. For instance, in ancient

Pakistan and Afghanistan, turmeric was used to cleanse wounds and stimulate their recovery by applying it on a piece of burnt cloth that was placed over a wound[125]. In Ayurvedic medicine, it was used on diabetic wounds[126]. Although modern medicine has neither held in very high esteem nor encouraged such empirical use of the natural product, recent emphasis on the use of natural and complementary medicines in western medicine has drawn the attention of the scientific community to this ancient remedy, as indicated by the over 3000 publications on turmeric emerging in recent decades, among which the importance of turmeric in its medicinal properties especially in wound healing has begun to be re-recognized. For example, Gujral et al. showed the healing properties of turmeric on wounds and ulcers in rats and rabbits models[127]. Subarna Kundu et al. also pointed out more recently in their preclinical study that turmeric paste as a topical medicament leads to significantly faster wound healing[128]. In addition to that, turmeric is considered to be generally safe in individuals of all age groups and there is no known interaction of drugs with turmeric that has been reported by the monographs of Commission E, the German regulatory authority[129]. As the constant search for novel compounds in western medicine has drawn new attention of the scientific community to this ancient remedy [130], extensive work has been carried out recently to establish the biological activities and pharmacological actions of turmeric and its extracts in the hope that they can be exploited in pharmaceutical drug discovery and drug design. Inspiringly, curcumin, the main yellow bioactive component of turmeric, has been identified and shown to have a surprisingly wide spectrum of beneficial biological actions, including anti-inflammatory, antioxidant, anti-cancer, anti-angiogenic and anti-microbial activity [130,131]. Furthermore it was shown to modulate wound healing processes [132,133]. Safety evaluation studies demonstrated that curcumin, just as its parent herb turmeric, is extremely safe as it is tolerated at a very high dose without any toxic effects[134]. For example, three different phase I clinical trials indicated that curcumin, when taken as

high as 12g per day, is well tolerated[135].

These therapeutic features attribute to curcumin's unique chemical properties. The generic structures of the turmeric-derived curcuminoids are, in order of their relative abundance in the root, comprised of curcumin (R_1 and R_2 = OCH3), demethoxycurcumin (R_1=H, R_2=OCH3), bis-demethoxycurcumin (R_1 and R_2 = H), and cyclocurcumin (Figure 4). Curcumin, or diferuloylmethane (chemical formula $C_{21}H_{20}O_6$ and molecular weight of 368.38), named by the IUPAC as (1E,6E)-1,7-bis(4-hydroxy-3-methoxyphenyl)-1,6-heptadiene-3,5-dione, has three chemical entities in its structure: two aromatic ring systems containing o-methoxy phenolic groups, connected by a seven carbon linkers consisting of an α,β-unsaturated β-diketone moiety which exhibits keto-enol-tautomerism (Figure 4, left). That is, a predominant keto form in acidic and neutral solutions and stable enol form in alkaline medium.

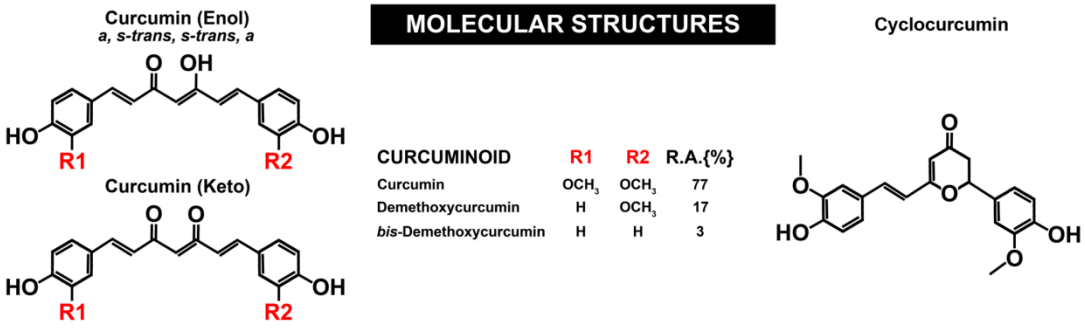

Figure 4: Molecular structures of turmeric-derived curcuminoids. The generic structure of the most abundant curcuminoid (R.A.= relative abundance) is the structure of the most energetically stable enol conformer of curcumin (R1 and R2 = OCH3), where R1 and R2 moieties have adopted the *a, s-trans, a* orientation (Kolev et al., 2005). The less abundant and less stable diketo form of curcumin, as opposed to enolic curcumin, is nonplanar, whereby the ketones are oriented *anti* relative to each other (Agnihotri and Mishra, 2011). The least abundant curcuminoid is cyclocurcumin.

Michal Heger et al. summarized several distinct chemical properties this amphipathic molecule possesses: (1) H-bond donating and accepting capacity of the b-dicarbonyl moiety, (2) H-bond accepting and donating capacity of the phenylic hydroxyl residues, (3) H-bond accepting capacity of the ether residue in the methoxy groups, (4) multivalent metal and nonmetal cation binding properties, (5) high partition coefficient (log P value), (6) rotamerization around multiple C-C bonds, and (7) behavior as a Michael reaction acceptor[136]. Studies to date have demonstrated a strong intrinsic activity and efficacy of curcumin as a therapeutic agent for various ailments, which is undoubtedly correlated to these physiochemical properties. For example, its diketone moiety and two phenolic groups are three main reactive functional groups that account for the important chemical reactions, with which curcumin may serve as hydrogen donator (leading to its oxidation), participate in reversible and irreversible nucleophilic addition (Michael reaction) reactions, hydrolysis and degradation [137]. Therefore, curcumin has been found to interact with numerous signaling molecules, such as inflammatory molecules, cell survival proteins, protein kinases, protein reductases, glyoxalase I, xanthine oxidase, proteasome metal ions and even DNA and RNA[138], reflectiong its pleiotropic biological activities.

Reactions with ROS

The antioxidant activity of curcumin is a consequence of its excellent ability to scavenge reactive oxygen species (ROS) of both free radical oxidants and molecular oxidants. During this process, all three active sites can sustain oxidation through the transfer of election and the abstraction of hydrogen, and the phenol-OH group is found to contain the most easily abstractable hydrogen, without which it forms resonance stabilized phenoxyl radicals across the keto-enol structure. For example, when curcumin reacts with peroxyl radicals, it turns into less reactive curcumin phenoxyl radicals, which provides protection against ROS-induced oxidative stress[139], and such reaction can

be reversed in the presence of water soluble antioxidants like ascorbic acid. Studies indicated that curcumin is able to scavenge various free radical ROS such as hydroxyl radicals, superoxide radicals and alkoxy radicals. Besides, it is considered as a superoxide dismutase mimic due to the fact that it can efficiently react with superoxide radicals comparable to well known lipid soluble antioxidants[140]. Likewise, curcumin can protect cells from molecular oxidants such as peroxynitrite and hydrogen peroxide being excessively produced in many biological processes[141].

Nucleophillic Addition Reaction

The α, β-unsaturated β-diketo moiety of curcumin facilitates nucleophilic addition reaction, known as the Michael addition, which takes place between the unsaturated ketone as an acceptor and anions such as -OH, -SH, -SeH as donors. During this process, pH conditions are found to be of great importance because both -OH and -SH are protonated at physiological pH while -SeH easily undergoes deprotonation that renders it a better nucleophile. Studies indicated that this reaction is extremely helpful for the biological chemistry of curcumin in living cells [137,138].

Curcumin-Metal Ion Interactions

Again, the α, β-unsaturated β-diketo moiety of curcumin makes it an excellent chelating agent, where the enolic proton is replaced by the metal ion and the o-methoxy phenolic moiety remains intact in the complexes. Studies indicated that with such a monobasic bidentate ligand, curcumin forms stable complexes with most of the known metal ions, such as those transition metals like Fe^{3+}, Mn^{2+}, Ni^{2+}, Cu^{2+}, Zn^{2+}, Pb^{2+}, Cd^{2+}, Ru^{3+}, Re^{3+} or those non-transition metal ions and rare earth ions like Al^{3+}, Ga^{3+}, Sm^{3+}, Eu^{3+}, Dy^{3+}, Se^{2+} and metal oxides like VO^{2+}[142]. The curcumin-metal complexion has novel physico-chemical properties, for example, it may act as new metal-based (Cu^{2+} , Mn^{2+}) antioxidant[143]. Researchers also found that the toxicity of the metal is

reduced by the complexion. Take Alzheimer's diseases as an example, due to its lipophilic nature, curcumin is found to chelate metal ions that are toxic to the neurons after it crosses the blood brain barrier[144]. Some studies reported curcumin-metal complexes to be better anti-tumor agents than curumin itself [145,146].

These chemical properties are closely related to biological processes that are benificial for therapeutic purposes especially in wound helaing. Therefore, interest in translating the use of curcumin to the clinic in these areas has increased remarkably over the recent years, leading to a burgeoning number of clinical trials and publications [147,148,149]. During the last two decades, collective scientific data (around 8000 peer-reviewed articles, reports, reviews, opinions, patents and clinical trials) from both animal models and in human studies suggests that curcumin is indeed a safe therapeutic molecule, and the US Food Drug Administration (USFDA) has considered this molecule to be " generally recognized as safe (GRAS)" (http://www.nutraingredients-usa.com/Suppliers2/Sabinsa-gets-FDA-no-objection-letter-for-GRAS-status-of-its-Curcumin-C3-Complex), which has, in a sense, paved the way for ongoing human clinical trials. Unfortunately, although the pharmacological safety and efficacy of curcumin makes it a potential compound in developing modern medicine for the treatment of wounds as well as other human diseases, progress in translating these findings into clinical application has so far been impeded and curcumin has not yet been approved as a therapeutic agent, most likely due to several of its physicochemical properties including relatively low bioavailability caused by low aqueous solubility, instability, poor absorption as well as rapid metabolism and systemic elimination [150,151].

1.4. Electrospinning: an encouraging approach for regenerative medicine

Developments in material sciences, now allow to remove some obstacles associate with curcumin's low bioavailability. One option to circumvent unwanted properties is nano-formulation of the pharmaceutical compound through electrospinning. This technique from the textile industry has recently emerged as a novel means to generate nanoscale scaffolds for regenerative medicine and controlled-release systems for therapeutic purposes[152].

1.4.1. Electrospinning history and fundamentals

Electrospinning is a notable fiber-fabrication technique to produce non-woven fibrous materials with typical fiber diameters in the order of a few micrometers down to tens of nanometers[153]. In 1900, it was first patented by Cooley[154], but the time electrospinning truly surfaced as a valid technique for spinning small-diameter fibers dates back to 1934, when Formhals patented a process and an apparatus using electric charges to spin synthetic fibers[155]. Around 30 years later, in 1969, Taylor studied how the polymer droplet at the end of a capillary behaves when an electric field is applied and described the formation of "Taylor cone" from the pendant droplet as the surface tension is balanced by electrostatic forces[156]. Shortly afterwards, interest shifted to deeper understanding of the relationships between processing parameters and the structural properties of electrospun fibers. For example, Baumgarten investigated the influence of different processing parameters such as solution viscosity, flow rate and applied voltage on electrospun fiber properties in 1971[157]. Till now, the process of elctrospinning has been known, especially in the textile industry, for over 100 years, however, this technique has not gained widespread interest as a potential polymer processing technique for applications in tissue engineering and drug delivery until recently, despite

some early efforts have been made [158,159].

A typical electrospinning setup consists of a capillary, a high voltage source with positive or negative polarity and a grounded collector (Figure 5). Generally, prepared polymer solution (or melt), so called spinning solution, is injected (by syringe pump, gravitational forces or pressurized gas) at a constant feed rate though a nozzle or needle which is charged to a high voltage (positive or negative) that injects a charge of a certain polarity into the polymer solution or melt. When the voltage is sufficiently high, the hemispherical surface of the liquid droplet elongates to form the Taylor cone, from which a charged liquid jet is ejected toward the earthed collector when the applied voltage increases further.

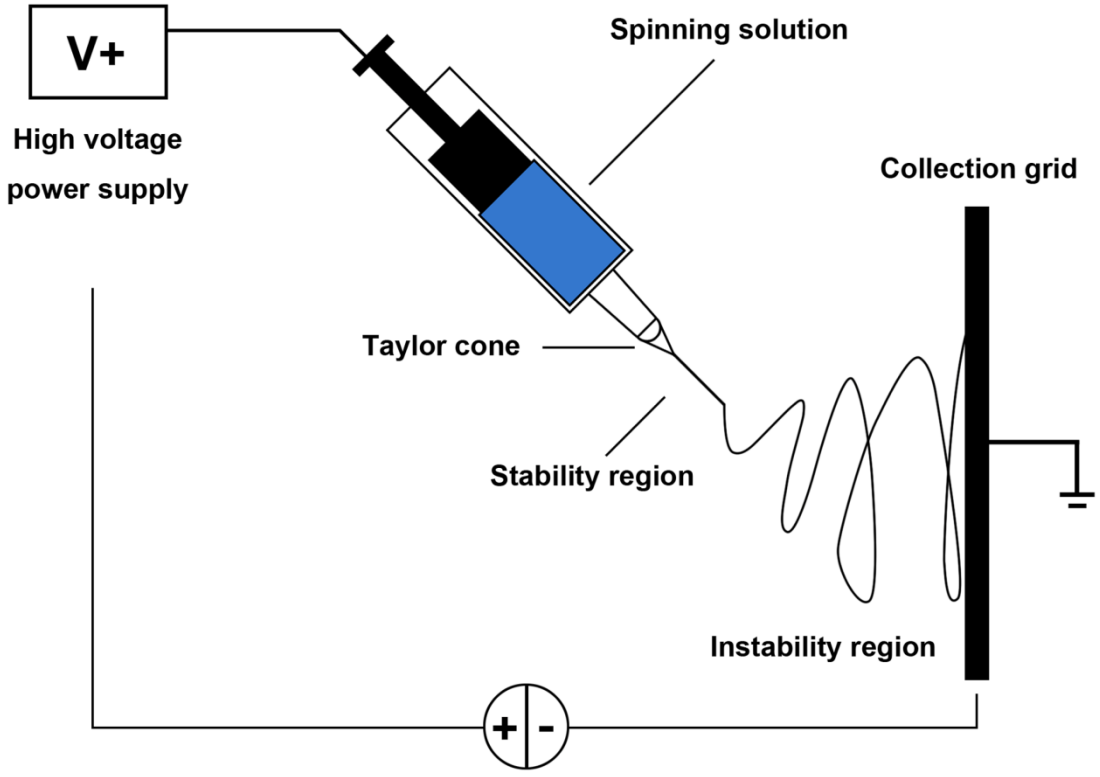

Figure 5: Electrospinning process. The standard laboratory setup for electrospinning consists of a spinneret, a high-voltage power supply, a syringe pump and a grounded collector. Polymer solution, sol-gel, particulate suspension or melt is stretched into a thin fiber under applied high voltage, whipping in a random manner before depositing on the grounded collector.

As the jet dries in flight (solvent evaporation), the mode of current flow changes from ohmic to convective. The charge migrates to the surface of the fiber, leading to the elongation and thinning of the jet by a whipping process initiated at small bends in the fiber. Then the motion of segments of the jet grows rapidly into an electrically driven chaotic bending instability, possibly due to repulsive interactions between like charges in the jet [160]. This ends up with increasing transit time and path length until the jet is finally deposited on the grounded collector [161], leaving dry polymer fibers with nanometer-scale diameters (Figure 6).

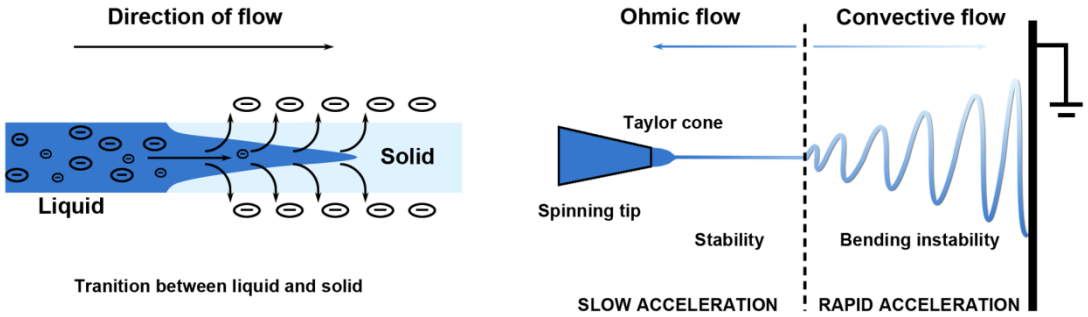

Figure 6: Bending instability. As the jet dries in flight, the mode of current flow changes from ohmic to convective as the charge migrates to the surface of the fiber. The jet is then elongated by a whipping process caused by electrostatic repulsion initiated at small bends in the fiber, until it is finally deposited on the grounded collector, forming uniform fibers with nanometer-scale diameters.

Technically, there are several processing parameters that greatly affect fiber formation and structure, such as voltage, polymer flow rate and capillary-collector distance, all of which have been found to be able to influence the formation of nanofibers with bead -like defects[162].

Applied voltage

Within the electrospinning process, applied voltage is the crucial factor. As described above, only when it is higher than the threshold value, charged jets

are ejected away from Taylor Cone, while suboptimal field strength ends up with bead defects or even failure in jet formation. There is evicdence that applied voltage controls the fiber diameter, however, results vary strongly with the polymer system being used[163,164,165]. Therefore, it is important that there is an optimal range of electric field for a certain polymer-solvent system, and either too weak or too strong a field will lead to the formation of beaded fibers.

Flow rate

Polymer flow rate also has an impact on fiber size as well as fiber porosity and geometry. If there is insufficient flow of polymer solution through the capillary to replace the ejected fiber jet, the cone shape at the tip of the capillary cannot be maintained. On the other hand, very high flow rate ends in bead fibers with thick diameter largely due to inadequate drying time of the jet prior to its arrival at the collector and low stretching forces. Incomplete drying has also been shown to form ribbon-like (flattened) fibers, as the later dried core layer brings about the collapse of the earlier dried skin layer[166]. Megelski et al. demonstrated that both fiber diameter and pore size is proportional to flow rate and significant amounts of bead defects were noticeable at high flow rates[167]. Therefore, lower flow rate is more recommended as the polymer solution will get enough time for polarization.

Capillary - collector distance

While playing a minor role, Capillary - collector distance can also influence fiber size by 1-2 orders of magnitude. Briefly, too short distance precludes the fiber from having enough time to solidify before arrival at the collector while too long distance gives rise to bead defect. Hekmati et al. precisely studied three important parameters of the electrospinning process including the needle-tip-to-collector distance using polyamide-6 (PA-6)/formic acid polymer solution and found that the nanofibers' diameter increased with the reduction

of the needle-tip-to-collector distance[168]. Correspondingly, Doshi and Reneker demonstrated that the fiber diameter decreased with increasing distances from the Taylor cone[169].

Literature also indicates that factors like humidity and temperature can affect the fiber diameter and morphology, and some researchers regarded them as ambient parameters. In a study to produce ultra-fine polyamide-6 (PA-6) fibers through electrospinning, Mit-uppatham et al. found that raising the temperature of the solution during spinning resulted in the reduction of the fiber diameters with higher deposition rate[170]. Regarding humidity, low humidity may dry the solvent totally and increase the velocity of the solvent evaporation. On the contrary, high humidity will lead to thick fiber diameter, because charges on the jet can be neutralized and the stretching forces become small. Nezarati et al. investigated the impact of humidity as an environmental parameter on fiber morphology, in which the resulting fiber architecture of three polymers (poly(ethylene glycol) [PEG], polycaprolactone [PCL], and poly(carbonate urethane) [PCU]) at a range of relative humidities (5%-75%) were characterized with scanning electron microscopy. They found that low relative humidity (< 50%) resulted in fiber breakage for all three polymers due to decreased electrostatic discharge from the jet, while at high relative humidity (>50%), three distinct effects were observed based on individual polymer properties, suggesting that the effects at high humidity were dependent on the polymer hydrophobicity as well as the solvent volatility and miscibility with water [171]. At last, depending on the application, different collector configurations can be chosen. For example, stationary collector results in the formation of a randomly oriented fiber mat while rotating collector generates mats with aligned fibers, with rotation speed as a critical determinant for the degree of anisotropy. Also, the geometry of the collector itself can influence the final outcome of the product. For example, collectors of two-dimmensional copper mesh or cylindrical rotating mandrel yield sheets or tubular constructs,

respectively.

It is important to realize that there are general trends which are useful when the optimum condition for a certain system is to be considered. The exact relationship, however, will differ for each polymer/solvent system. Thus, it is difficult to give quantitative relationships that can be applied across a broad range of polymer/solvent systems.

1.4.2. Electrospinning for advanced wound dressing

As being mentioned above, electrospinning is a remarkably simple method for generating nanofibers of polymers. Many parameters can influence the morphologies of the resulting electrospun fibers. Appropriate adjustment of all or some of these parameters optimizes the electrospun fibers with desired morphologies and structural properties. Thus, electrospinning is able to produce nanofiber structures that closely resemble the architecture of the ECM, thereby providing an initial support for the healing process[172]. For this reason, electrospinning is the preferred technique of the majority of researchers for wound dressing development with several advantages outlined above. Various electrospinning techniques are available for the fabrication of nanofibrous meshes that provide essential requirements for effective wound care. However, for fabricating ideal mats with all the required properties, many parameters need to be optimized depending on the selected polymers and compounds to be loaded, some of the elementary aspects of the fabrication process are still poorly understood. With the advancement of innovative research as well as deeper understanding of electrospinning sets-ups, it is expected to achieve future "smart dressing devices" capable of treating all aspects of wound for real clinical translation.

1.4.3. Electrospinning for drug delivery

A drug-delivery system carries a therapeutic agent into the body and enhances its efficacy as well as safety by controlling the rate, time, and site of release, so as to deliver and retain a satisfactory amount of drug for an adequate period of time. Meanwhile, it is expected to avoid degradation of non-released drugs within the body. During the past few decades, polymeric micro/nanostructures have gained huge interest as drug-delivery systems because of their increased surface area that enhances the drug-dissolution rate[173]. Electrospinning, as one of the most important methods of electrohydrodynamic (EHD) techniques, uses electrostatic forces as the driving force to fabricate fibers of different shapes with sizes in the nano-scale to a few microns through electrically charged fluid jet. Therefore, it provides great advantages for drug delivery applications thanks to its great flexibility in modulating the shape, size, morphology, and composition of micro/nanostructures through process parameters and material selection. It enables direct encapsulation of a variety of drugs into the electrospun fibers, including hydrophobic and hydrophilic drugs as well as biomacromolecules, e.g., proteins and DNA. With its large surface area that ensures high therapeutics take-up and its three-dimensional open porous structure that reduces the constraint to drug diffusion, electrospinning brings about a more efficient drug-release system [174].

2. HYPOTHESIS

In view of the above, we hypothesized that therapeutic curcumin could be loaded into a biomimetic vehicle of electrospun gelatin nanofibers to enhance its solubility and availability and that these mats can be used to improve acute wound healing processes *in vitro* and *in vivo*.

3. MATERIALS AND METHODS

We set out to design a treatment system with clinical translation in mind. As fiber forming material, gelatin was selected. It is a mixture of peptides and proteins acquired by partial hydrolysis and denaturing of the triple-helix structure of collagen, the most abundant protein in the ECM [175] [176,177]. Recent evidence suggests that gelatin is an attractive polymer for tissue engineering because of its biological origin, which exhibits favorable biodegradability and non-antigenicity[178] [179]. We also showed recently that appropriate crosslinking could improve the mechanical properties of the electrospun gelatin nanofibers to values comparable to human skin [180,181]. This also prevented its rapid dissolution at temperatures at or above 37 °C, a crucial condition for topical application [182].

3.1. Materials

3.1.1. Reagents

Trifluoroethanol (Sigma, Germany), Glutaraldehyde (Sigma, Germany), Ethanol (Apotheke, Germany), Trypsin-EDTA (PAA Laboratories, Germany), Fetal bovine serum(Gibco®, USA), Bovine serum albumin (Sigma, Germany), Antibiotic/Antimycotic (Capricon Scientific, Germany), Dimethyl Sulfoxide (Sigma, Germany), Buffy coats (Institute for Clinical Transfusion Medicine and Immunogenetics Ulm, Ulm, Germany), Ficoll Paque Plus (Amersham Biosciences, Sweden), MitoTracker® Deep Red FM (Life Technologies, USA), NucBlue® Live Ready Probes (Life Technologies, USA), Formaldehyde (Otto Fischar, Germany), WAY 262611(abcam, UK), Hematoxylin & Eosin (Carl Roth, Germany), Triton X-100 (Sigma, Germany), Sodium citrate dihydrate (Sigma, Germany), TWEEN® 20 (Sigma, Germany), Picro-Sirius red (IHC World, USA), Xylene (Carl Roth, Germany), Roti®-Histokitt (Carl

Roth, Germay), Goat serum (Sigma, Germany), H_2O_2 (Carl Roth, Germany).

3.1.2. Cell culture mediums

Dulbecco's Modified Eagle's Medium (DMEM, Biochrom, Germany), AIM V® Serum Free Medium (Life Technologies, USA).

3.1.3. Buffers

PBS (Biochrom, Germany), Sodium citrate buffer (self prepare).

3.1.4. Cell lines

Human Macrophage cell line MV-4-11 (ATCC® CRL-9591™), Human fibroblast cell line HS-27(ATCC® CRL1634™).

3.1.5. Commercial kits

LDH (lactate dehydrogenase) assay kit (Roche, Germany), WST-1 (Water-soluble tetrazolium-1) assay kit, LIVE/DEAD assay kit (Invitrogen, Germany), Ibidi wound healing assay kit (Ibidi, Germany), Human XL Proteome Profiler Array Kit (R&D Systems, USA), Quantikine ELISA kit (R&D Systems, USA), CytoselectTM 24-well cell migration/chemotaxis kit (Colorimetric Format, Cell Biolabs, USA), DAB Substrate Kit (Thermo Fisher Scientific, Germany).

3.1.6. Antibodies

β-catenin (D10A8 XP® Rabbit mAb, Cell signaling, USA), fluorochrome-conjugated secondary antibody (Alexa Fluor 568 goat anti-rabbit IgG, Invitrogen, Germany), Human Dkk-1 antibody (R&D Systems, USA), MCP-1 blocking antibody (abcam, UK), CD68/ED1 antibody (abcam, UK),

Goat anti-Mouse IgG (H+L)-HRPO second antibody (Dianova, Germany).

3.1.7. Devices

Milli-Q system (Millipore, Billerica, MA, USA), syringe pump (Cole-Parmer, USA), Scanning electron microscopy (SEM, JSM-5600LV, JEOL, Japan), X-ray diffractometer (D/Max-2550PC, RigaKu, Japan), Nicolet-Nexus 670 Fourier transform infrared (FTIR) spectrometer (Thermo Fisher Scientific, USA), High-performance liquid chromatography (HPLC) system (Agilent 1200, USA), Universal material tester (H5K-S, Hounsfield, UK), Analytical balance (KERN&Sohn, Germany) Laminar flow bench(BDK LUFT-UND RINIRAUM Technik, Germany), Cell culture incubator (Thermo Scientific Heracell™ 150, Germany), 4°C Refrigerator (SIEMENS, Germany), -20°C Freezer (LIEBHERR, Germany), -80°C Freezer (Thermo Scientific, Germany) CASY® Cell Counter (Innovatis, Germany), Bath vessle (IKA® EH4 Basic, Germany) , Autoclave (Systec, Germany), Microwave (SHARP R239, Japan), Mithras LB940 Microplate Reader (Berthold Technologies, Germany), Nanodrop2000 specrophotometer (Thermo Scientific, Germany), AxioCam camera light microscope (PrimoVert, Carl Zeiss, Germany), fluorescent microscope (Carl Zeiss, Germany), tube rotator (MACS Miltenyi Biotech, Germany), Axio polarized Microscope (Carl Zeiss, Germany), Well plates (Greiner CELLSTAR, USA), Glass slide and cover slip (MENZEL-GLÄSER Superfrost®Plus, Gerhard MENZEL B.V.&Co, Germany), Skin biopsy punch (AcuPunch, USA).

3.2. Methods

3.2.1. Electrospinning of Curcumin/Gelatin blended nanofibrous mat

Gelatin (from bovine skin) and curcumin powder were purchased from

Sigma-Aldrich. Spinning solutions were prepared by dissolving 1g gelatin and 0.1g curcumin in 10 ml trifluoroethanol. During the electrospinning process, spinning solution was loaded into a 10 ml syringe with a 20 gauge nozzle 10cm away from an aluminium foil wrapped copper plate as collector. Feed rate of the syringe pump (Cole-Parmer, USA) was set to 1.5 ml/h with the DC voltage of 15 kV. As-prepared samples were vacuum dried to remove residual organic solvents and underwent a crosslinking process. Briefly, 25% glutaraldehyde solution was mixed with ethanol (1% V/V) and transferred to the bottom of a vacuum dryer covered by a porous ceramic plate with the as-prepared NM on top. The dryer was vacuumized for 24 h at 4°C, then the cross-linked nanofibrous mats were rinsed in ultrapure water and dried for 24 h in a freeze-dryer.

3.2.2. Scanning electron microscopy (SEM)

Prior to imaging by SEM, samples were put on a sample holder and sputter-coated with gold for 50 seconds under argon to increase the conductivity. A scanning electron microscope (JEOL JSM-5600LV, Japan) operating at an excitation voltage of 8-10 kV was used to assess the macroscopic morphology and surface texture of the electrospun fibrous mats and to compare the cross-linked and as-prepared electrospun samples.

3.2.3. X-ray diffraction (XRD) spectroscopy

XRD spectroscopy of the electrospun nanofibrous mats was carried out by the aid of X-ray diffractometer (D/Max-2550PC RigaKu Inc., Japan), with Cu-Kα radiation. The operating voltage and current were kept at 40 kV and 300 mA, respectively. The electrospun nanofiber samples were examined between 0 and 60° (2θ) at a scanning rate of 1° (2θ) per minute.

3.2.4. Fourier transform infrared (FTIR) spectrometer

A Nicolet-Nexus 670 Fourier transform infrared (FTIR) spectrometer (Thermo Fisher Scientific, Waltham, MA) was used to obtain the FTIR spectra of the electrospun nanofibers over a range of 500–4000 cm^{-1} at a scanning resolution of 2 cm^{-1}.

3.2.5. Curcumin release profile

The *in vitro* dissolution of Cc/Glt NM and free curcumin was examined in 50 ml phosphate-buffered saline (PBS, pH 7.4) at 37 °C. At predetermined time intervals, 200 µL aliquots were withdrawn for sampling and replaced with an equal volume of PBS to maintain a constant volume. Samples were analyzed using a high-performance liquid chromatography (HPLC) system (Agilent 1200, USA) combined with a quadrupole mass spectrometer (API-4000, AB SCIEX, USA). An analytical column (4.6×150 mm, 3.5µm, Agilent Eclipse XDB-C18, USA) was selected as the separation column and maintained at 45 °C. The mobile phase, with a total rate of 300µL/min in gradient mode, was composed of water and methanol, each containing 0.2% formic acid. The key parameters for curcumin analysis, the declustering potential (DP), collision energy (CE) and collision cell exit potential (CXP) were fixed at -70, -50 and -12V, respectively. The release profile of each sample was performed in triplicates. Average values of the dissolved drug at specified time periods were plotted versus time (h).

3.2.6. Tensile mechanical properties

The tensile mechanical properties of curcumin loaded nanofibrous scaffolds (crosslinked or non-crosslinked nanofibrous mats) were examined according to the standard ISO 7198 “Cardiovascular implants - Tubular vascular prostheses” by using a universal material tester (H5K-S, Hounsfield, UK). Briefly, rectangular samples (10mm ×

50mm) were cut and subjected to strain-stress measurements (50N load cell at 20°C and humidity of 60%) at a cross-head speed of 10mm/min. At least 5 specimens from each sample were tested to study its Young's modulus and elongation at breaking point.

3.2.7. Cell isolation and culture

The human fibroblast cell line HS-27 (ATCC ® CRL-1634™) was cultured in Dulbecco's Modified Eagle's Medium (DMEM, Biochrom, Germany) supplemented with 10% FCS at 37°C and 5% CO_2. For subculturing, the cells were washed with PBS and detached by adding 0.25% trypsin-EDTA solution followed by incubation at 37°C until cells detach. Fresh culture medium was added and the cells were seeded in new culture flasks in a 1:4 ratio. The growth medium was renewed 2 to 3 times a week. For most experiments, cells were plated into 6 well or 96 well plates (Greiner CELLSTAR, USA) in serum-free medium.

Peripheral blood mononuclear cells (PBMC) were freshly isolated from buffy coats from healthy donors (Institute for Clinical Transfusion Medicine and Immunogenetics Ulm, Ulm, Germany) based on the Ficoll density gradient centrifugation technique. Briefly, heparinized human peripheral blood was diluted with warm (37°C) phosphate-buffered saline (PBS, Biochrom, Germany) before being carefully layered over Ficoll Paque Plus (Amersham Biosciences, Sweden). After centrifugation at 350 g for 30 min without brake, the monocyte-enriched hematopoietic precursors were carefully collected at the interface between PBS and Ficoll Paque solution. Cells were subsequently counted and resuspended in AIM V® Serum Free Medium (Life Technologies, USA) at a density of $1x10^6$ cells/ml for direct experiments.

Human Macrophage cells MV-4-11 (ATCC® CRL-9591™) were cultured in DMEM supplemented with 10% FCS at 37°C and 5% CO_2. Growth medium

was renewed every 2 to 3 days. For subculturing, fresh medium was added or replaced to maintain a cell concentration between $1x10^5$ and $1x10^6$ cells/ml.

3.2.8. LDH and WST-1 assay

HS-27 cells were used to assess the cytotoxicity of electrospun NM based on a procedure adapted from the ISO10993-5 standard test method. Briefly, $6cm^2$ of different NM (Cc/Glt NM or Glt NM) were incubated in 1mL DMEM without serum at 37±1°C for 72±2 h to obtain sample extracts. Then, conditioned medium of the nanofibrous mat (CM- NM) were prepared by mixing sample extracts with an appropriate amount of cultured medium (DMEM supplemented with 10% FCS) for cytotoxicity assay[183]. HS-27 were trypsinized when 80%-90% confluency was reached and seeded into a 96-well plate at a density of $5x10^3$ cells/well. 24 hours after cell seeding, the supernatant was replaced by either CM-Cc/Glt NM or CM-Glt NM. A mixture of equal amounts of DMEM and culture medium was used as control. The LDH (lactate dehydrogenase) and WST-1 (Water-soluble tetrazolium-1) assay were performed every day according to manufacturer's instructions (Roche, Germany), data was collected by Mithras LB940 Microplate Reader (Berthold Technologies, Germany).

3.2.9. Live and dead assay

HS-27 was seeded in a 6-well plate at a density of $1x10^5$ cells/well. 24 hours after cell seeding, the supernatant was replaced by CM-Cc/Glt NM, CM-Glt NM or control medium, respecitvely. The cells were incubated at 37°C and 5% CO_2 for 5 days. For the fluorescence based dual-color cell LIVE/DEAD assay, calcein AM (green, Ex/Em=494/517 nm) and ethidium homodimer-1 (red, Ex/Em=528/617 nm) were added to the culture every other day according to the manufacturer's instructions (Invitrogen, Germany). Images were taken via fluorescent microscope and analyzed via Axiovision software (Carl Zeiss, Germany).

3.2.10. Cell visualization on the scaffold

HS-27 were trypsinized and re-suspended in DMEM supplemented with 10% FCS at a concentration of $1x10^6$ cells/ml. Disk shaped scaffolds were prepared by sampling the electrospun NM using biopunch (φ=6mm, Acuderm, USA). The scaffolds (n=5) and cell suspension (10ml) were transferred into a 15ml falcon tube (Greiner CELLSTAR, USA), which was fixed on a tube rotator (MACS Miltenyi Biotech, Germany) and incubated at 37°C and 5% CO_2. On day 7 and day 14, samples (n=5) were harvested. For live cell imaging, mitochondria were stained by MitoTracker® Deep Red FM (Life Technologies, USA) and nuclei were counter stained using NucBlue® Live Ready Probes (blue, Ex/Em= 360/460 nm, Life Technologies, USA) according to the manufacturer's instructions. Before fluorescent microscopy, samples were cut into smaller pieces and were fixed between two glass slides (SuperFrost Ultra Plus, Thermo Scientific, Germany).

3.2.11. Fibroblasts in vitro wound healing assay

HS-27 cells were seeded at $5x10^5$ cells/ml in culture inserts (Ibidi, Germany). Calcein AM was applied to better visualize and track cells as described above. Once cells reached confluency, the insert was removed and the medium was replaced by CM-Cc/Glt NM, CM-Glt NM or control medium, respectively. After 36 hours, images were taken and cell migration in the open wound area was quantified (Adobe Photoshop CS5, Adobe Systems, USA). Results were expressed as the percentage of the open wound compared to the original wound.

3.2.12. Fibroblasts cytokine profile array

From this and the following *in vitro* assay, AIM V® Serum Free Medium, instead of the cultured medium (DMEM supplemented with 10% FCS), was mixed with its extracts of electrospun NM (see LDH and WST-1 assay) to obtain CM-Cc/Glt NM or CM-Glt NM. They were then added to replace the

medium from a 6-well plate with pre-seeded (24h before) HS-27 ($1x10^5$ cells/well), fresh AIM V® Serum Free Medium was used as control. Subsequently, the cell cultures were incubated at 37°C and 5% CO_2 for 5 days, before supernatants were collected and subjected to semi-quantitative cytokine analysis using Human XL Proteome Profiler Array Kit (R&D Systems, USA) according to the manufacturer's instructions. In brief, 102 different cytokines were analyzed in duplicates using spotted capture antibodies, followed by incubation with detection antibodies and chemiluminescent visualization. Membranes were finally exposed to X-ray films for 10 min. The mean (blank corrected, n = 2) pixel density was calculated using Image J software.

3.2.13. Quantified ELISA assay for Dkk-1, SDF-1 α, MCP-1 and TSP-1

Cultured supernatants from above mentioned cytokine array experiments were sampled and analyzed by Quantikine ELISA (R&D Systems, USA) for Dickkopf-related protein-1(Dkk-1), Stromal cell derived factor 1α (SDF-1α), Monocyte chemoattractant protein-1 (MCP1) and Thrombospondin-1 (TSP-1) according to the manufacturer's instructions. Briefly, supernatants were added to 96-well plates coated with specific monoclonal antibodies of interest, incubated at room temperature for 2 h before the washing steps. Respective cytokine specific, luciferase-conjugated antibodies were added to each well, incubated for 2 h at room temperature and washed again. Substrate solution was then added, incubated for 20 min in the dark, followed by addition of 50 µL stop solution. The concentrations of cytokines were determined by measuring absorbance at 450 nm using a microplate reader (Mithras LB940, Berthold Technologies, Germany) and plotting a standard curve.

3.2.14. β-catenin immunofluorescence and fibroblast migration

HS-27 cells were seeded at $5x10^5$ cells/ml in culture inserts (Ibidi, Germany). Once cells reached confluency, the insert was removed and the medium was

replaced by CM-Cc/Glt NM, CM-Glt NM or control medium respectively for 24 hours. Cells were then fixed by 4% formaldehyde for 20 minutes. Samples were washed twice and treated with 400 µL blocking buffer (5% goat serum in PBS) for 45 minutes. Then, primary antibody for β-catenin (D10A8 XP® Rabbit mAb, Cell signaling, USA) were added and incubatet overnight at 4°C. Next, samples were treated with fluorochrome-conjugated secondary antibody (Alexa Fluor 568 goat anti-rabbit IgG, Invitrogen, Germany) for 1–2 hr at room temperature in the dark. After the washing step, slides were mounted and images were recordes by fluorescent microscopy with Axiovision software (Carl Zeiss, Germany).

3.2.15. Dkk-1 mediated fibroblast migration

HS-27 migration assay was measured with CytoselectTM 24-well cell migration kit (8µm, Colorimetric Format, Cell Biolabs, USA) according to the manufacturer's protocol. Briefly, HS-27 was seeded in a 6 well plate at $1x10^5$ cells/well and were treated with CM-Cc/Glt NM or CM-Glt NM respectively until near confluency. For each assay, 500µL supernatant of each well were added to the corresponding lower well of the migration plate. Additionally, Dkk-1 was inhibited via addition of either 10 µg/mL Human Dkk-1 antibody (R&D Systems, USA) or 1µM WAY 262611(abcam, UK), a small molecule inhibitor of Dkk-1, to the supernatant. In the next step, 300µL HS-27 were added to the upper insert at $1x10^6$ cells/ml. After 24 h of incubation, the inserts were taken out and the non-migratory cells were removed by gently swabbing the interior of the inserts. Inserts were then transferred to a clean well and each was treated for 10 minutes with staining solution followed by extraction solution. Finally, 100µl of each reaction solution was transferred to a well of a 96-well plate and measured in a plate reader at 560 nm. For a better visual investigation of fibroblasts migration, the cells were also examined under a light microscope.

3.2.16. MCP-1 mediated PBMC and macrophage chemotaxis

The PBMC and macrophage chemotaxis assay was also based on Cytoselect^{TM} 24-well cell migration kit (8µm, Colorimetric Format, Cell Biolabs, USA) according to the manufacturer's protocol as described in aforesaid HS-27 migration assay, only that in the lower well, MCP-1 was selectively inhibited by adding 5 µg/ml MCP-1 blocking antibody (abcam, UK) to the supernatant. Similarly, 300µL newly prepared PBMCs or MV-4-11 (see cell culture and harvesting) were added to the upper insert at 1x10^{6} cells/ml and incubated for 12 h for the final measurement in a plate reader at 560 nm. For a better visualization of PBMCs and non-adherent MV-4-11 chemotaxis, cells were also observed either via light microscopy(PBMC) or an fluorescent microscopy (MV-4-11) using fluorescence based Two-color LIVE/DEAD staining supplemented with NucBlue® (Life Technologies, USA) to counter stain the cell nucleus.

3.2.17. Animal housing conditions

All protocols of animal studies were approved by the Institutional Review Board of the Animal Care and Use Committee of Shanghai Jiaotong University. 12 Sprague-Dawley rats (Department of Laboratory Animal Science, Shanghai Jiaotong University, China) weighting 250–300g were used in this study. They were randomly assigned to three groups (n = 4 /group) and were given food and water ad libitum.

3.2.18. Surgical procedure for acute wound animal model

On the day of surgery (d0), rats were shaved closely on the dorsum under anaesthesia (ketamine 100mg/kg, I.P.) and operations were performed aseptically with a hole-punch creating two round, full-thickness skin defects (Φ = 6mm) on the dorsal midline in each animal. Next, animals from different groups were subjected to different treatments: (1) received Cc/Glt NM; (2) received pure Glt NM of the same size; (3) received no treatment (control group). All wounds were fixed by sterile Medical Infusion Fixation Paster

(RENHE, China). Fresh nanofibrous membranes were reapplied every other day while in the control group, only Fixation Paster was changed. On day 15, animals were euthanized. The reconstituted skin was cut to the control depth determined as the layer of panniculus carnosus and harvested including surrounding skin area of 0.5 cm. Samples were fixed with 10% formaldehyde, embedded in paraffin, and then sectioned to obtain 5μm-thick paraffin sections for histological and immunohistochemical studies.

3.2.19. Wound closure analysis

All wounds were photographed from a standard height at same intervals over a period of 15 days. Three independent, blinded observers evaluated the wound appearances and measured the wound size from the digital photographs through pixel-based process of calibration, tracing, and area calculation using Adobe Photoshop software (CS5, Adobe Systems, USA) [184]. The percentage of wound healing is defined as the quotient of the initial wound area and the wound area after a fixed time interval in percent.

3.2.20. Histological analysis

To harvest tissue samples, an area of 8 mm in diameter including the complete epithelia margins was excised and embedded into paraffin blocks. Serial sections (5-μm) were performed until reaching the central portion of the wound. These sections were stained with hematoxylin and eosin for anaylsis.

3.2.21. Collagen content analysis

For collagen detection, sections were stained with Picro-Sirius red (IHC World, USA) following the manufacturer's protocol. Briefly, de-paraffinized sections were first stained with Weigert's haematoxylin for nuclei. After the wash step, slides were stained by Picro-Sirius red for 1 h and were washed in two changes of acidified water followed by dehydration and mounting. Fluorescence and polarized (orthogonal polarizing) microscopy were applied to evaluate collagen content and quality [185,186].

3.2.22. Macrophage immunohistochemistry

Macrophage infiltration was detected by immunohistochemistry, which was performed using a standard technique with slight modification [187]. In brief, newly prepared paraffin sections were dried overnight at 37°C and then at 57°C for 8 h. After de-paraffinization in xylene and rehydration in a graded series of ethanol, the sections were placed in a 10 mmol/L sodium citrate buffer and boiled for 15 minutes for antigen retrieval. Sections were then incubated for 10 minutes with 3% H_2O_2 (Carl Roth, Germany) to inactivate endogenous peroxidase, followed by a blocking step with 10% goat serum for 1 h. Subsequently, slides were incubated with monoclonal antibodies against macrophage marker CD68/ED1 (abcam, UK) and incubations were carried out overnight at 4°C. After that, sections were incubated with a peroxidase coupled goat anti-mouse antibody for 1 h, and the peroxidase was disclosed using the DAB Substrate Kit (Thermo Fisher Scientific, Germany). The sections were later counterstained with Mayer's haematoxylin and mounted. Images were taken with an AxioCam camera microscope (PrimoVert, Carl Zeiss, Germany). All histological and immunochemical analyses were independently and blindly assessed by three observers and images presented were representative of all replicates.

3.2.23. Statistical analysis

Data were collected and expressed as means ± standard deviation (SD). Depending on the number of groups and normal distribution of the results, statistical analysis was performed using Student's t test, one-way ANOVA with Tukey post hoc test or non-parametric Kruskal-Wallis H test (GraphPad Prism5.0, USA). Statistical differences are indicated in the figures by asterisks dependant on the p-value: $p<0.01$*, $p<0.001$** and $p<0.0001$***. All *in vitro* assays were conducted in at least duplicate per experiment and replicated in three separate experiments.

4. RESULTS

4.1. Material characterization

4.1.1. Morphology of electrospun nanofibrous mat

Addition of curcumin to the electrospun nanofibrous mats (NM) was macroscopically evident through a change in colour (Figure 7A).

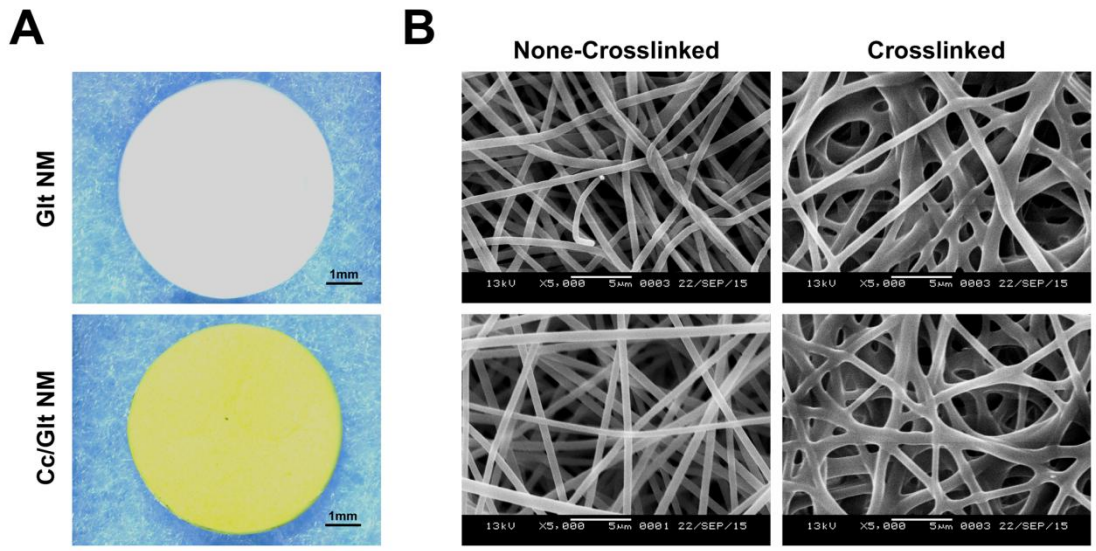

Figure 7: Morphology. (A) Gross view of the electrospun nanofibrous mat with color change due to curcumin incorporation (left). (B) Representative SEM images (5,000x) of electrospun nanofibers. Both crosslinked (lower row) and non-crosslinked (upper row) nanofibers exhibited smooth fiber matrix. Further, curcumin loaded nanofibers (right column) existed without any visible aggregates, suggesting a nanosolid dispersion derived from a successful electrospinning process without phase separation.

To evaluate the extent to which curcumin was nano-formulated, we examined the morphology of the NMs by scanning electron microscopy (SEM, Figure 7B). The surface of both crosslinked and non-crosslinked fibers exhibited smooth surface morphology without beading or visible aggregates separating from the fiber matrix. Moreover, the arrangement of these non-woven fibers mimicked the natural structure of ECM.

4.1.2. Electrospinning nanoformulates curcumin

Under X-ray diffraction (XRD) spectroscopy, pure curcumin exhibited sharp peaks in the range of 10°-30°, within which two characteristic peaks at diffraction angles 2θ of 8.78° and 17.16°, as well as various peaks of lower intensity were observed, implying a high crystalline structure. In the case of blended nanofibrous mats, the discrete peaks of curcumin disappeared in the spectrum, revealing that curcumin existed as amorphous nanosolid dispersion instead of crystalline material in the electrospun nanofiber (Figure 8).

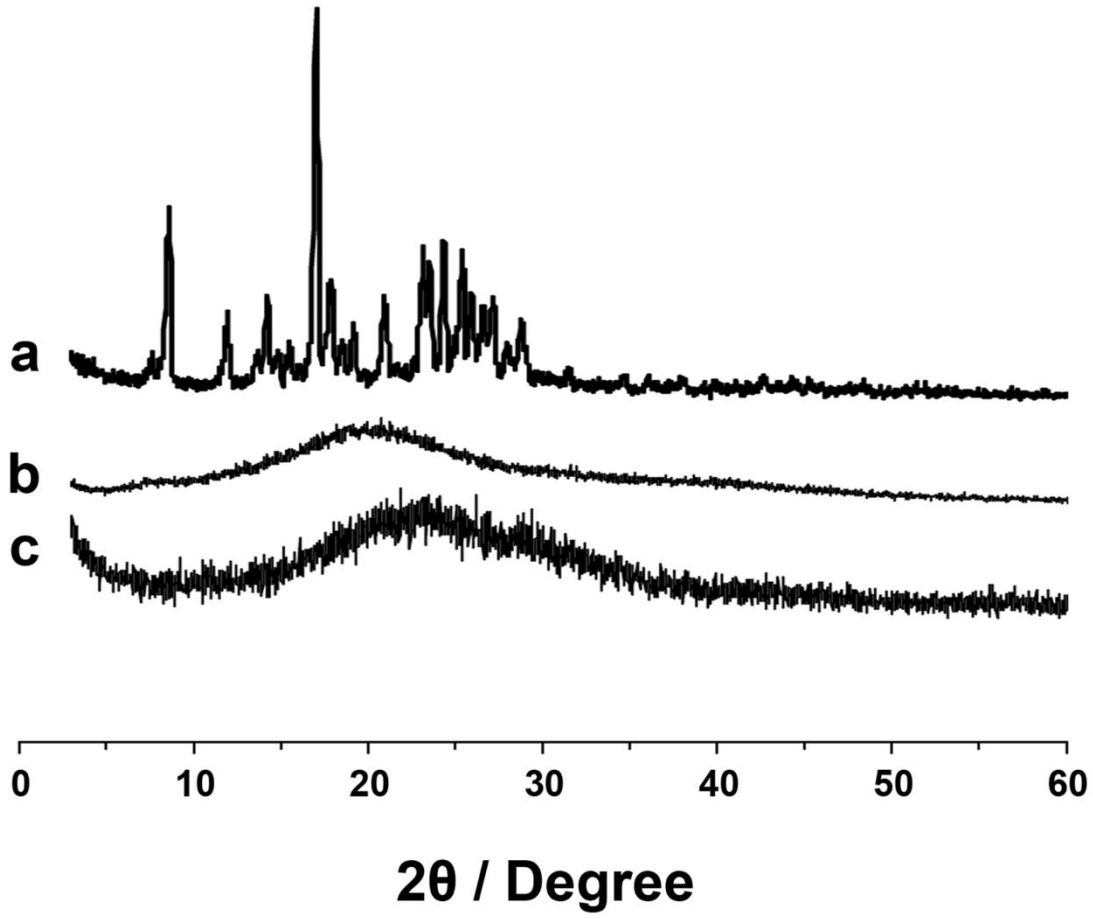

Figure 8: Curcumin nanoformulation. The X-ray diffraction spectrum of pure curcumin in the crystalline form exhibited numerous notable peaks (a), while the spectrum of amorphous gelatin with disordered molecular orientation and polymer arrangement was completely devoid of any diffraction peak (b). However, when curcumin was optimally nanoformulated into the gelatin nanofiber through electrospinning, it was completely converted into the amorphous state manifested by the disappearance of its original discrete peaks from the spectrum of the blended nanofibers (c).

4.1.3. Curcumin incorporation in nanofiber

We further scrutinized the fibers with Fourier transform infrared (FTIR) spectrometry for an indication of the presence of curcumin in the fibers (Figure 9).

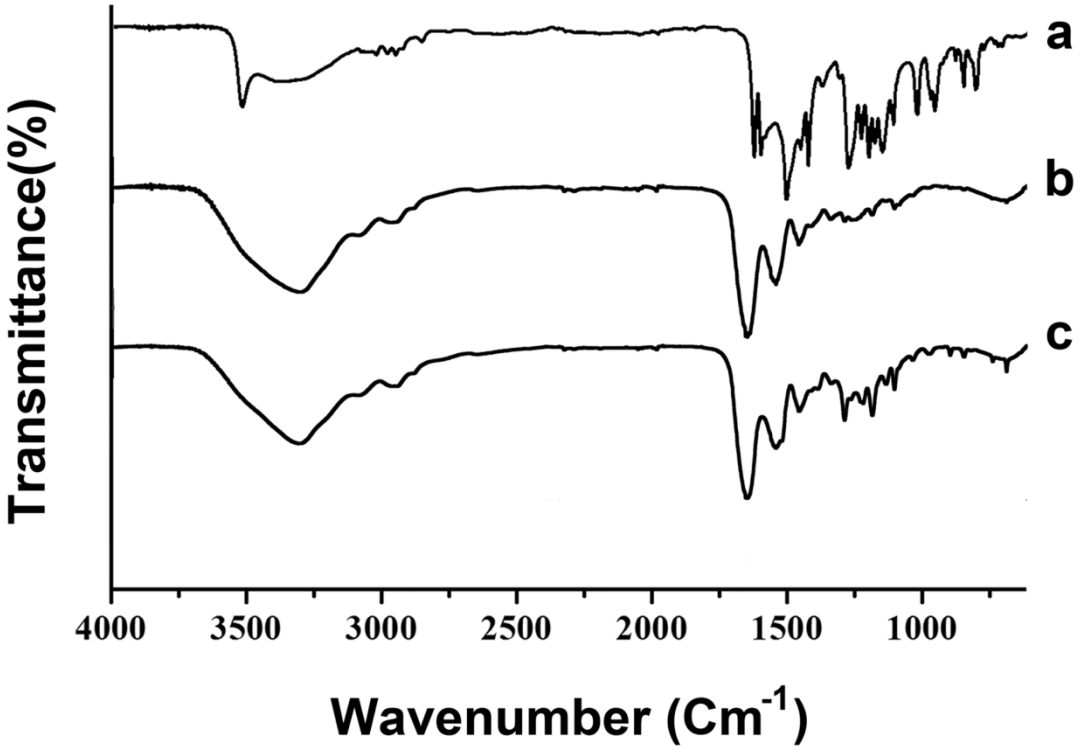

Figure 9: Curcumin incorporation in gelatin nanofiber. FTIR spectrum of pure curcumin (a) showed a dominant peak of 1500 cm^{-1} and the band at 1293 cm^{-1} while the spectrum of gelatin (b) exhibited typical absorption bands at 3302 cm^{-1}, 1643cm^{-1} and 1540 cm^{-1}. FTIR spectrum of an optimized curcumin formulation through electrospinning (c), however, show both characteristics peak (1293 cm^{-1}) and band (3302 cm^{-1}) of curcumin and gelatin, indicating a successful incorporation of curcumin into gelatin nanofibers.

For pure curcumin, the most dominant peak appears at 1500 cm^{-1}, corresponding to mixed vibrations of v(C=O), δ(CCC), δ(CC=O) and aromatic v(CC), v(CCH); the band at 1293 cm^{-1} belongs to the pure in-plane C-H vibrations of aromatic rings (Figure 9 a). The spectrum of gelatin (Figure 9 b) showed typical absorption bands at 3302 cm^{-1} (N-H stretching vibration), 1643cm^{-1} (C=O stretch) and 1540 cm^{-1} (N-H bend and C-H stretch). The spectrum of curcumin-gelatin blended nanofibers (Figure 9 c) exhibited features comprising composite characteristic bands of both curcumin and

gelatin, such as the N-H stretching band (3302 cm^{-1}) from gelatin; the O-H absorption band (3510 cm^{-1}) of curcumin disappeared while its aromatic signature (1293 cm^{-1}) was apparent, indicating a successful incorporation of curcumin into gelatin nanofibers and interactions between both components.

4.1.4. Curcumin release profile

Curcumin release from the blended nanofibrous mat was analyzed and displayed in Figure 10.

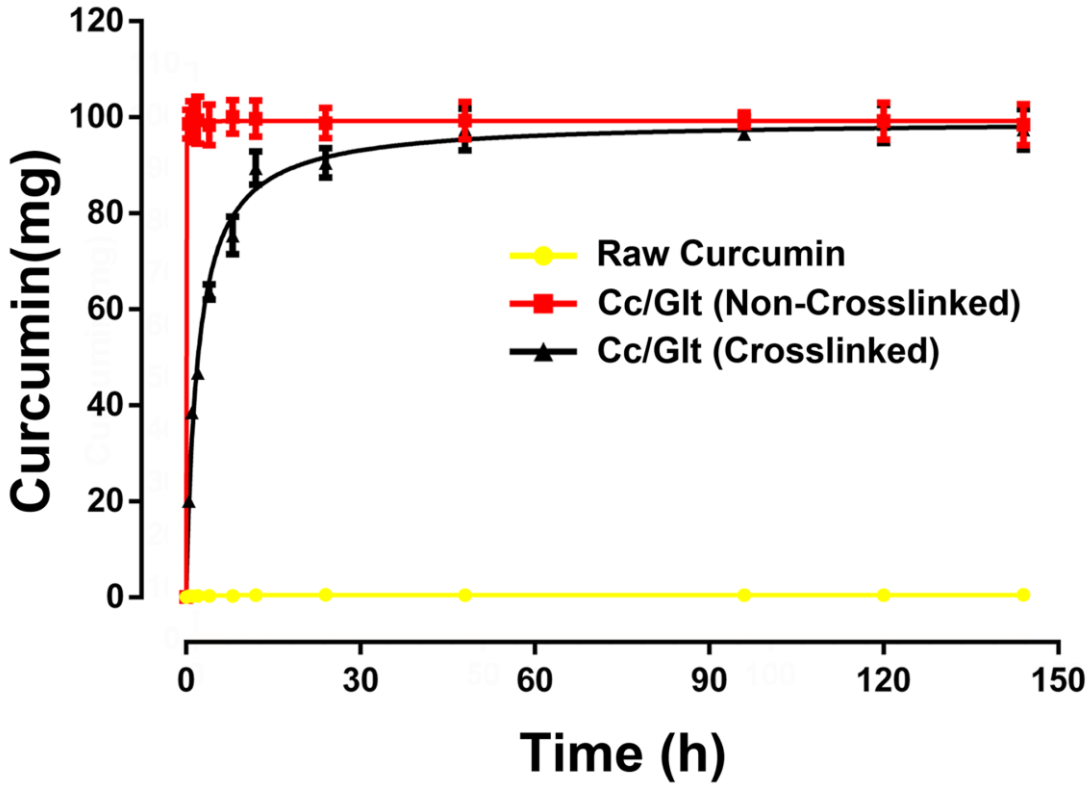

Figure 10: Curcumin release *in vitro*. The release profiles of the pure curcumin and Cc/Glt NM demonstrated a marked improvement of the dissolution rate of curcumin from electrospun blended nanofiber compared to that of the pure drug (yellow). Additional crosslinking further improved the release kinetics (black), avoiding initial burst release of curcumin from non-crosslinked nanofibrous mat (red).

Significant improvement of the dissolution rate and a sustained release pattern were seen in blended nanofibrous membranes compared to that of the raw curcumin, which was almost insoluble in this study. For the crosslinked blended nanofibrous mat, 75.34% and 90.46% of curcumin was released in the

first 8 h and 24 h respectively, and after 120 h, nearly all curcumin was released, whereas at the same time only 0.46% of the drug was freed from raw curcumin particles. It is noteworthy that the as-spun (as-spun fiber means initially electrospun fiber without further processing) nanofibrous mats only released curcumin and collapsed immediately (Figure 10, red curve), characterized by a steep curve that almost vertically ascends and reaches its peak in the initial phase (initial burst release). Therefore, an additional crosslinking process was necessary to achieve agreeable controlled release profiles of the entrapped curcumin from the blended nanofibers.

4.1.5. Tensile mechanical properties of Cc/Glt NM

Except for the therapeutic function of bioactive curcumin released, the mechanical properties of the topically applied electrospun curcumin-gelatin nanofibrous mat are also important for their effect on wound healing. We found that an additional crosslinking process enhanced the tensile strength of the medicated nanofibrous mat. The tensile stress-strain curves of electrospun Cc/Glt NM are shown in Figure 11. Young's modulus of the non-crosslinked fibrous mat was calculated to be 0.367 N cm^{-2}, whereas the crosslinked fibrous mat achieved a Young's modulus of 3.376 N cm^{-2} (****P<0.0001), which correlates with values reported for human skin and artificial skin substrates with structures similar to Integra [180]. This result indicates that crosslinking significantly improved the mechanical properties of the electrospun curcumin-gelatin nanofibrous mat in a way to support possible future use for wound dressing purposes.

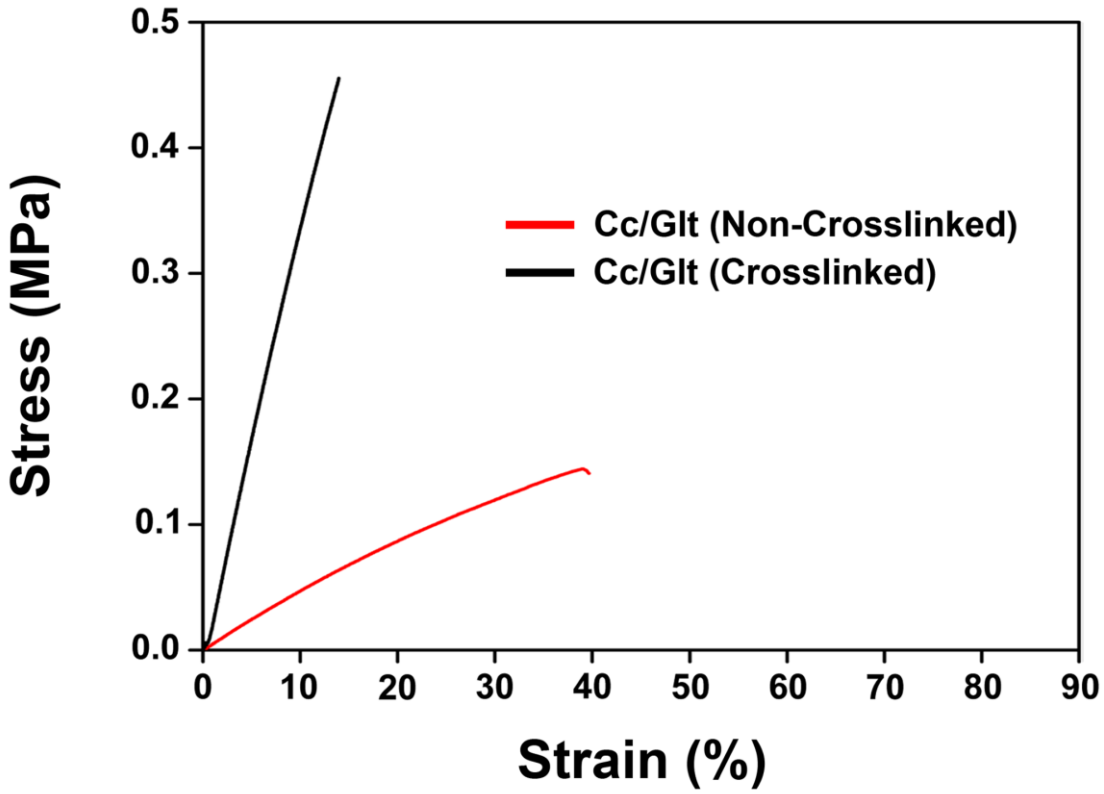

Figure11: Mechanical properties of Cc/Glt NM. Typical stress-strain plots of both crosslinked (black) and non-crosslinked (red) electrospun curcumin gelatin blended nanofibrous mats indicated that the crosslinking process significantly enhanced the mechanical properties of the fabricated nanofibrous mat.

4.2. Biocompatibility and cytotoxicity

4.2.1. Cytotoxicity of electrospun NM *in vitro*

Next curcumin/gelatin nanofibrous mats (Cc/Glt NM) were tested for their biocompatibility and cytotoxicity. Since fibroblast cells are key players in wound healing [188], we chose them for our experiments. Lactate dehydrogenase (LDH) is an oxidative enzyme widely distributed in cell membranes and cytoplasm that is released into the culture medium when the cell membrane loses integrity due to cell injury or death. Therefore, it serves as a reliable means to assess cytotoxicity due to environmental toxic factors. Cells treated with supernatants from NMs with or without curcumin did not show significantly different levels of LDH release, suggesting no cytotoxic

effect of either the NMs or the entrapped curcumin (Figure 12A). However, viability of HS-27 measured by WST-1 assay, which is based on the reductive cleavage of tetrazolium salt to the soluble formazan by a mitochondrial dehydrogenase that is only active in viable cells, demonstrated a significantly increased cell metabolism over time with conditioned medium of curcumin/gelatin nanofibrous mats (CM-Cc/Glt NM) as compared to CM-Glt NM and unconditioned medium, as illustrated in (Figure 12B).

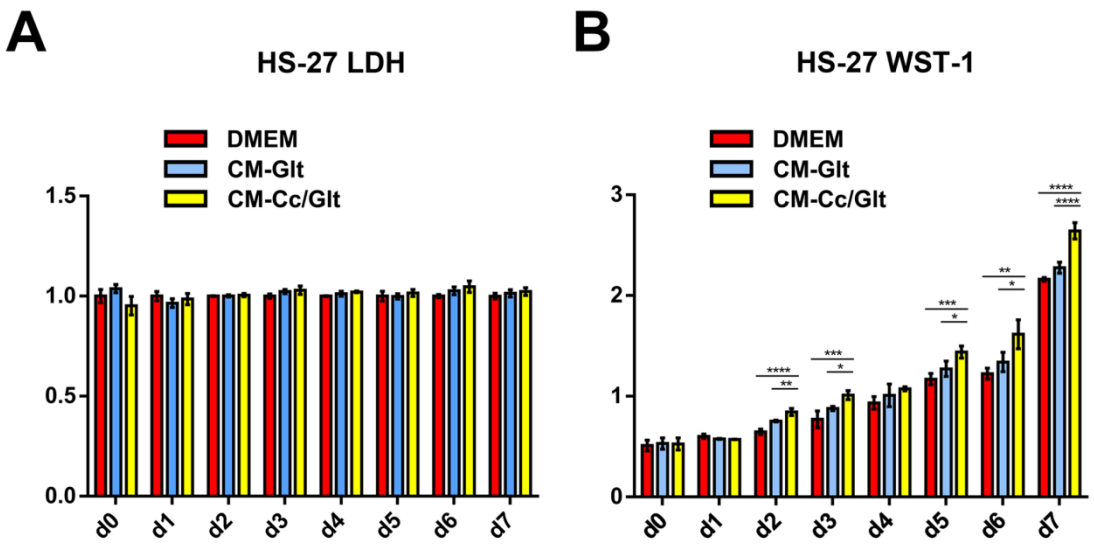

Figure 12: Cytotoxicity of electrospun NM *in vitro*. Human fibroblast cells were treated with conditioned medium of NMs with or without curcumin. Relative cell death was determined by LDH assay where level of LDH release didn't show significant change over time (A). Cell viability (metabolism) quantified by WST-1 assay, on the contrary, was significantly increased over time upon the treatment of conditioned medium with curcumin (B). Both assays verified that either fabricated NMs or the entrapped curcumin had no cytotoxic effect on cells.

4.2.2. Fluorescence-based cytotoxicity *in vitro*

Evaluation of cell viability was performed by fluorescent dual-color LIVE/DEAD assay in a 6-well plate where Calcein-AM as a nonfluorescent, cell-permeant fluorescein derivative is converted by cellular enzymes into cell-impermeant, highly fluorescent calcein that accumulates inside live cells with intact membranes and causes cells to fluoresce green. Ethidium-homodimer-1, on the other hand, enters dead cells with damaged membranes and undergoes a

drastic enhancement of fluorescence upon binding to their DNA causing the nuclei of the dead cells to fluoresce red. Thus the double-staining allows for simultaneous examination of both live and dead cells under fluorescent microscopy shortly after the assay begins[189]. Our data illustrated that cell viability under CM-Cc/Glt NM or CM-Glt NM was well maintained as the overwhelming majority of cells gave off green fluorescence (Calcein-AM) while dead cells, stained red (Ethidium-homodimer-1), were barely found. Moreover, with the lapse of time, it was obvious that cell proliferation under conditioned medium with curcumin was higher than that without curcumin (Figure 13).

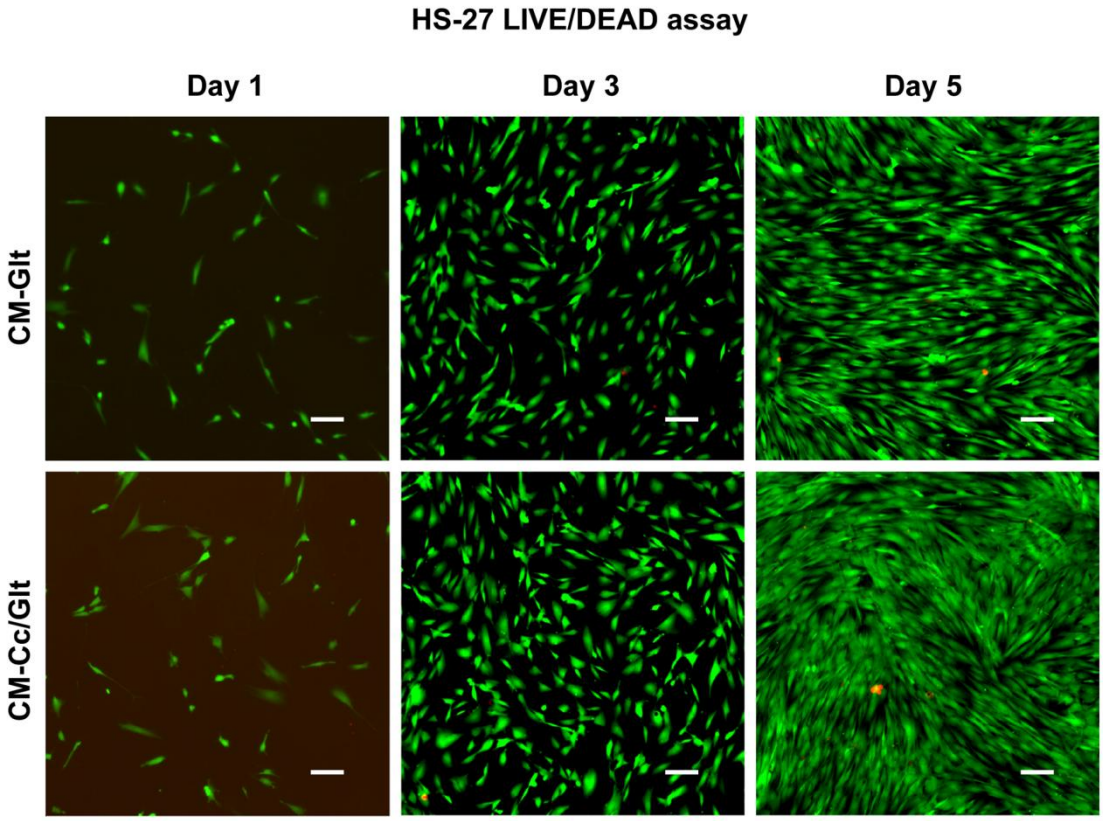

Figure 13: Fluorescence-based cytotoxicity *in vitro*. HS-27 cells were treated with conditioned medium with or without curcumin for 5 days and evaluated by the fluorescent based dual-color LIVE/DEAD (viablility/cytotoxicity) kit *in vitro*. No significant difference was observed from scarcely scattered dead cells (red) between the two groups while the overwhelming live cells (green) displayed enhanced cell proliferation over time upon CM-Cc/Glt NM treatment than those subjected to CM-Glt NM.

4.2.3. Cell visualization on the nanofibrous mat

To evaluate cell adhesion, spreading as well as cell interaction with the nanofibrous membrane, cells and NM were 3D co-cultured in a tube rotator and the cell-scaffold complexes (n=5) were later examined by fluorescent microscopy at a fixed time interval. We used MitoTracker Red, a membrane-permeable dye that localizes to functional mitochondria, to trace active viable cells on the material surface. Since Glt NM may have higher background fluorescence from this dye than Cc/Glt NM, an additional nucleus counterstaining was performed to distinguish cells from underlying scaffold. We demonstrated a direct interaction between cells and scaffolds as well as cell spreading over time, shown in Figure 14, where cells were distributed on the surface of both NMs and exhibited uniformity, as observed by the presence of fluorescent labeled live cells (blue nucleus, red cytoplasm), suggesting agreeable interaction between cells and NMs. Furthermore, co-delivering of curcumin through Cc/Glt NM exhibited substantially more proliferative cells over time: at a certain time point (day7 and day14), cells on Cc/Glt NM appeared to be substantially more than those on simple Glt NM, providing further proof of synergistic effects of both enhanced bioactivity of nano-formulated curcumin and biomimetic NM with an appropriate mechanical property through electrospinning for cellular attachment and activity. Notably, Cc/Glt NM exhibited green auto-fluorescence, another evidence of curcumin (Ex/Em = 420 /470 nm) presence in the nanofibers [190].

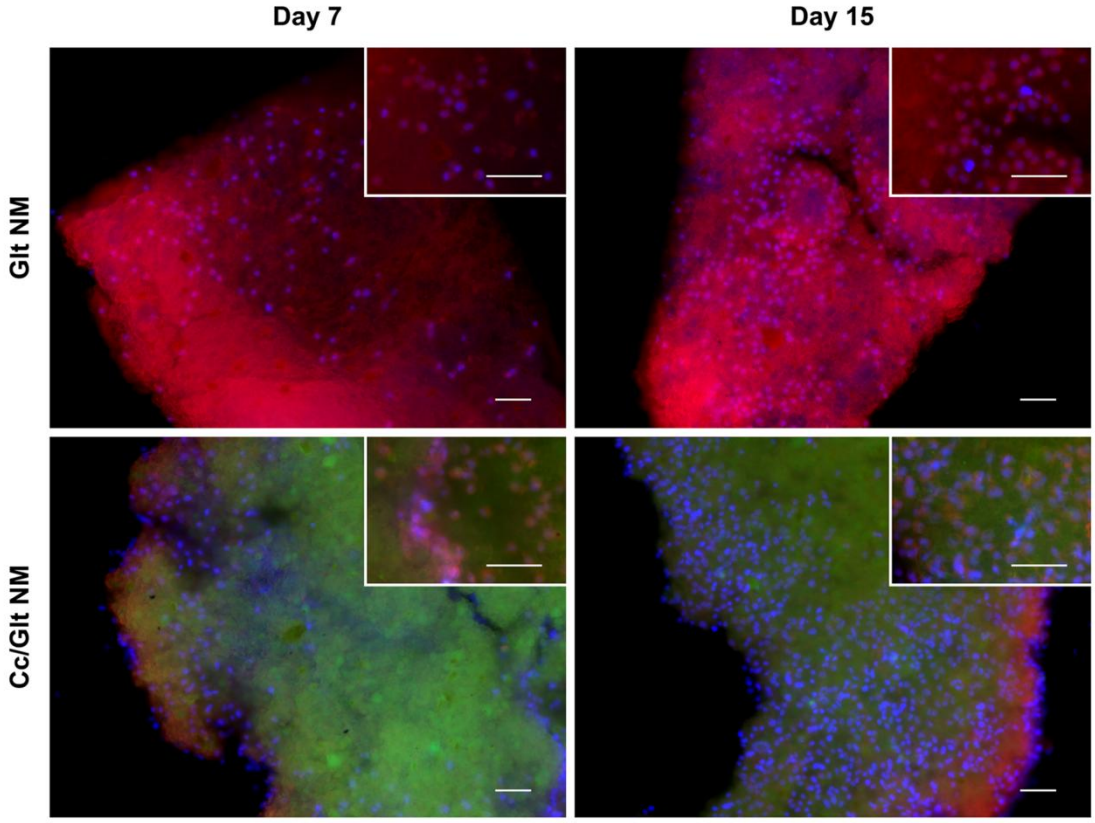

Figure 14: Cell visualization on the nanofibrous mat. Live cells (nucleus/blue, cytoplasm/red) adhere and expand on the surface of the mat overtime. Different from Glt NM (upper row), Cc/Glt NM displayed green autofluorescence due to the presence of curcumin in its nanofibers (lower row). Left and right panels show representative images of cell distribution and growth on the mat at different time points, respectively. Embedded images with higher magnification further illustrate cell morphology and quantity in detail (scale bar, 50µm).

4.3. Curcumin activates fibroblasts

4.3.1. Fibroblasts *in vitro* wound healing

Next, we investigated *in vitro* via scratch assay whether activated curcumin delivered by Cc/Glt NM could influence fibroblasts migration [191]. A gap in the confluent monolayer of HS-27 was generated by lifting a culture-Insert, and the extent of cellular infiltration toward the gap area was assessed 36 hours after the start point (Figure 15, left). We found that 36 hours after scratching, HS-27 subjected to CM-Cc/Glt NM left the open wound only 28.39% of the initial gap area, significantly lower than that of the control group (49.35%, ****P<0.0001)

and that from HS-27 subjected to CM-Glt NM (40.44%, ***P<0.001), indicating the distinct effect of bioactive curcumin in mobilizing fibroblasts (Figure 15, right).

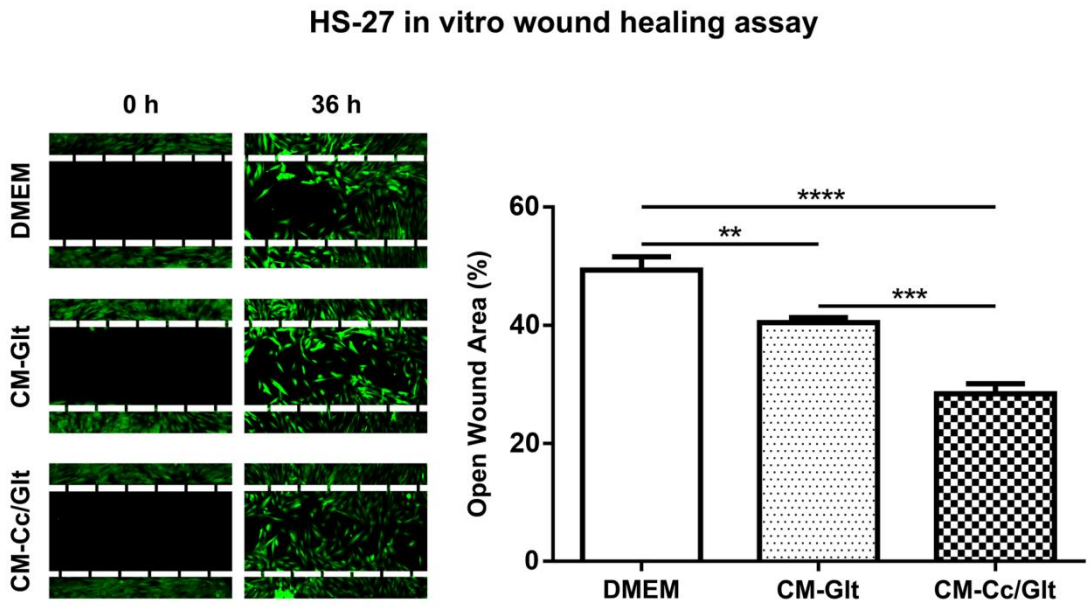

Figure 15: Fibroblast *in vitro* wound healing. HS-27 was plated in ibidi chambers for 24h prior to scratch wounding by removing the chambers. Cells were cultured for an additional 36h and migration potential was evaluated by measuring the movement of cells into the gap. The images are representative samples of images obtained at 0 and 36 h after the scratch.

4.3.2. Fibroblasts cytokine paracrine profile array

To better understand the paracrine mechanism behind the increased migration and proliferation of fibroblasts upon curcumin stimulation, we screened 102 different cytokines, chemokines, and growth factors aided by Human XL Cytokine Array, and identified 6 significantly down regulated proteins upon curcumin stimulation (Figure 16).

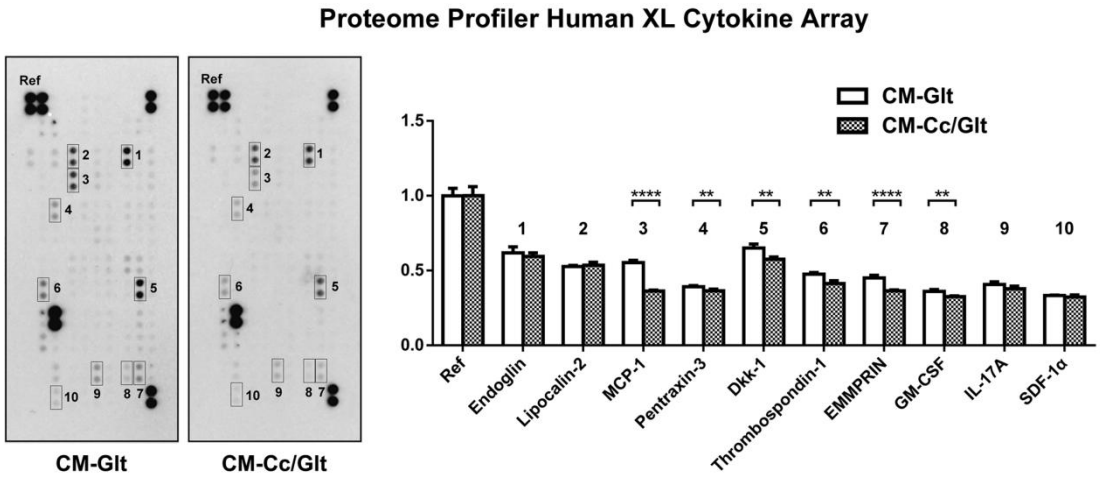

Figure 16: Paracrine profile of fibroblasts under curcumin treatment. The release of bioactive molecules from HS-27 was evaluated by cytokine protein array. Upon curcumin treatment, several bioactive molecules were found significantly down regulated in the conditioned medium with curcumin including MCP-1, Pentraxin-3, Dkk-1, TSP-1, EMMPRIN and GM-CSF. Relative secretion was evaluated as pixel intensity relative to the positive control.

4.3.3. Quantified cytokine expression of Dkk-1, SDF-1α, MCP-1 and TSP-1

After literature review, we selectively double checked the secretion of two of the significantly regulated cytokines, dickkopf-related protein-1(Dkk-1) and stromal cell derived factor 1α (SDF-1α) by ELISA, as recent evidence implies that SDF-1/CXCR4 axis and Wnt signaling pathway play important roles in fibroblast migration[192,193], and Dkk-1 is known as a Wnt antagonist [194,195]. While the decrease in SDF-1α expression could not be verified, secreted Dkk-1 level was indeed found significantly decreased (**$p<0.001$) in fibroblasts subjected to CM-Cc/Glt NM (Figure 17A,B). Except for Dkk-1 and SDF-1α, another two cytokines, namely monocyte chemoattractant protein-1 (MCP-1) and thrombospondin-1 (TSP-1), were also noticeably down-regulated in the cytokine array assay described above. Both were previously affirmed as essential participants in wound healing with reportedly common effects pertaining to inflammation[196,197,198]. As an immunomodulatory role of

curcumin on wound healing is discussed [199,200], we further investigated if they may be potential players. Again we validated the cytokine expression through ELISA and found that MCP-1 level was indeed significantly down regulated (****p<0.0001) whereas TSP-1 expression remained unchanged when fibroblasts were subjected to CM-Cc/Glt NM (Figure 17C,D).

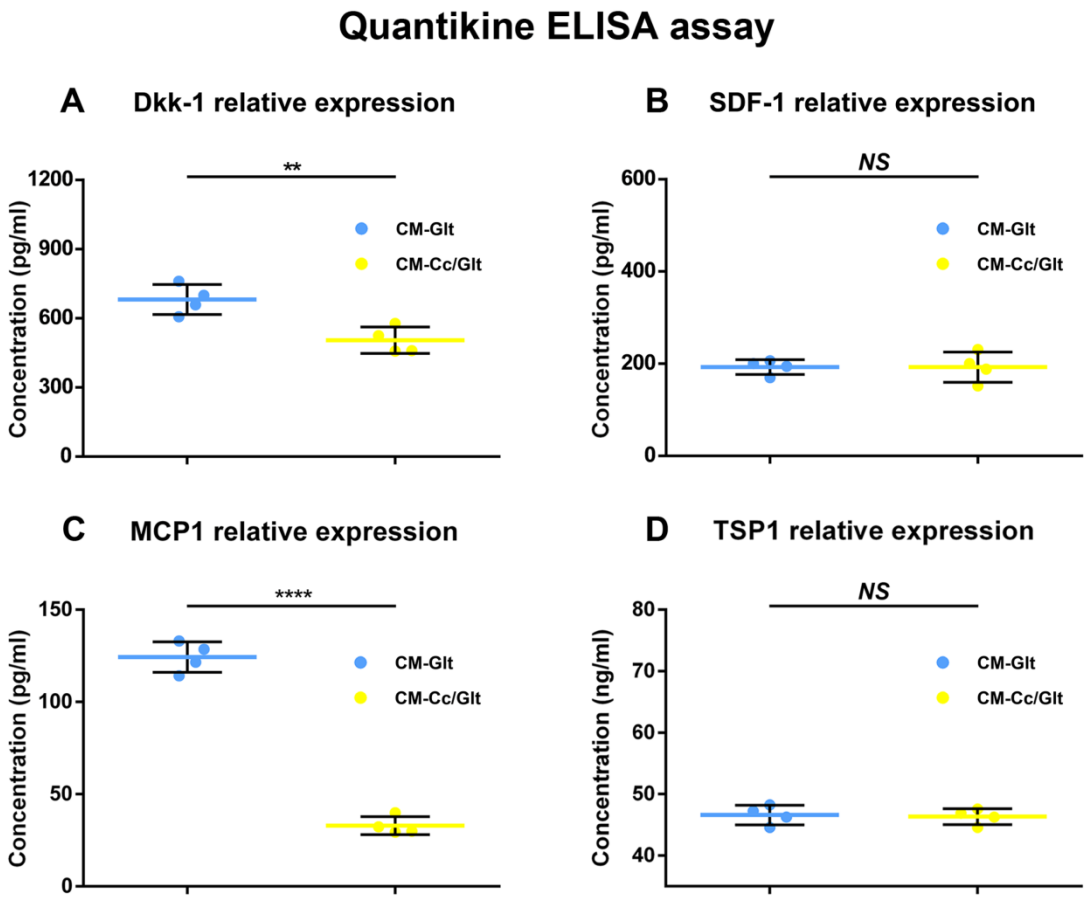

Figure 17: Quantified cytokine expression. Levels of 4 different cytokines, Dkk-1(A), SDF-1(B), MCP-1(C) and TSP-1(D), were analyzed by quantikine ELISA from HS-27 subjected to CM-Cc/Glt NM or CM-Glt NM.

4.4. Dkk-1 mediates curcumin induced fibroblasts mobilization

4.4.1. β-catenin signaling in migrated fibroblasts

In a scratch assay (see 3.3.1) we detected immunofluorescence of β-catenin, the transcriptional co-activator of Wnt signaling pathway[201], and observed

that migrating cells at the leading edge of wounded fibroblast monolayers displayed evidently stronger β-catenin signal (Figure 18, arrow). Treatment with curcumin did result in enhanced fibroblasts migration associated with active β-catenin accumulation (Figure 18, first and second row) which suggested a vital role Dkk-1 plays therein.

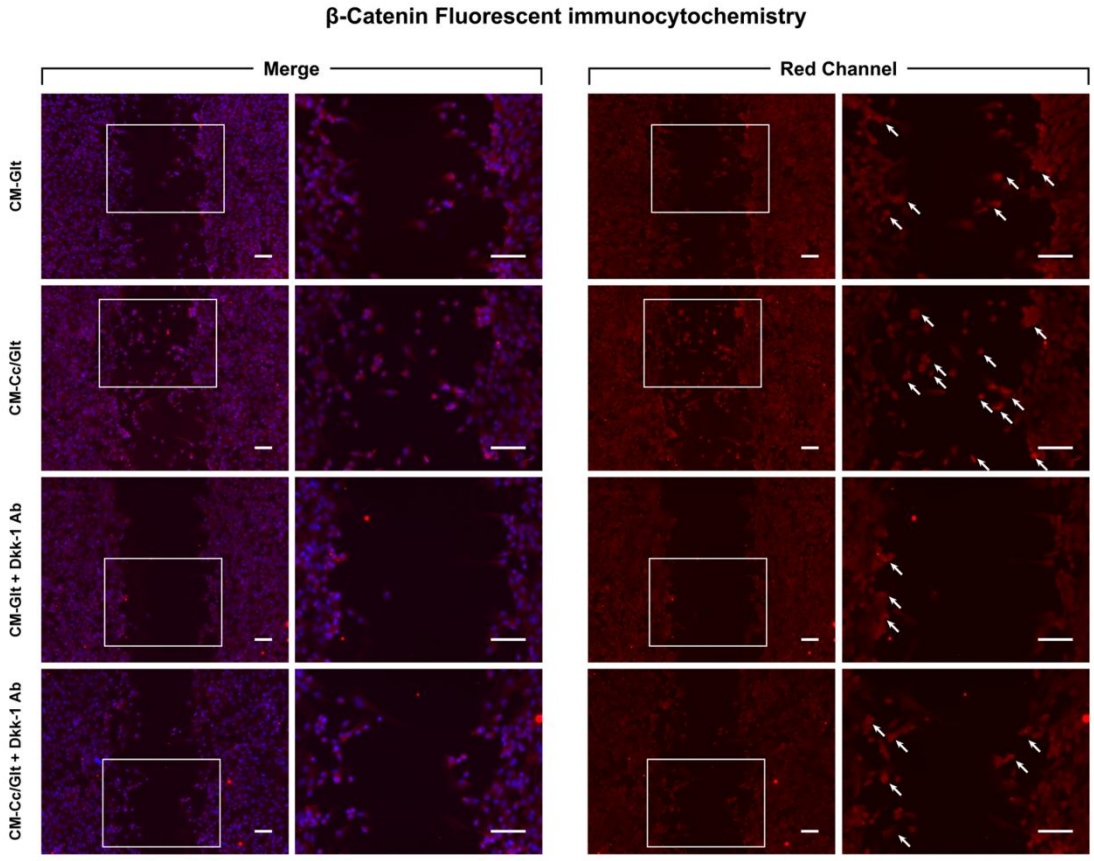

Figure 18: β-catenin signaling in migrated cell. Representative image of fluorescent immunocytochemistry against β-catenin (red) with nuclei counterstain (blue) on fibroblasts that underwent scratch assay 24h post wounding are shown (left panel). A single red channel image (right panel) was extracted to better visualize β-catenin expression, where migrating fibroblasts at the leading edge of the scratch wounding return to an active β-catenin signal (arrow). Moreover, cells subjected to CM-Cc/Glt NM result in enhanced fibroblasts migration associated with active β-catenin accumulation than those of CM-Glt NM (first and second row, arrow). Dkk-1 neutralizing via antibody abrogated such difference but failed to intensify β-catenin expression (third and fourth row, arrow). Scale bar, 100µm.

4.4.2. Dkk-1 mediates fibroblast migration

To further investigate whether curcumin induced fibroblasts migration is

through Dkk-1 regulated Wnt signaling, we performed the following blocking experiments on Dkk-1. Selectively blocking Dkk-1 via antibody abrogated the difference between curcumin treated scratch assays and control, however, failed to intensify β-catenin expression (Figure 18, third and fourth row). These data were further validated by Boyden chamber-based, quantified fibroblasts migration assay using either antibody or WAY262611, a small molecule to inhibit Dkk-1 with high selectivity [202], which led to exceedingly consistent results (Figure 19). Such results indicated that Dkk-1 is at least partially, involved in the regulation of curcumin induced fibroblasts migration, and that a physiological concentration of this cytokine is of critical importance to maintain its biological function.

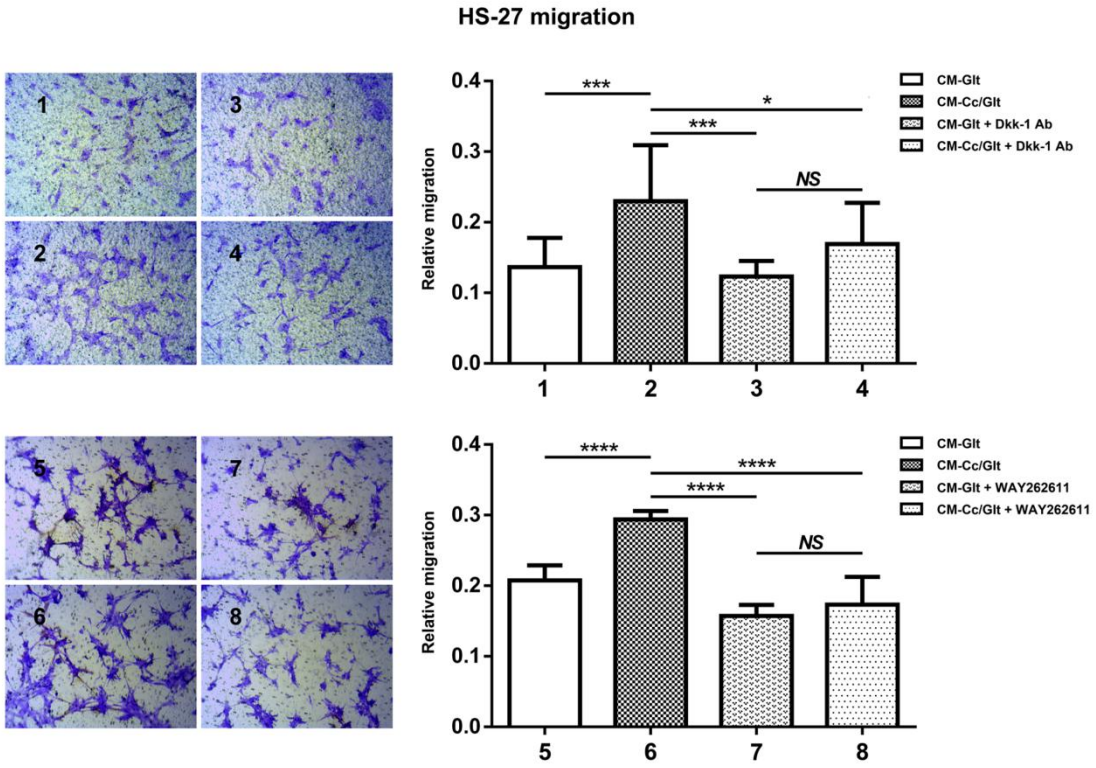

Figure 19: Dkk-1 mediates fibroblast migration. Quantified fibroblasts migration under Dkk-1 mediation was analyzed by Boyden chamber assay using either Dkk-1 antibody (1-4) or WAY262611 (5-8). Curcumin existence led to significant enhanced fibroblast migration (2 to 1 and 6 to 5). Blockade of Dkk-1 annihilated the discrepancy of curcumin induced cell migration by both Dkk-1 antibody (4 to 3) and its small molecule inhibitor (8 to 7).

4.5. MCP-1 mediates curcumin induced anti-inflammation

Because MCP-1 is widely accepted as one of the key chemokines that regulate migration and infiltration of monocytes/macrophages to inflammatory site due to tissue injury or infection[203], we then selectively blocked MCP-1 with antibodies in an *in vitro* functional chemotaxis assay using both peripheral blood mononuclear cells (PBMC) and a macrophage cell line (MV-4-11) to test whether MCP-1 mediates their chemotaxis in the presence of curcumin with the aid of CytoselectTM 24-well cell migration kit.

4.5.1. Curcumin inhibits PBMC chemotaxis

PBMCs in the upper insert indeed demonstrated a significantly diminished migration towards the lower well when the latter contain conditioned medium with curcumin than without curcumin (***P<0.001, Figure 20).

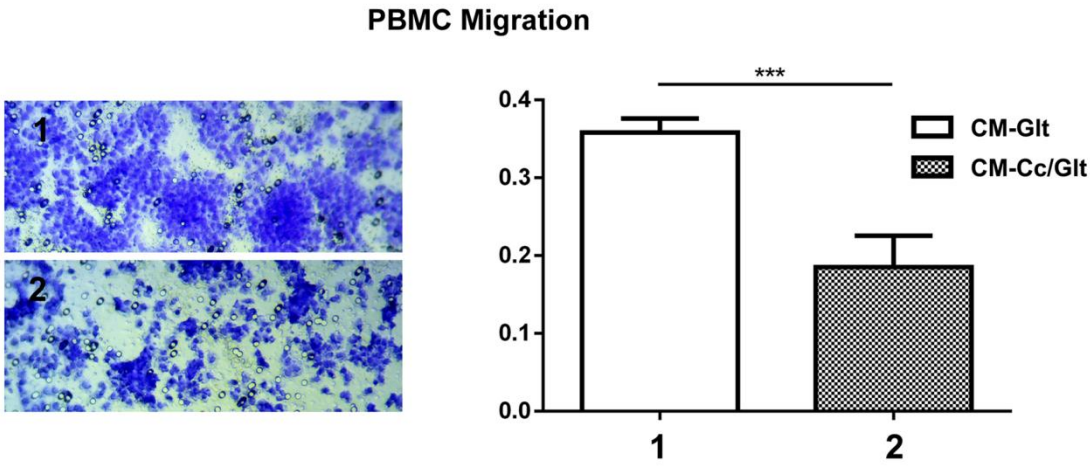

Figure 20: Curcumin inhibits PBMC chemotaxis. Supernatant of fibroblasts subject to conditioned medium with or without curcumin were added to the lower well of the migration plate and served as chemoattractant while newly prepared PBMCs were at the upper insert and were allowed for chemotaxis for 12h. Chemotactic PBMCs crossed to the opposite site of the membrane were stained for a better visualization (left). Chemotaxis was significantly decreased upon curcumin treatment (right, 2 to 1).

4.5.2. Curcumin inhibited macrophage (MV-4-11) chemotaxis is mediated by MCP-1

Similarly, an evident inhibitory effect of curcumin on MV-4-11 chemotaxis was observed as well and furthermore, such effect could be annihilated when exogenous MCP-1 antibody was applied (****P<0.0001, Figure 21).

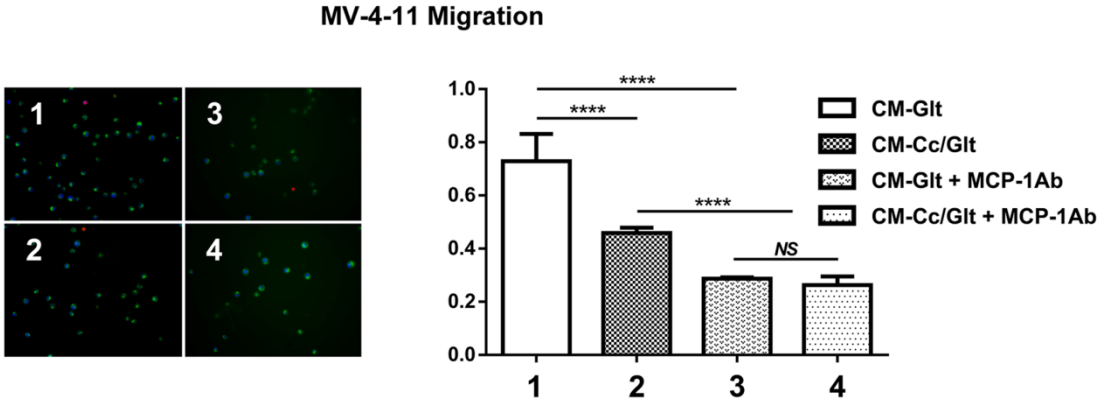

Figure 21: Curcumin inhibited macrophage (MV-4-11) chemotaxis is mediated by MCP-1. Supernatant of fibroblasts subject to conditioned medium with or without curcumin were added to the lower well of the migration plate and served as chemoattractant while macrophages (MV-4-11) were at the upper insert and were allowed for chemotaxis for 12h. Chemotactic MV-4-11 crossed the membrane to the lower well was further fluorescently stained (dead cell/red, alive cell/green and cell nucleus/blue) for a better visualization (left). Existence of curcumin significantly reduced MV-4-11 chemotaxis (right, 2 to 1), however, addition of MCP-1 antibody annihilated the difference (right, 4 to 3).

It should be noted that the elimination of curcumin provoked discrepancy in PBMCs chemotaxis could not likewise be achieved by using MCP-1 antibody in our attempt. This is likely due to the multiple cellular components in the isolated PBMCs from buffy coat [204], which tend to conceal the effect of one single cytokine from a designated cell type. Nevertheless, highly consistent results obtained from both PBMC and macrophage indicated that MCP-1 is a pivotal downstream mediator of curcumin induced anti-inflammatory response manifested by impeded chemotaxis of inflammatory cells, typically macrophages, in the healing process.

4.6. Wound healing *in vivo*

We finally evaluated whether this approach of curcumin nano-formulation by engineering electrospun Cc/Glt NM could be used to enhance wound healing *in vivo*. We used Sprague-Dawley rats and treated full-thickness back-skin wounds of these rats (two wounds per rat, n = 12 rats) with Glt NM, Cc/Glt NM or left untreated (control).

4.6.1. Cc/Glt NM accelerates wound closure *in vivo*

Wound closure was analyzed after 3, 7, 11 or 15 days (Figure 22). Although wounds that received Cc/Glt NM did not differ from wounds treated with Glt NM on early days post wounding (*P<0.05 to control group on day 3), the delivery of curcumin by Cc/Glt NM led to significant faster wound closure at time points of day 7(****P<0.0001), day 11(****P<0.0001) and day 15 (****P<0.0001 to control group and ***P<0.001 to Glt NM group).

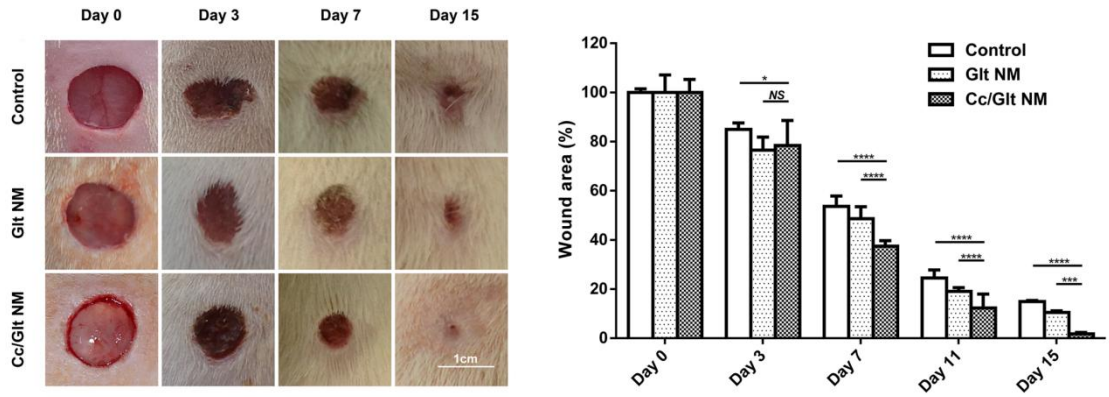

Figure 22: Topical application of Cc/Glt NM accelerates wound closure *in vivo*. A rat model of acute wounds was used to evaluate the healing ability of Cc/Glt NM, in which three groups were tested: wounds treated with Cc/Glt NM, with Glt NM only or without treatment (control). Representative photographs of wound size at each different time point are shown (left). Delivering curcumin from the Cc/Glt NM markedly enhanced wound healing, especially after 7 and more days post wounding (right).

4.6.2. Cc/Glt NM enhances dermal regeneration

Representative wound histology (H&E) for all three groups at the end time point (day 15) showed clear differences in the extent of re-epithelialization and the granulation tissue between wounds subject to Cc/Glt NM and other conditions (Figure 23). Specifically, complete re-epithelialization and differentiated epithelium characterized by well developed epidermis layers were shown in wounds subjected to Cc/Glt NM (Figure 23-c,f,i,3), which clearly differed from less differentiated epidermis in wounds treated with Glt NM (Figure 23-b,e,h,2) or epithelial incompletion accompanied by fibrinous debris in wounds of the control group (Figure 23-a,d,g,1). Moreover, there was noticeable fibroblast proliferation accompanied with markedly increased deposition of connective tissue in the wounds from the Cc/Glt NM treated group in comparison to the other two groups (Figure 23-4,5,6,7,8,9). These results indicated a superior performance of Cc/Glt NM over Glt NM and control in healing the wound.

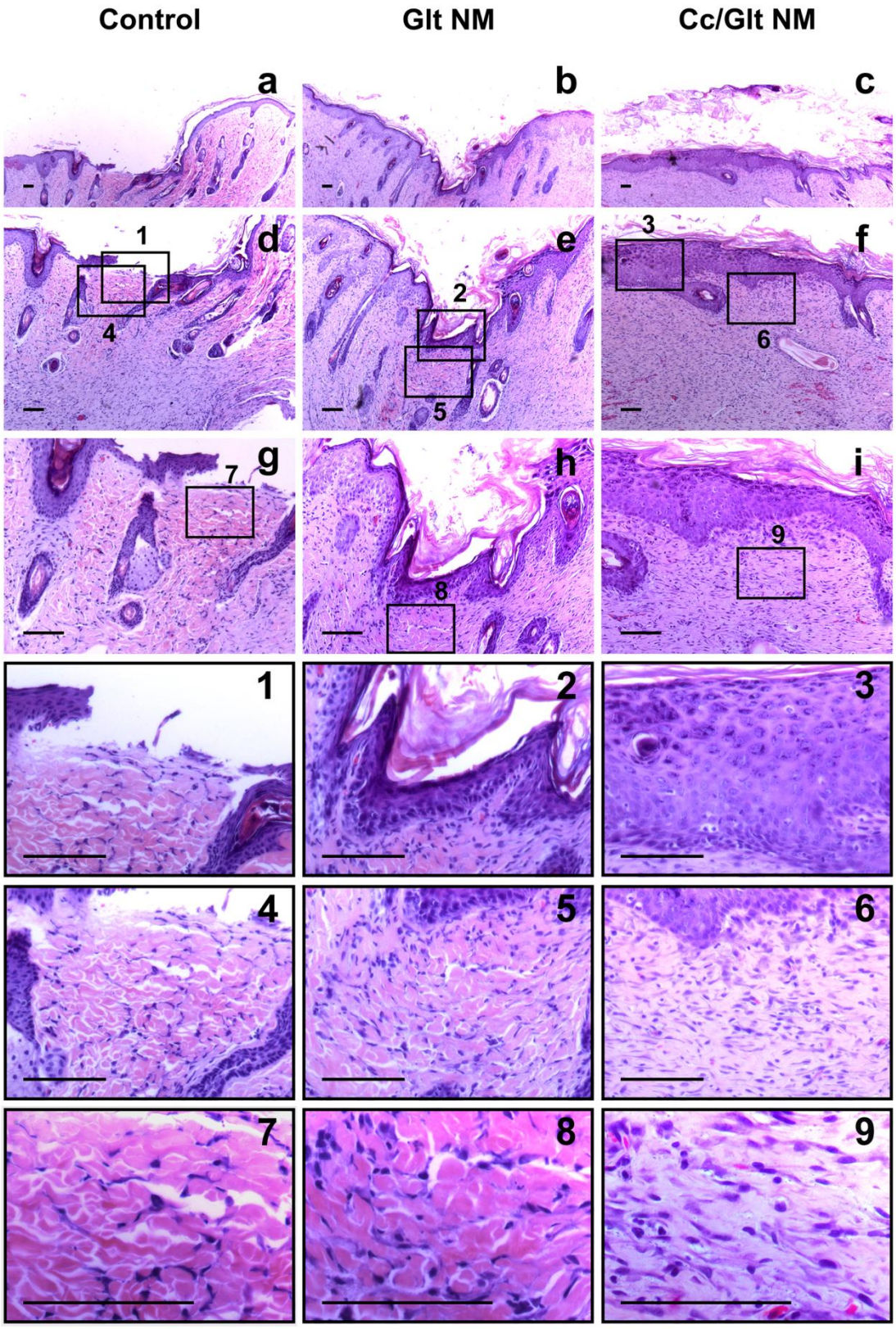

Figure 23: Topical application of Cc/Glt NM enhances dermal regeneration. Histological evaluation of repaired skin stained with H&E 15 days post wounding were performed to

compare rate of re-epithelialization and granulation tissue formation from three different groups: wounds treated with Cc/Glt NM (c,f,i,3,6,9), with Glt NM only (a,d,g,1,4,7) or without treatment (control, b,e,h,2,5,8). Different levels of re-epithelialization and epithelium differentiation are further shown in detail with higher magnified images (1- 3). Also, varying degrees of the maturation of granulation tissue (pink-violet) is shown in detail in images with higher magnification (4-9). Both of which demonstrated the superior performance of Cc/Glt NM over Glt NM and control in improving dermal regeneration to accelerate wound healing *in vivo* (scale bar, 100µm).

4.6.3. Cc/Glt NM enhances collagen deposition

Collagen deposition is another crucial step in granulation tissue formation within the wound bed [205]. Hence, through Picro-sirius red (PSR) staining [185,206], we evaluated the extent to which collagen content and quality differed between the treatments. As shown in Figure 24, merged fluorescence microscopic images demonstrated a clear distinction between cells (green auto-fluorescence) and extracellular collagen fibers (PSR stained red fluorescence, Figure 24-a,b,c). To focus only on collagen deposition, single red channel was used for evaluation (Figure 24-d,e,f), in which Cc/Glt NM treated wounds displayed more collagen deposition, evidenced by higher density and intensity of the PSR signal (Figure 24-f) as compared to wounds subjected to other conditions (Figure 24-d,e). Besides, this collagen was more compact and better interwoven (Figure 24-f), obviously differring from the loose reticular arrangement of collagen formed in Glt NM treated (Figure 24-e) or untreated (Figure 24-d) wounds, indicating formation of a more matured collagen. These findings were further confirmed by polarized microscopy (orthogonal polarizing field), as collagen fibers in Cc/Glt NM treated wounds (Figure 24-i,l) appeared to be not only brighter and thicker than those from wounds receiving Glt NM (Figure 24-h,k) or left untreated (Figure 24-g,j), but also presented well curved and more regularly aligned collagen bundle structures that were clearly in contrast to what was found in wounds from the other two groups (Figure 24-j,k,l, red arrow).

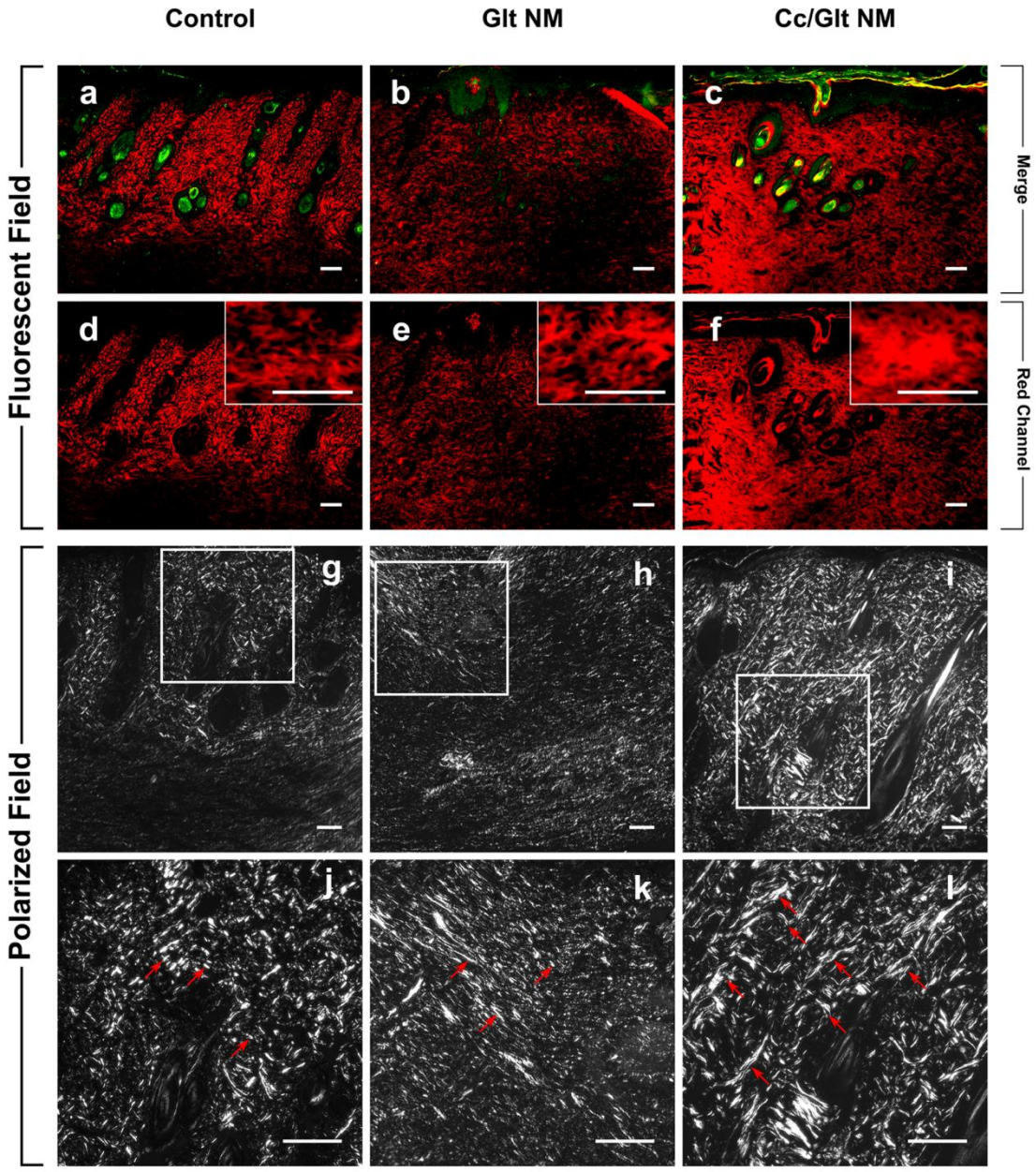

Figure 24: Topical application of Cc/Glt NM enhances collagen deposition. Picrosirius red staining was used to detect the content and quality of newly deposited collagen in the wound bed by fluorescent (a-f) or polarized (g-l) microscopy. Collagen (red) is in clear contrast to cells (autofluorescence green) in the merged image (a-c). To focus only on collagen content, single red channel image (d-f) is used to compare the relative fluorescent intensity, with more details shown in the higher magnification insert (d-f, upper right corner). Quality of collagen bundles was further evaluated by using polarized light to detect bifringence. Wounds subjected to Cc/Glt NM had brighter and thicker collagen with better curved and more regularly aligned collagen bundle structures (l, red arrow) as compared to wounds treated with Glt NM (k, red arrow) or no treatment (j, red arrow). Scale bar: 100µm.

4.6.4. Cc/Glt NM inhibits macrophage infiltration *in vivo*

We have shown *in vitro* that curcumin impeded the chemotaxis of inflammatory cells, typically macrophages, through MCP-1 (See 3.5.2). Presumably, such impediment acts throughout the healing process given that MCP-1 originated from mobilized wound site fibroblasts. We therefore further investigated *in vivo* the interstitial macrophage infiltration on tissue samples harvested at end time point (day 15) in a rat model of acute wounds by CD68/ED1 immunohistochemistry and confirmed a marked decrease of CD68/ED1 positive macrophage influx in interstitial areas in Cc/Glt NM treated wounds as compared to those from Glt NM treated (**P<0.01) or left untreated (control, ***P<0.001) wounds (Figure 25).

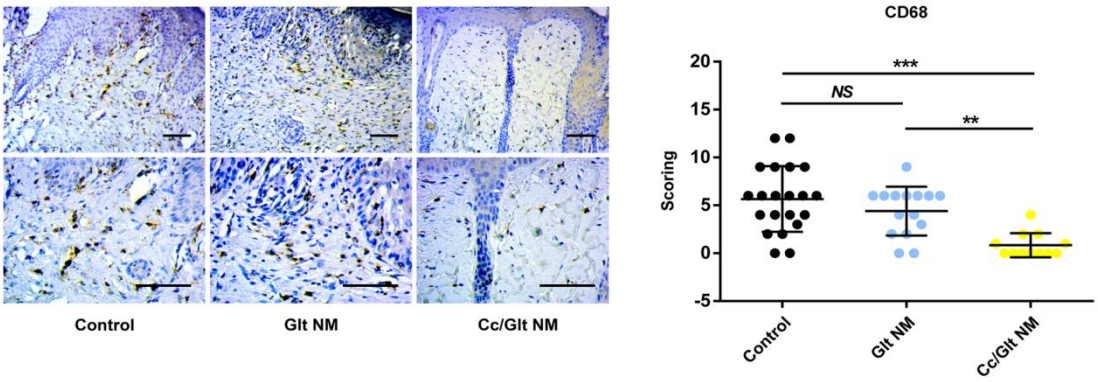

Figure 25: Topical application of Cc/Glt NM inhibits macrophage infiltration *in vivo*. Expression and localization of CD68 (macrophage marker) in wound bed were examined by immunohistochemistry. Representative photographs from different treatmens were shown (left: upper row, low maginification; bottom row, high magnification). Macrophage infiltration was quantified by morphometry (right).

5. DISCUSSION

The human practice of wound care following the study of wound healing has evolved over the ages. Hippocrates (460-377 BC), known as the father of western medicine, used vinegar and wrapped dressings to treat open wounds[207]. The famous "Wound Man" from medieval medicine in Western Europe first appeared in print in *Fasciculus Medicinae* (a collection of medical texts, Venice, 1492) from a German physician (Johannes Kirchheimer), which laid out schematically the various wounds a person might suffer with surrounding notes stating treatments for these various injuries (*In disem biechlin find ma[n] gar ain schöne underwysung un[d] leer wie sich die Cyrurgici oder wundartz gegen ainen jeglichen verwundten menschen, Es sey mit schiessen, howen, stichen…*- "In this booklet one finds a nice instruction and teaching of how the surgeons or wound doctor towards any wounded person, be it with shots, strikes, slashes…")[208,209]. In the east, Traditional Chinese Medicine (TCM) has been practiced for thousands of years and has deeply emphasized an artistic and holistic approach to healing based on the theory of Yin and Yang balance [210]. However, the science of wound healing has had an arduous journey full of contradictions and uncertainty. Galen (120-201 A.D), a prominent physician and surgeon in the Roman empire, was first to recognize that pus from wounds inflicted by the gladiators preceded wound healing, which was unfortunately misinterpreted until 12th-13th century, when his doctrine (pus bonum et laudabile - "good and commendable pus") was challenged and discarded in favor of an antiseptic technique raised by Ugo Borgogni from Bologna [211]. Another interesting example is the present widely accepted concept of moist wound healing, which is in sharp contrast to early practice of wound exposure to allow it to dry [212], had already been empirically noted by Galen even earlier in his time.

The progress in dealing with wounds or defects by surgical intervention, mainly based on reconstructive plastic surgery that began in 1917 when Sir Harold Gillies used skin grafts to treat a British sailor who sustained terrible facial injuries during World War I [213], is undoubtedly a big stride forward toward modern wound therapy. However, surgical techniques such as skin or flap transplantation, except for its many advantages like high-quality repair, shortened therapeutic course and low recurrence rate, always face the problem of donor tissue insufficiency, post-operative flap compromise, host immunological rejection or even loss of function. Concerning the innevitable extra injuries and post-operative complications, non-surgical wound therapy has always been necessary.

As a matter of fact, noninvasive wound therapy especially the utilization of plants and their products has a long history and is still being widely practiced in many cultures [214]. One example from Asia is the use of turmeric. This plant has been used empirically for nearly 4000 years to cleanse wounds and stimulate their recovery [125]. The constant search for novel compounds in western medicine has drawn new attention of the scientific community to this ancient remedy [130]. Curcumin was identified as the principle biologically therapeutic compound of turmeric and was found to possess a wide range of beneficial pharmacological properties including anti-inflammatory, anti-oxidant, anti-microbial and anti-cancer activity [130,148]. Thus, the interest in translating the use of curcumin to the clinic in these areas has increased remarkably over the recent years, leading to a burgeoning number of clinical trials and publications [148].

In the current study we lay the foundation for clinical use of topical curcumin for acceleration of wound healing through electrospinning. We show how bioavailability and application of curcumin for wound treatment can be massively improved by nanoformulation and embedding in blended

nanofibrous mats produced by electrospinning. To be more specific, we demonstrated that through electrospinning, curcumin was successfully formulated as amorphous nanosolid dispersion and favorably released from gelatin based biomimetic nanofibrous mats that could be easily applied topically to experimental wounds. We also show a significant acceleration of wound healing with this approach in a rat model. In vitro analysis of this effect revealed a combined mode of action through modulation of fibroblast migration by DKK-1 mediated Wnt signaling and immunomodulation based on altered MCP-1 expression by topical fibroblasts. Our study provides evidence that current material technology can be used to open a new avenue to translate an ancient Asian remedy for modern wound therapy.

5.1. Electrospun Cc/Glt NM successfully nano-formulates crucmumin and enhances its bioavailability for wound therapy

Although currently there is increasing interest regarding curcumin's pleiotropic activities against human diseases[147] including its ability to modulate wound healing processes [199], clinical use of the drug has been restricted mainly because of the low bioavailability of curcumin due to several of its physicochemical properties, especially its feeble solubility (hydrophobicity) [215], fast aqueous degradation, instability, poor absorption and rapid systemic elimination[151]. These defects are largely in connection with its structure. Chemically, Curcumin (chemical formula: $C_{21}H_{20}O_6$; (1E,6E)-1,7-Bis(4-hydroxy-3-methoxyphenyl)-1,6-heptadiene-3,5-dione) contains polar central and flanking regions being separated by a lipophilic methine segment, which facilitate its intermolecular interaction as well as association with biomolecular targets to participate in various molecular interactions in biological process [216]. However, as a hydrophobic molecule with a log P value (partition coefficient) of around 3.0, it is almost insoluble in water or aqueous medium at neutral pH due to the strong hydrophobicity of its

conjugated alkene chain. Besides, the unavailability of a strong polar group renders it insoluble or sparingly soluble in polar aprotic or polar protic solvents but soluble in some nonpolar solvents with comparable εr values (relative permittivity) such as benzene (2.3), toluene (2.38), diethyl ether (4.3) and chloroform (4.81). The relatively high log P value of curcumin is reflected by its order of solubility in different solvents: acetone >2- butanone > ethyl acetate > methanol > ethanol > 1,2-dichloroethane > 2-propanol > ether > benzene > hexane. It is noteworthy that it does not dissolve well in some aliphathic or alicyclic organic solvents such as hexane and cyclohexane [217]. Interestingly, some studies alleged that curcumin can be dissolved in slightly basic water or aqueous buffer. Several curcumin suppliers also recommend to raise the pH value in aqueous medium to improve its solubility. However, Tønnesen et al. pointed out that alkaline conditions couldn't achieve tremendous increase in solubility as compared to neutral condition (pH=7.3)[218].

Furthermore, curcumin becomes very susceptible to degradation under alkaline conditions, partly because of the formation of phenylate anion that gives rise to curcumin radicals which mediate further degradation of curcumin, react with other curcumin radicals to form dimeric catabolites and react with other biomolecules in the cells, all of which may disturb the experimental outcomes[219]. As a result, scientific studies based on curcumin inevitably rely on chemical solvents that are miscible in water, such as acetone, butanone, methanol, ethanol, 1,2-dichloroethane (up to 8.7 g/l w/w), 2-propanol and dimethyl sulfoxide (DMSO), of which the toxic effects need to be taken into account extremely cautiously, such as judging the lethal 50% dose values (LD50). As an example, suggested amount of some solvent being used for oral administration of curcumin in rat models (data from respective material safety data sheet) are: acetone 9.8 g/kg; 2-butanone 2.7 g/kg; methanol 5.6 g/kg; ethanol 7.1 g/kg; isopropanol 5.0 g/kg and DMSO 18.0 g/kg. Accordingly, DMSO is currently a relatively suitable solvent for in vitro and in vivo studies,

which dissolves curcumin up to a concentration of 11 mg/ml (versus 1 mg/ml for ethanol) [220]. Despite all this, proper controls (solvent alone) should always be employed in all assays[221], and the exploration of new and safer methods to increase curcumin's solubility has become a kind of urgent need.

In addition to this, curcumin undergoes chemical degradation in aqueous-organic solutions at physiological pH or greater. It was demonstrated that in 0.1 M phosphate buffer and serum-free medium with pH 7.2 at 37 degrees C, about 90% curcumin decomposed within 30 min. Studies indicate that its α,β-unsaturated β-diketo moiety rather than the phenolic group is responsible for its fast degradation, leaving degradation product like trans-6(4'-hydroxy-3'-methoxyphenyl)-2,4-dioxo-5-hexanal, ferulic aldehyde, ferulic acid, feruloylmethane, vanillin,vanillic acid and other dimerization end-products[222]. Different from the hydrolytic degradation (hydrolysis through the diketo moiety), curcumin is also sensitive to light and degrades much faster upon its exposure. For example, curcumin is rapidly decolorized upon exposure to UV light. Studies also indicates that the rate of curcumin photodegradation was influenced to a large extent by the nature of solvents used, for example, the measured half-life of curcumin in various solvents are found to be methanol (92.7 h) > ethyl acetate (15.1 h) > acetonitrile (6.3 h) > chloroform (2.7 h) [223]. The mechanism of its photodegradation is not yet clear, but it is likely that the β-diketone moiety participates in scavenging of the hydroxyl radical and redox reactions, thus forming smaller phenolic compounds such as vanillin, ferullic acid, and other small phenols[224]. Fortunately however, lipids, liposomes, albumins, cyclodextrin, cucurbituryl, surfactants, polymers and many other macromolecular and microheterogenous systems are found to be able to significantly decrease its degradation, making it possible to prepare stable curcumin solutions in culture medium containing 10% Fetal Bovine Serum (FBS) and also in human blood [225].

Moreover, studies related to absorption, distribution, metabolism and excertion of curcumin have, unfortunately, indicated only poor absorption and rapid elimination of this polyphenolic compound that contribute to its low bioavailability. Wahlström et al. observed an extrmely low serum curcumin levels in blood plasma which is negligible from Sprague-Dawley rats subjected to an oral administration of 1 g/kg curcumin[226]. A similar study indicated a maximum serum concentration of 1.35 ± 0.23 μg/mL (0.83h) in rats subjected to 2 g/kg curcumin orally, while either undetectable or extremely low (0.006 ±0.005μg/mL at 1 h) serum levels were detected in humans given same dose of curcumin[227]. In a phase I clinical trial of curcumin, a larger oral dosing of 4-8 g of curcumin resulted in peak plasma levels of 0.41-1.75 μM after 1 h of administration [228], while another recent human clinical trial found a plasma curcumin level of 11.1 nmol/L one hour after 3.6g curcumin was given orally [229]. Second, in a study investigating the absorption and tissue distribution of curcumin in rat model, Ravindranath et al. showed that after 400 mg of curcumin was administrated orally, only traces (less than 5 mg/ml) in portal blood and negligible quantities of unchanged drug in liver and kidney (< 20 mg/tissue) were observed. No curcumin was detectable in urine, as a matter of fact, the urinary excretion of conjugated glucuronides and sulfates significantly increased [230]. They further evaluated its tissue distribution using tritium-labeled curcumin (400, 80 or 10 mg of [^{3}H]-curcumin) and found that the percentage of curcumin absorbed (60-66% of the given dose) remained constant regardless of the dose administered, that is, more curcumin does not bring about higher absorption, which limited its bioavailability [231]. Perkins S et al. used single dose of [^{14}C] curcumin (100 mg/kg) via the i.p. route in C57Bl/6J Min/+ mice and found that [^{14}C] Curcumin disappeared rapidly from tissues and plasma within 2-8 h after dosing. Furthermore, they also observed that after the termination of dietary curcumin intake, tissue levels of curcumin declined rapidly to unquantifiable amounts within 3-6h [232]. Although there

are no data of serum or tissue curcumin level through intravenous administration available, these studies clearly suggest the poor rate of systematic absorption and distribution of this compound. Studies have also evaluated the metabolism and systemic elimination of curcumin. Once absorbed, curcumin is found to be subjected to conjugations such as sulfation and glucuronidation at various tissue sites. Liver is the major organ responsible for metabolism of curcumin. Holder et al. concluded that the major biliary metabolites were glucuronides of tetrahydrocurcumin (THC) and hexahydrocurcumin (HHC) and a minor biliary metabolite was found to be dihydroferulic acid together with traces of ferulic acid[233]. Pan et al. investigated the pharmacokinetic properties of curcumin in mice and found that 99% of curcumin in plasma was present as glucuronide conjugates. They pointed out that curcumin was first biotransformed to dihydrocurcumin and THC, which were subsequently converted to monoglucuronide conjugates. With these results, they drew similar conclusions that curcumin-glucuronoside, dihydrocurcumin-glucuronoside, THC-glucuronoside, and THC are major metabolites of curcumin in vivo [234]. More recently, Vareed SK et al. examined the pharmacokinetics of a curcumin in healthy human volunteers 0.25 to 72 h after a single oral dose (10 g or 12 g) and concluded that major metabolites are curcumin conjugates, present as either glucuronide or sulfate instead of mixed conjugates, in plasma [235]. Hoehle and colleagues examined the metabolism of curcumin by rat liver tissue slices and showed the formation of reductive metabolites as THC, HHC, and octahydrocurcumin (OHC) [236]. As clearance of curcumin is also an important factor that determines its relative biological activity, one clinical study with daily oral curcumin (36 and 180 mg) for up to 4 months found neither curcumin nor its metabolites in urine, but from feces, which indicated that curcumin has low oral bioavailability in humans and may undergo intestinal metabolism [237]. Similar findings were indicated in mice models that the termination of dietary curcumin intake led to rapid declination of tissue curcumin levels to

unquantifiable amounts shortly afterwards (3-6h) [238]. All these data suggest that curcumin undergoes extensive metabolic conjugation and reduction, most likely through alcohol dehdrogenase [239], which severely curtail its bioavailability.

Due to these defects, progress in translating the findings of curcumin's pleiotropic activities into clinical application has so far been impeded. In the case of wound treatment, topical administration of curcumin could avoid most of the problems that associate with its systemic administration, such as inherently poor intestinal absorption and rapid metabolism as well as elimination (first-pass effect) of curcumin from oral administration. Unfortunately however, again because of its insolubility, problem associated with curcumin's bioavailability still need to be addressed first before a success in translating curcumin's potential into tangible benefits for wound treatment from bench to bedside.

Seeking to overcome this obstacle, researchers have tried several approaches aiming to enhance curcumin bioavailability, including the application of adjuvants, nano-fuormulation, liposomes, micelles and phospholipid complexes. For example, curcumin has been traditionaly designed and produced as emulsion, cream, solution, pill, gel, band aid, etc., in which appropriate adjuvant is able to improve curcumin bioavailability via the impediment of its metabolic pathway. In a study led by shoba et al., combined piperine was found to inhibit glucuronidation in the liver and intestine, increasing its bioavailability increased up to 154% in rat and 2000% in the humans[227]. Except for the piperine, quercetin derived from soy beans (that inhibits sulfotransferases) and genistein (that inhibits alcohol dehydrogenase) have also been found to counteract detoxification enzymes implicated in curcumin metabolism, and thereby increase its absorption, serum concentration and subsequent bioavailability[240].

Recently, nanoformulation has been found to be a very effective approcch to enhance the bioavailability of the drug. Through literature review, there are several frequently reported forms of nanoformulation, which include: (1) Nanoparticles, especially biodegradable nanoparticles, which have been used for encapsulation of curcumin due to its biocompatibility and biodegradability; (2) Liposomes, generated from phospholipid bilayers, which are the second most widely used vehicle to solubilize/encapsulate curcumin. Various types of liposomes have been tested and are clinically used with normal size of liposome/lipid nanoparticle ranging from 50-150nm; (3) Cyclodextrins, which are cyclic oligosaccharides bearing solubilized curcumin in its lipophilic cavity and hydrophilic outer surface facilitating greater dispersion of the cyclodextrin-curcumin complex, thus offers enhanced stability, bioavailability, minimal curcumin degradation[241]; (4) Micelles, or polymeric micelles, which are composed of amphiphilic block copolymers that spontaneously form 20-100 nm micelles in aqueous solution. Their hydrophobic core can effectively entrap curcumin for solubilization and targeted delivery[242]; (5) Nanogels, which are designed to transport various drug molecules including curcumin. They are made from a cross-linked network of polycationic (e.g. polyethylenimine, polylysine, spermine, etc.) and neutral polymeric (e.g. PEG, Pluronic/Poloxamer, etc.) components. Briefly, swollen nanogels contain a water-filled interior volume and have excellent dispersion stability, they bind and encapsulate drug molecules with opposite charge, via hydrophobic interactions, hydrogen bonding or due to participation of all these forces. They emerged as novel environmentally responsive systems as they can mimic human tissues due to higher hydrophilicity in the system for the swollen nature[243]. (6) Polymers, which have been extensively studied to exploit a wide variety of polymeric carriers to improve curcumin solubility and bioavailability. For example, nanoencapsulation of curcumin with polymers has been proven to be a promising approach to simultaneously improve the

bioavailability and reduce curcumin degradation [148]. Some other nano-formulation approaches such as dendrimers, lipid nanoparticles, gold nanoparticles or magnetic nanoparticles have also been investigated by different research groups, which will not be described in detail. All these attempts imply that nanoformulation may be an ideal option to obtain sustained release of curcumin at the cellular targets to improve therapeutic benefit. As a matter of fact, attempts have been made to nanoformulate curcumin so as to facilitate its use *in vitro*, *in vivo*, and pre-clinical settings. These processes, shown to improve its solubility, stability, cellular uptake efficacy, specificity, tolerability, and therapeutic index to varying degrees, have been proven to be effective and therefore become the focus of attention.

From a clinical point of view, nanoformulate curcumin in a suitable carrier system, most ideally in a form of wound dressing, is well suitable and therefore very necessary to help deliver therapeutic doses of curcumin favorably for an optimized wound therapy. Inspiringly, the developments in material sciences now have shed some new light on this old subject, which allows to remove some of the obstacles related to curcumin translation. One option to circumvent unwanted properties of curcumin while provide suitable vehicle for topical wound treatment is to nano-formulate the pharmaceutical compound into a nanofibrous structure through electrospinning, a technique from the textile industry that has recently emerged as a novel means to generate nanoscale scaffolds for application in tissue engineering and regenerative medicine. The simplicity of the electrospinning process itself, and the ability to incorporate therapeutic compounds into the nonwoven nanofiber meshes during spinning enables a useful controlled-release system for therapeutic purposes [152]. Literature review indicated that a variety type of drugs, such as antibiotics[244], anticancer drugs[245], proteins[246] and DNA[247] have been found to be able to incorporated into nanofiber through electrospinning. Studies have also demonstrated that electrospun fibers could significantly

improve drug encapsulation efficiency as compared to other forms of drug carriers, such as liposomes, hydrogels, nano/microspheres and cast films derived from conventional methods, while reducing the burst release through optimized drug-polymer-solvent system or electrospinning technique [248]. In a local drug delivery application, electrospun fibrous mats would facilitate the diffusion of drug molecules into the surrounding tissue but decrease the minimum required dosage of the drug with less systemic absorption so as to avoid unwanted side effects. For example, electrospun fibrous mats have been investigated for their application in transdermal drug delivery systems or as wound dressings[249,250].

In regard to material used for electrospinning based drug release system, there are several concerns. First, the material should protect the drugs from decomposition in the blood stream. Second, due to the application in tissue engineering and regenerative medicine, biodegradable materials are generally more favored since they exclude the need of explantation. However, they may be more complex in use as drug delivery vehicle than their non-degradable counterparts, which release incorporated drug primarily through diffusion. In other words, drug in a biodegradable vehicle may be released by both diffusion and degradation of the material itself, which may end up with dose dumping that causes local toxic effect of the drug. Therefore, special care must be taken to tailor both the release and degradation rate when biodegradable materials are to be used. Third, materials should allow controlled release of the therapeutic agent over a time period with a constant release rate and continue as long as necessary for the treatment. Therefore, the dispersion of drug in the polymer matrix is of great importance for its release profile. Jiang et al. prepared ibuprofen-loaded electrospun PEG-g-chitosan with PLGA for controlled drug delivery applications and demonstrated that the presence of PEG-g-chitosan significantly moderated the burst release rate of ibuprofen from the electrospun PLGA membranes. Besides, they also found that

ibuprofen was conjugated to the side chains of PEG-g-chitosan for prolonged release of more than 2 weeks, indicating chitosan nanofibers as an ideal candidate material for controlled drug delivery applications[251]. In an another study, Chew et al. investigated the feasibility of encapsulating human beta-nerve growth factor (NGF), which was stabilized in a carrier protein, bovine serum albumin (BSA) in a copolymer of epsilon-caprolactone and ethyl ethylene phosphate (PCLEEP) by electrospinning. Due to the relatively hydrophobic backbone PCLEEP has, a slow degradation rate was found with a sustained release of NGF via diffusion process for at least 3 months[252]. Studies also indicated that the use of polymer blends improves the tuneability of the physicochemical and mechanical properties of the drug loaded fibers, which benefits the development of controlled drug release formulations, in that the release rate can be modified by altering the ratio of the polymers in the blend. For example, Tipduangta et al. made an in depth study of the electrospinning process on the phase separation of a model partially miscible polymer blend, PVP K90 (Polyvinylpyrrolidone K 90) and HPMCAS (AquaSolve Hypromellose Acetate Succinate), in comparison to other conventional solvent evaporation based processes including film casting and spin coating. They found that electrospinning led to an enhanced apparent miscibility between the polymers while microscale phase separation was seen in the same blends being processed using film casting and spin coating. Therefore, they achieved electrospun polymer blend nanofibers for tunable drug (paracetamol) delivery: a biphasic drug release profile with a burst release from PVP-rich phases and a slower, more continuous release from HPMCAS-rich phases [253].

In our study, we use trifluoroethanol (TFE) as the common solvent for curcumin and gelatin to prepare spinnable solution and then formulated it into curcumin/gelatin nanofibrous mat through a simple elecrospinning process. We found in XRD measurements, the characteristic peaks of raw curcumin

originating from its crystalline structure no longer existed in the spectrum of Cc/Glt NM, fully suggesting that the nano-formulation through electrospinning has successfully achieved the amorphization of raw curcumin (Figure 8), which is consistent with the result from FTIR, as characteristic O-H streatching band of curcumin was not observed in FTIR spectrum of Cc/Glt NM (Figure 9), this may possibly due to intermolecular hydrogen bonding.

Most importantly, the engineered nanofibrous mat was found to be able to control-release loaded curcumin efficiently, where the time span of curcumin release falls in the range of empirical regularity of dressing exchange in clinical practice (Figure 10). Therefore, this approach has been proven to attained water solubility of integrated curcumin and thus overcome its drawbacks from topical administration for wound healing (Figure 26).

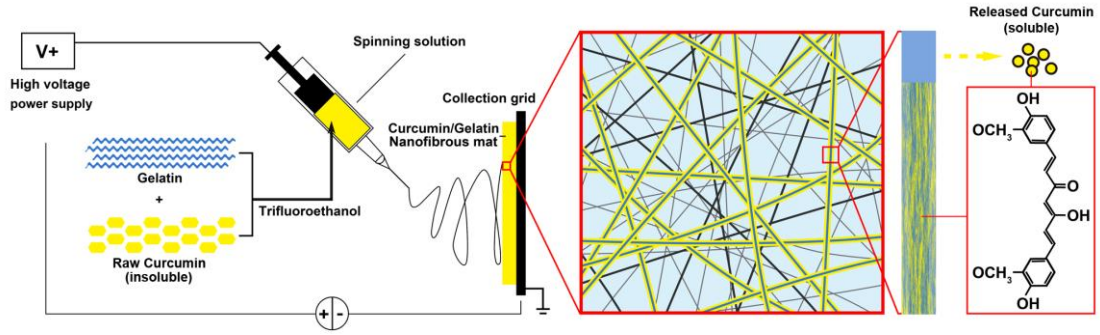

Figure 26: Scheme of curcumin nanoformulation through electrospinning. Curcumin and gelatin were co-dissolved in TFE to obtain spinnable solution that could be electrospun toward the collection grid to form the Curcumin/Glatin nanofibrous mat. Through such simple approach, the bioavailability of curcumin can then be significantly improved as it can be further control-released from the blended nanofiber to enhance its solutility.

Similarly, some recent attempts have also investigated different drug loading

methods together with electrospinning techniques, such as coatings, embedding and encapsulating (coaxial and emulsion electrospinning), aiming to obtain better control over drug release kinetics[254]. Take acute wounds for example, following an invasive surgery or trauma, it is common to deliver antibiotics either systemically or locally in order to prevent infection at the wounded site. In this case, thanks to the ability of fabricating scaffolds with inherently high surface area, which allows for high drug loadings and the ability to overcome mass transfer limitations associated with other polymeric systems, electrospun matrices are able to exquisitely meet the requirement of drug delivery necessary to prevent infection as potential complication. Kim et al. evaluated the controlled release of a hydrophilic antibiotic (Mefoxin®, cefoxitin sodium) from electrospun PLGA and PLGA/PEG-b-PLA/PLA (80:15:5 by wt%) mats and found that the morphology and density of the electrospun scaffold was dependent on drug concentration, in which solutions without drug leading to a bead-and-string morphology but solutions containing 5 wt% drug giving a completely fibrous structure (possibly due to the effect of ionic salt on the electrospinning process). They also observed the intact structure of the drug after electrospinning through UV-vis and ^{1}H NMR analysis, demonstrating retained bioactivity of the incorporated antibiotic. Interestingly, in all tested PLGA mats, the maximum dosage of drug was released after 1 h of incubation in water at 37 °C, whereas the addition of the amphiphilic block copolymer (PEG-b-PLA) reduced the cumulative amount of the released drug at earlier time points and prolonged the drug release rate at longer times (up to a 1-week period). It is likely that the drug is primarily located at the surface of the PLGA fibers while being embedded in the polymer nanofibers when the amphiphilic PEG-b-PLA block copolymer was incorporated. Thus, the authors demonstrated that antibiotic loaded electrospun mats can be used to effectively reduce infection with greater than 90% inhibition of Staphylococcus aureus growth and proposed that the combination of mechanical barriers based on non-woven nanofibrous biodegradable scaffolds and their capability

for local delivery of antibiotics increases their desired utility in biomedical applications, particularly in the prevention of post-surgical adhesions and infections [255].

In an other study, in order to confer capability of immobilizing diverse macromolecular bioactive agents to the fibers, Lu et al. prepared composite mats composed of cationized gelatin (CG)-coated polycaprolactone (PCL) by coaxial electrospinning, in which cationized gelatin (by derivation with N,N-dimethylethylenediamine) was used as a shell material while PCL formed the core section thereby improving the mechanical properties of the nanofibrous CG hydrogel. They found that the core-shell fibers could effectively immobilize the two types of agents, bovine serum albumin (BSA) and heparin, under mild conditions, where the adsorption amount reached about 12μg of BSA and 23μg of heparin per mg of the fiber mat, respectively. Besides, they also demonstrated that VEGF could be conveniently impregnated into the fibers through specific interactions with the adsorbed heparin in the outer CG layer, with sustained release of bioactive VEGF for more than 15 days. With these results, the author concluded that the advantage of the electrospun CG-coated PCL fibrous mat such as high mechanical strength, bioactive surface characteristics and capacity for immobilization of various macromolecular bioactive agents under very mild conditions, is well suitable for tissue engineering applications [256].

5.2. Electrospun Cc/Glt NM is ideal for topical wound treatment

Once the protective skin barrier is broken, a native process of dermal and epidermal tissue regeneration starts with a set of complex biochemical actions (physiological process of wound healing). Wound healing dressings are usually applied during this process to protect the wound, exude extra body

fluids, cleanse the exogenous microorganisms, sometimes improve appearance and accelerate the healing as a whole. As being described above, if curcumin nanoformulation could be in a form of wound dressing, it may ideally allow easily topical administration for both drug delivery and wound protection. A very useful option is to prepare a solid dispersion of curcumin in a suitable matrix. Among various techniques including phase separation or self-assembly used for fabricating such meshes, electrospinning, except for its aforesaid ability to incorporate drug into the nanofibers for medical treatment, has been found to be a simple, cost-effective and versatile approach to engineer highly porous mesh structure with well-interconnected pores and high surface area. Therefore, it is the most frequent method of choice in developing candidate nanofibrous mats as wound dressing. We therefore reasoned that with appropriate selection of fiber forming material and adoption of electrospinning parameters, the inherently high surface to volume ratio of electrospun nanofibrous mats can enhance cell attachment, drug loading and subsequent controlled-release as well as mass transfer properties. In our study, we successfully prepared Cc/Glt NM through electrospinning (Figure 7, Figure 26) and demonstrate that such system allows considerably enhancing the solubility and availability of curcumin (Figure 10) by embedding it into gelatin based electrospun nanofibrous mats (Figure 26) and could be easily applied as an agreeable biomimetic wound dressing for accelerated healing process (Figure 22). Thus, the electrospun Cc/Glt NM could potentialy serve as "smart dressing" for topical wound treatment.

Literature review indicates that despite some preliminary work in tissue engineering decades ago, electrospinning has not gained widespread interest as a potential polymer processing technique for its applications in tissue engineering until the last few years. However, it has soon been recognized of its unique advantages to engineer scaffolds with extremely fine polymer fibers with diameters ranging from micrometers to nanometers, allowing the

production of suitable vehicle in a form of wound dressing with the ability to deliver insoluble drugs [257]. By using different polymers (biodegradable or non-degradable), especially those natural polymers, electrospun nanofibers can be oriented or arranged randomly, giving control over both the bulk mechanical properties and the biological response to the mat. In a form of two-dimensional non-woven meshes, electrospun wound dressings have been shown to promote hemostasis, fluid absorption and gas permeation when implanted onto open wounds [258]. Electrospun meshes have also been shown several intrinsic properties that make them particularly interesting in its application for wound healing. **First and foremost**, the synthetic mesh is able to mimic the natural structure and functional biology of ECM, which is largely due to its randomly aligned nanofibers within the mesh, leading to promoted cell migration and proliferation for new tissue formation. This has been proven in our study through the observation of fibroblast adherence and expansion over time on both electrospun Cc/Glt NM and Glt NM (Figure 7, Figure 14). This is very useful as the fabricated nanofibrous mat can not only offer mechanical protection, but also provide positive topological signaling for cell activity. For example, Merkle et al. reported that core-shell PVA/gelatin electrospun nanofibers promote human umbilical vein endothelial cell and smooth muscle cell proliferation and migration [259]. Thus, this technique is expected to be able to develop advanced bioactive wound dressings that can actively initiate the healing process. **Second**, the presence of small interstices and the high surface area of the fibers is also essential for fluid absorption, dermal drug delivery and surface modification with specific chemical functionalities [260], so that electrospun nanofibrous meshes have been shown to promote the hemostasis of injured tissue. **Third**, the high interconnected porosity of nanofibrous meshes (60-90%) facilitate cell respiration and high-gas permeation while avoiding wound desiccation and dehydration. Studies indicate that none woven electrospun nanofibrous mats for wound dressing usually have pore sizes ranging from 500nm to 1μm, small

enough to protect the wound from microorganisms penetration through aerosol particle-capturing mechanisms [261] while allowing gaseous and fluid exchanges through inherent small interstices[262,263]. **Fourth**, although the electrospun naofiber mesh induces cell migration and proliferation within the wound bed, its nanoscale pores prevent tissue ingrowth into the fibrous structure. Hence, it will be easily removed without additional injury during dressing exchange or once the wound has healed. This is in accordance with what we have observed in our study, that the nanoscale pores presented in our electrospun NM avoid cell infiltration and tissue ingrowth (data not shown). Bearing these favorable traits, the applications of electrospinning in developing favorable candidates for wound dressing and drug delivery are deemed nearly limitless. For example, electrospinning of suspensions containing living cells have recently been reported [264].

In terms of fiber forming materials for this purpose, a wound dressing material is expected to not just provide a physical barrier to a wound, but reduce loss of protein, electrolytes and fluid from the wound bed and be permeable to moisture and oxygen as well as help to minimize pain and infection [265,266]. For these reasons, polymeric nanofirous meshes have recently attracted enough attention from researchers. Till now, there are various synthetic and natural-based biodegradable polymers being investigated through electrospinning to develop materials that actively support and supplement the deposition of healthy tissue, such as poly(vinyl alcohol) (PVA), poly(lactic-co-glycolic acid) (PLGA), silk fibroin and chitosan [267]. Zahedi et al. reviewed the most frequently selected polymers and pointed out that by virtue of unique properties of nanofibrous bandages, the applications of these materials on various types of wounds are abundant with respect to other modern wound dressing materials, such as hydrocolloids, hydrogels, and so forth [268]. Generally, synthetic polymers ensure easy processability and good mechanical properties of the resulting mesh while natural polymers increase

the capability of the fibers to actively interact with biomolecules involved in the healing process [269]. Sometimes, considering the advantages and disadvantages of both synthetic and naturally derived materials, mixtures of different polymers instead of single polymer solutions are prepared to electrospin the so called "polyblended" nanofibers.

We chose gelatin as the fiber-forming material in this study because of its biological origin from its parent collagen, the principal structural element of skin ECM [270]. It contains the Arg-Gly-Asp (RGD)-like sequences which are essential for cell adhesion and migration in wound healing [271]. Also, it has been found as a repository for a large family of cytokines[272]. Thus, the nonwoven electrospun nanofibers could resemble ECM structures to provide mechanical protection as well as nanotopography and chemical signaling in the guidance of cell function and also serve as an ideal biodegradable scaffold for *in situ* dermal regeneration [273]. Additionally, gelatin has excellent water absorption and fluid affinity, supporting a moist wound healing [274]. Several *in vitro* assays demonstrated that our approach endowed the biomimetic construct with appropriate properties necessary for fibroblast growth and activity similar to what granulation tissue ECM would do in physiological wounds [275].

Considering the fact that wound dressings also need to serve as a mechanical support and barrier while covering the wound, an appropriate tensile strength of the mat is necessary [276]. We took additional cross-linking steps to engineer the modulus of elasticity of Cc/Glt NM into the range reported for normal human skin, which has been thought to be crucial for wound dressings and skin replacement constructs [277,278]. Most importantly this changed the release kinetics for curcumin from our NMs - since the most common way of electrospinning to get drug release system is to dissolve or disperse the drug in the polymer solution before they are electrospun into nanofibrous mats, drug

under such circumstances may present either on the fiber surface or being encapsulated inside the fiber, which could lead to burst release in the initial stage. To address this problem, some methods are being investigated by other groups, for example, to encapsulate the therapeutic agents inside polymeric nanofibers by coaxial electrospinning so as to obtain core-shell structures[279]. This approach has the reportedly advantage of high loading efficiency and controllable release behavior with suppression, but not complete elimination, of the burst release effect. To further overcome the problem, additional coating on the drug reservoir of electrospun fiber could be adopted[266]. He et al. described a coaxial electrospinning technique to fabricate core-shell ultrafine fiber mats for drug delivery application, in which Poly (L-lactic acid) (PLLA) and tetracycline hydrochloride (TCH) were employed as the shell and core materials, respectively. They showed that a reservoir-type drug release device can be conveniently obtained through encapsulating TCH in the PLLA ultrafine fiber. Since a subsequent sustained TCH release from these fiber mats was therefore achieved, they proposed that the electrospun ultrafine fiber mats containing drugs may be used as drug release carriers or made into biomedical devices such as sutures and wound dressings[280].Similarly, Xu et al. investigated the release behavior of a water soluble anti-cancer drug, Doxorubicin hydrochloride (Dox), from the drug-loaded nanofibers prepared by emulsion-electrospinning, which successfully incorporated the drug into amphiphilic poly(ethylene glycol)-poly(L-lactic acid) (PEG-PLA) diblock copolymer nanofibers, forming "core-sheath" structured drug-loaded nanofibers. They found that the release behavior of this drug-loaded system showed a three-stage diffusion-controlled mechanism, in which the release rate of the first stage was slower than that of the second stage, but both obeyed Fick's second law [281]. In our study, we found that an appropriate crosslinking process efficiently solved the problem of initial burst release to achieved controlled release of the imbedded curcumin to a time window that is conform with accepted clinical dressing change intervals[282]

(Figure 10), while favorably improving the mechanical property of the electrospun Cc/Glt NM as a whole (Figure 11). Therefore, together with gelatin's wide commercial availability at a relatively low cost, the easily produced Cc/Glt NM turns out to be a very promising candidate for clinical translation.

It should be noted that based on the nature of action, present wound dressings are generally classified as passive, interactive and bioactive products [283]. Similarly, electrospun nanofibrous mats for wound healing application can also be classified according to the criterion adopted for commercial dressings: passive, interactive, advanced and bioactive. **Passive** electrospun mats, derived from both natural and synthetic polymers, simply provide physical (such as water and gas permeability) and morphological (such as adequate porosity and nanometer scale fiber size) properties of wound dressing. They allow the maintenance of appropriate level of moisture in the wound bed and protection of tissue against additional mechanical trauma. Khil et al. fabricated a nanofibrous polyurethane (PU) membrane by electrospinning and evaluated its performance as a wound dressing. They found that due to the porosity and inherent property of PU, this wound dressing exhibited controlled evaporative water loss, excellent oxygen permeability, and promoted fluid drainage ability. Besides, neither toxicity nor permeability to exogenous microorganism was observed with the nanofibrous membrane, which has also been shown to increase epithelialization rate and well control the exudate in the dermis in an in vivo animal experiment. They therefore concluded that nanofibrous PU membrane prepared by electrospinning could be properly employed as wound dressing. **Interactive** electrospun mats combine properties from passive electrospun mats with the value-added capability to address optimal cell responses and limit bacterial proliferation in the wound bed, the main strategy of which consists of the combination of synthetic polymers and biopolymers in order to exhibit antibacterial properties and affinity toward ECM components.

Given the fact that gelatin is a natural polymer derived from collagen that often been chosen for biomedical applications with it is biodegradable, non-toxic, and easily available at low cost, Kim et al. prepared a blended nanofiber scaffold using synthetic and natural polymers (PU and gelatin) by electrospinning for wound dressing and found that the blended nanofibrous scaffolds were elastic, with increasing elasticity as the total amount of PU increased. Moreover, as the total amount of gelatin increased, the cell proliferation increased with the same amount of culture time. Therefore, they demonstrated that this gelatin/PU blended nanofiber scaffold has potential application for use as a wound dressing[284]. Despite the therapeutic benefit interactive electrospun mats have been shown, their translation to the clinic are not yet available as there are still problems associated with the electrospinning of natural polymers reproducibly in large scale. For example, issues of impurities that may induce immunogenic reactions upon implantation together with the complexity of processing natural polymers are currently limiting the transference of these mats into real devices for clinical wound treatment [285]. **Advanced interactive** electrospun mats are deemed to be capable of treating additional bacterial infection. Several studies have been performed to develop drug loaded nanofibrous mats. Meinel et al. recently overviewed drug loaded electrospun nanofibers for wound healing applicatons [286]. The most frequently selected drugs for wound healing applications have also been summarized by Abrigo and colleagues [262]. Undoubtedly, the improvement of loading antibiotics or antimicrobials into electrospun fibers represents a great advantage in treating infections in the wound bed. With the aid of developing techniques, electrospun fibers is even able to load bioactive ingredients such as growth factors, vitamins and other biomolecules known to encourage the healing processes [287]. For example, coaxial electrospinning produces ore-shell fibers with a polymeric external shell and an internal solution containing drugs or other biomolecules. However, given the complexity of wound type and situations, optimal drug release profiles and

rates of release are of great importance. Also, the common problem of initial burst release from drug loaded nanofibers which may bring about local toxic drug concentration toward tissue cells at the wound site. Therefore, these systems have not been translated into real clinical therapy and more studies are needed to develop adaptive devices to fit for various kinds of wounds. **Bioactive** electrospun mats aim to act as multifunctional systems with adequate mechanical and physico-chemical properties that is expected to protect the wound, stimulate the healing process as well as to control the bacterial load in the wound bed. For example, electrospinning natural polymer nanofiber as biomimetic infrastructure with agreeable mechanical property, which is loaded with multifunctional drugs like curcumin, which have been recently demonstrated as powerful wound healing agent with potent bactericidal, antiviral, and antifungal activity [288,289]. In some other attempts, researchers tried to include wound status monitoring (such as PH and temperature) as an indicator of the progression of healing and/or the bacterial load. Based on electrospun nanofibers and conductive magnetic nanoparticles (MNPs), Luo et al developed a lateral-flow immunobiosensor for rapid detection of Escherichia coli (E. *coli*) O157:H7 bacteria. They found that due to high surface area and unique nanostructure, the conductive pathogen/nanoparticle complex in the purified solution is effectively captured on the nanofiber membrane by antibody-antigen binding with bacterial load as low as 67 CFU/mL in a total detection time of 8 min [290].

Here in our attempt, we are able to combine the advantage of both therapeutic curcumin and fiber-forming gelatin with its excellent biometic properties through electrospinning and found that this simple engineering process is indeed an apt choice for producing suitable candidate materials as bioactive wound dressings. We speculate that owning to the high porosity of the electrospun nanofibrous mat (Figure 7) as well as gelatin's favorable biodegradability, the degradation products of the Cc/Glt NM will not

accumulate at the site of implantation that hinders wound closure. On the contrary, the easiness of being cut into any size and shape make the Cc/Glt NM suitable for various types wounds in clinical settings [291]. Taken together, the electrospun Cc/Glt NM fabricated in this study is well promising as a bioactive wound dressing for topical wound treatment.

5.3. Delivered curcumin exterts synergistic signalling to accelerate wound healing

Through further study, we found that delivered curcumin was able to enhance recruitement of wound site fibroblasts *in vitro* and *in vivo* (Figure 15, 23, 27) by inducing proliferation and migration (Figure 12-15, Figure 23, Figure 27), which is at least partially mediated by Dkk-1 (Figure 18-19). Presumably, such mobilization takes place once bioactive curcumin is released from the topical applied Cc/Glt NM (Figure 27), so that activated fibroblasts may immediately play active roles comparable to the proliferative phase of wound healing, leading to granulation tissue formation as well as apoptosis of unwanted cells. Several studies have assessed the effects of curucmin for wound healing in this phase. According to these studies, the presence of fibroblasts at the wound site is arguably most critical in ensuring normal wound healing. For example, if the fibroblasts are not activated, or sub-optimally migrate into the provisional matrix, there will be reduced autolytic debridement of the denatured proteins and fibrin clot [292]. Additionally, in the process of granulation tissue formation, fibroblasts differentiate into myofibroblasts, which contract and pull the wound edges together [293]. All these findings verified that impaired fibroblast activity such as proliferation and migration within the wound area, could lead to failure of normal healing [294]. Toward this end, studies have also shown a dose dependent effect of curcumin on human fibroblasts [295,296,297]. Mohanty C and colleagues prepared

oleic acid based polymeric (COP) bandages loaded with curcumin and compared its potency of wound healing to void bandage and control (cotton gauze treatment) in a rat model, which led to the conclusion that comparative acceleration in wound healing is due to early implementation of fibroblasts and their differentiation (increased level of α-smooth muscle actin) [298]. However, another *in vitro* study led by Topman et al. showed no evidence that curcumin influences the *en mass* fibroblast migration kinematics post infliction of localized mechanical damage. This contradictory result is probably due to, as the author pointed out, the complexity of *in vivo* wound healing that could hardly be adequately mimicked in an *in vitro* setting. Whether curcumin induces other pathways warrants further exploration [299].

In the current study, we provide evidence that Dkk-1 is an important mediator of fibroblast mobilization in this context. Our results agree with previous reports showing decreased expression of Dkk-1 and enhanced expression of β-catenin in fibroblasts from pachydermoperiostosis (abnormal fibroblast proliferation) patients than normal ones [300,301]. Similarly, Dkk-1 mediated Wnt signaling has also been found as a positive regulator of cell migration in other tissues like breast cancer [302]. Interestingly, Koch et al. found that wounding of epithelial monolayers returned the leading edge cells to a nonquiescent state with activated β-catenin signal and subsequent induction and secretion of Dkk-1[194]. Given that Wnt signaling cascade and its antagonist Dkk-1 have been proposed to play crucial roles to maintain homeostasis of a variety of tissues including skin [303], and that the physiologic Dkk-1 level is of vital importance to maintain its biological functions [194,304], we speculate that curcumin could precisely control Dkk-1 level in a temporospatial manner so as to correctly regulate the downstream Wnt signaling pathway, in that Dkk-1 has been shown to participate in a negative feedback loop in Wnt signaling as well [305]. Yet more studies are required to fully elucidate its less well understood role in wound healing.

Except for fibroblast activation, apoptotic processes have also been recently draw enough attention in curcumin related wound healing studies. It has been suggested that curcumin is able to cause apoptosis because of its capability to induce ROS. Scharstuhl A et al. observed that 25μM curcumin give rise to fibroblast apoptosis due to the generation of ROS, which could be inhibited by antioxidants like N-acetyl-l-cysteine (NAC), biliverdin or bilirubin. On a subsequent functional wound contraction model in vitro, they demonstrated that fibroblast-mediated collagen gel contraction was completely prevented by 25μM curcumin, whereas this could be reversed by co-incubation with NAC, which is partially mediated by heme oxygenase (HO). Their findings suggest that curcumin induced fibroblast appoptosis together with antioxidants, HO-activity and its effector molecules as its possible fine-tuning regulator, may modulate pathological scar formation of wound healing [306]. Similarly, curcumin induced apoptosis has also been found in the early stage of wound healing, as Mohanty et al. confirmed the presence of greater amounts of apoptosis (by DNA fragmentation) 4 days after the treatment with curcumin loaded oleic acid based polymeric bandage than void bandage and control (cotton gauze) [298]. According to their result, it is reasonable to speculate that wounds subjected to curcumin treatment can more readily progress from inflammatory to the proliferative phases and proceed to heal, since a series of apoptotic processes eliminate unwanted inflammatory cells from the wound site, at least it is possible to accelerate the healing cycle with minimal prolongation of the inflammatory phase. In our study, we didn't observed apoptotic effect of curcumin on fibroblasts, instead, it was shown to induced fibroblasts mobilization manifested by enhanced cell proliferation and migration. We speculate that it is possibly due to the favorable controlled release profile of curcumin from the Cc/Glt NM, through which the therapeutic dose of curcumin could be accumulated locally so as to exert its healing potential at the greatest extent.

On the other hand, acute inflammation is induced almost immediately upon tissue injury, controlling inflammation is therefore important and can optimize the wound repair process, as uncontrolled inflammatory responses may result in tissue damage and the turnover into problematic wound. In our study, we also found that curcumin action on fibroblasts lead to inhibition of inflammatory responses by suppressing MCP-1 levels and subsequent inflammatory cell infiltration *in vitro* and *in vivo*. Our data is in accordance with most studies that conclude that curcumin enhances wound healing by inhibiting the inflammatory response. In a recent review, Joe et al. stated that curcumin potentially modulates inflammation through a variety of mechanisms, most particularly of which being its inhibitory effect on tumor necrosis factor alpha (TNF-α) and interleukin-1 (IL-1). Both of the cytokines are produced by monocytes and macrophages that crucially regulate inflammatory responses [307,308]. Curcumin has also been proven to be able to inhibit the activity of NF-κB (nuclear factor kappa-light-chain-enhancer of activated B cells), a transcription factor that accounts for a group of genes implicated in the initiation of inflammatory responses [309]. Buhrmann C et al. found that curcumin induced down-regulation of gene products that mediate matrix degradation (matrix metalloproteinase-1, -9, and -13), prostanoid production (cyclooxygenase-2), apoptosis (Bax and activated caspase-3) and cell survival (Bcl-2). All of these genes are all known to be regulated by NF-κB. Furthermore, they observed the abrogated effects of IL-1β induced NF-κB activation by wortmannin, a specific inhibitor of phosphoinositide 3-kinase (PI3K), indicating the role PI3K plays in IL-1β signaling pathway which led to the conclusion that curcumin suppressed IL-1β-induced PI3K p85/Akt activation and its association with I kappa B kinase (IKK) [310].

Based on previous studies, Frey and Malik pointed out that NF-κB has long been considered to be oxidant responsive[311]. However, uncontrolled

inflammation may in turn induce oxidative stress. Take diabetic wounds for example, they stagnated in the inflammatory phase characterized by a continuing influx of neutrophils that release cytotoxic enzymes, free radicals, and inflammatory mediators. As the consequence, the overproduction of free radicals inevitably results in extensive collateral damage that counteract the healing process [312]. All these facts highlight the close correlation between oxidation and inflammation in wound healing. Generally, both inflammation and oxidative stress during wound healing are considered to inhibit tissue remodeling. Recent studies proved that curcumin is able to scavenges free radicals (a major cause for the inflammation) and inhibits the peroxide induced oxidative damage in human keratinocytes and fibroblasts by down regulation of the PI3K/AKT/NF-κB pathway [313]. In a very special type of acute wounds, cutaneous burns are dynamic injuries characterized by a central zone of necrosis surrounded by a zone of ischemia, which may progress to full necrosis over the days and therefore poses a great challenge for its treatment. The anti-oxidant effect of curcumin has been found to be able to reduce the burn progress. Singer et al. evaluated the unburned interspaces (ischemia zone) in a rat model of burn wounds (by using brass comb) with animals randomized to oral curcumin or vehicle administration 30 minutes before injury and at 24, 48, and 72 hours after injury and found that the percentage of interspaces that progressed to full-thickness necrosis in the curcumin group were significantly lower than vehicle groups at one, two, three, and seven days after injury [314]. While most literature concludes that curcumin reduces inflammation during wound healing, there are some studies suggesting that curcumin enhances wound healing by promoting the inflammatory response. Kulac et al. investigated the healing effect of burn wound through topical treatment of curcumin in rats and found that curcumin treated wounds heal much faster with imcreased numbers of inflammatory cells [315]. Unfortunately, the authors did not mention the type of inflammatory cells being evaluated in the study. Similarly, Jagetia GC examined the effect of curcumin

on the healing of deep excision wounds of mice exposed to fractionated irradiation (IR), as a result, fractionated IR reduced the synthesis of collagen, deoxyribonucleic acid (DNA) and nitric oxide (NO) at different post-IR times but curcumin treatment before IR significantly elevated the synthesis of collagen, DNA and NO. They therefore concluded that increased NO is essential to initiate inflammatory reaction in wound microenvironment as it helps in the repair and regeneration of wounds [316]. However, as NO can modulate the release of various inflammatory mediators from a wide range of cells participating in inflammatory responses (e.g., leukocytes, macrophages, mast cells, endothelial cells, and platelets), it could not simply be identified either as an "inflammometer" [317] or "therapeutic for inflammatory conditions" [318] in wound healing. As a matter of fact, NO has both anti-inflammatory and pro-inflammatory properties depending on the type and phase of the inflammatory reaction. For example, production of large amounts of NO by activated macrophages accounts for their ability to suppress lymphocyte proliferation [319]. Given the fact that prolonged and uncontrolled inflammation delays the subsequent phases of wound healing leading to the slow down or even impediment of the healing process, such as diabetic wounds, curcumin is more likely to modulate inflammatory responses via anti-inflammation so that the damaged skin can more readily access the following phases of wound healing. In our study, we showed that through MCP-1 mediation, curcumin induced inhibition of inflammatory cell infiltration existed lastingly through the entire healing process (Figure 25), not just in the inflammatory phase. This means bioactive curcumin released from the topical applied Cc/Glt NM exhibits persistant anti-inflammatory effects during wound healing. This is complementary to the knowledge [320] (Figure 27). However, further work is still needed to fully elucidate curcumin's function of immunomodulation in this complex physiological process of wound healing.

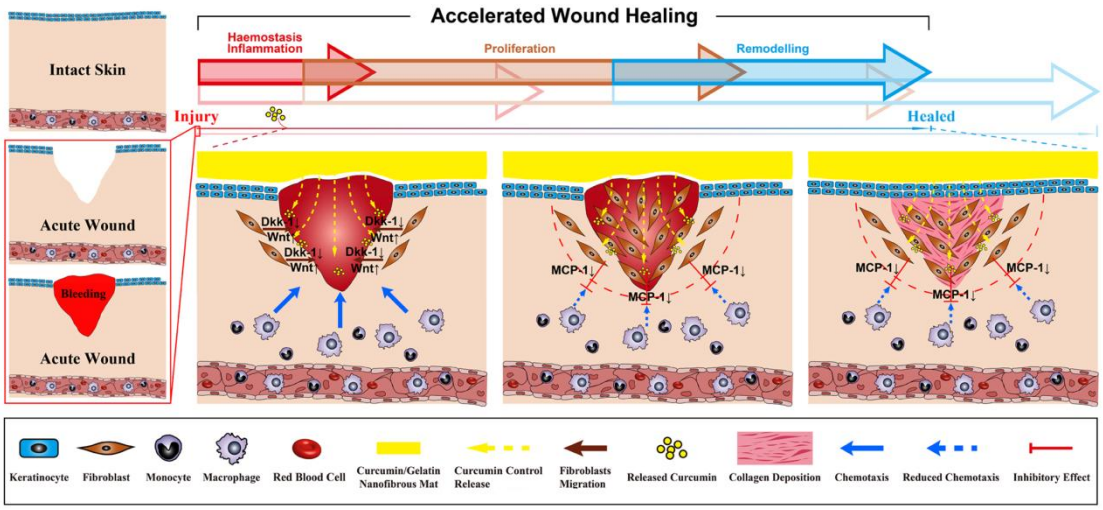

Figure 27: Scheme of potential mechanism of curcumin induced accelerated wound healing. Upon injury, topically applied Cc/Glt NM leads to controlled release of bioactive curcumin, which in turn, mobilizes wound site fibroblasts through the enhancement of both cell proliferation and migration, a process partially mediated by Dkk-1 regulated Wnt/β-catenin pathway signaling. In the mean time, fibroblasts decrease the expression of MCP-1, which mediates monocyte/macrophage chemotaxis, leading to lasting inhibition of inflammatory responses during the healing process. As a result, the wound environment turns out to be more in favor of later stages of wound healing, with faster re-epithelialization, granulation tissue formation as well as collagen deposition and maturation from proliferative fibroblasts.

Presumably, this is beneficial for the formation and maturaion of granulation tissue, because it protects the newly formed granulation tissue from degradation by proteases, particularly the matrix metalloproteinases (MMPs) produced by the immune cells like macrophages and neutrophils [321]. Studies have also shown that the prolonged exposure of wound tissues to pro-inflammatory cytokines, e.g. interleukin (IL-1) and tumor necrosis factor (TNF-α), may act to stimulate the production of MMPs [322] while inhibiting the synthesis of tissue inhibitors of metalloproteinases (TIMPs) [323]. As a matter of fact, MCP-1 has recently been shown to upregulate MMP-1 and MMP-2

mRNA expression in human skin fibroblasts, in which IL-1α has been found to take part as the mediator through an autocrine loop [324]. This is consistant with the observation that the improved response *in vivo* is only evident in the later stages of wound healing. In this study, we did observe improved granulation tissue formation, accompanied by more collagen deposition with higher quality (Figure 23,24,26), which comfirmed our previous result that curcumin induces fibroblast proliferation and migration, because granulation tissue is mainly formed by small capillaries and fibroblasts, which produce extra cellular matrix(ECM) [76]. Our findings are also consistent with what has been reported previously, that curcumin promotes granulation tissue formation through TGF-β, induces angiogenesis, stimulates fibroblast chemotaxis and proliferation, and induces the synthesis and release of matrix proteins. Similarly, these effects have been found to continue through to the remodeling phase of wound repair [325]. Based on findings in open excisional wounds in diabetic rats, Kant V et al. recently reported that curcumin application caused markedly faster wound closure with well-formed granulation tissue dominated by fibroblast proliferation, collagen deposition, enhanced neovasculogenesis with increased microvessel density and early completion of the regenerated epithelial layer [326]. In a study by Nguyen et al. 10% curcumin loaded chitosan-alginate sponges demonstrated a better wound closure, more advanced granulation tissue and collagen alignment in rabbit wounds compared to the composite sponge without curcumin and non-treatment [327]. Similarly, in a rat model, collagen content was shown higher in chitosan-alginate sponge (C2A2) treated wounds compared to gauze-treated control wounds. The resulting collagen appeared to be thicker, more compact and well-aligned [328]. Given the fact that collagen is the major protein in skin ECM (70-80% of skin[306]) and wound repair finally leads to the formation of scar tissue being composed mostly of collagen fibers, substantial collagen deposition at the wound site facilitates wound healing.

In the final phase of the wound healing, re-epithelialization (overlap with other phases), the process where keratinocytes migrate from the lower skin layers and divide, should be robust enough to restore adequate barrier function of the epidermis. In our study, curcumin has been shown to promote re-epithelialization. Similarly, Sidhu et al. evaluated the efficacy of curcumin treatment by oral and topical applications on impaired wound healing in diabetic rats and genetically diabetic mice using a full thickness cutaneous punch wound model and found earlier re-epithelialization together with increased migration of dermal myofibroblasts and fibroblasts in wounds treated with curcumin [329]. Comparable results have also been found in a rat model of burn wounds [330]. Panchatcharam et al. scrutinized the role of topically applied curcumin on cutaneous wound healing in rats and proved that curcumin reduced the epithelialization period of the treated wounds significantly from 23 days to 11 days when compared to the control group. It also increased cellular proliferation and collagen synthesis at the wound site, as evidenced by increased DNA, total protein and type III collagen content in wound tissues. Histopathological examinations confirmed wound contraction with enhanced tensile strength. Using biochemical techniques they further demonstrated that curcumin decreased the levels of lipid peroxides (LPs), while it significantly increased the levels of superoxide dismutase (SOD), catalase (CAT), glutathione peroxidase (GPx) activities, indicating the antioxidant properties of curcumin. All these results suggest different roles curcumin plays in accelerating wound healing especially in the later proliferative and remodeling phase[133]. Accumulating evidence shows that the presence of persistent inflammatory stimuli with prolonged inflammatory response consisting of neutrophils and macrophages are characteristics associated with impaired wound healing among patients with diabetes [331]. From our data, it is highly possible that fastly mobilized fibroblasts in combination with inhibition of degrading cells lead to an earlier formation and maturation of the granulation tissue with quicker and better re-epithelialization

by the surrouning epithelium. If this were indeed the case, the engineered Cc/Glt NM would stand a good chance at improving problematic wounds such as diabetic chronic ulcers.

In terms of scar formation, which is a natural outcome towards the end of normal wound healing, a complex series of interactions between cells, cytokines, growth factors, proteases and their inhibitors and ECM components is indispensable before a wound progresses to fibrous scar [332]. Interestingly, Scharstuhl et al. reported that curcumin treatment in high doses induces fibroblast apoptosis through the generation of reactive oxygen species (ROS) and proposed that it may provide novel way to modulate pathological scar formation under the fine-tuning regulation of antioxidants, heme oxygenase (HO) activity and its effector molecules [297]. Since curcumin itself has been widely known for its anti-oxidant effect in wound healing [333], more works are needed to reveal the way by which curcumin accurately act to regulate the complicated biological process for an improved wound healing.

Preclinical evaluation of acute wound healing includes animal models of full thickness skin defects, usually in the mouse and rat [334,335], but also in large animals such as porcine [336]. We used here rat skin defects to answer questions about the biocompatibility of the engineered material and more importantly, help elucidate the potential mechanisms of curcumin for accelerated wound healing before putting them into a clinical setting. The rodent system remains the model of choice for mechanistic investigation of the healing process [337,338]. But as loose-skined animal, the rat does not perfectly mimic human skin wound healing mostly due to the post wounding contracture caused by an extensive subcutaneous striated muscle layer (panniculus carnosus) which is largely absent in humans [339]. Our data from early wound closure suggests a superior performance of topical NM over the initial wound contracture. The healing process in this model also provides

sound evidence of enhanced bioavailability of curcumin that in turn exhibits prominent healing capacity through multiple mechanisms. It is worth mentioning that this simply engineered Cc/Glt NM may be well suited for future biological studies of curcumin, both *in vivo* and *in vitro*, without the fear of possible toxicity by using organic solvents like dimethyl sulfoxide (DMSO) for the enhancement of curcumin's aqueous solubility, which used to be very common [136].

5.4. Electrospun Cc/Glt NM could be a benificial complement to current wound therapy

In this study, we nano-formulate curcumin via electrospinning to improve its bioavailability and proved that topical application of the Cc/Glt NM significantly accelerated wound healing through synergistic effects between biomimetic NM and bioactive curcumin. Thus, the simple approach to engineer a smart integrated system that can act as a mechanically competent carrier as well as topically applied agent may be promising to open an avenue to translate this ancient medicine for modern wound therapy. However, it must be stressed that our current conclusions are based on research data from an animal model of normal physiological wound healing (Class I/Clean wounds), from a clinic point of view, a clean wound or wound with thorough debridement is a prerequisite for topical application of such medicated nanofibrous mat, as foreign body or bacteria from a contaminated wound inevitably lead to persistent or uncontrollable inflammatory responses. Likewise, for more complicated chronical or non-healing wounds such as diabetic wounds, which have not yet been investigated in this study, more work is still needed to explore the healing potential of the engineered Cc/Glt NM. As a matter of fact, when dealing with a wound, a comprehensive regime of wound treatment combining several techniques will usually be necessary.

For acute wounds, although curcumin has shown some antibacterial activity (usually at high doses) [340], it can not be considered to be comparable to special debriding agents in cleaning the wound bed. Therefore, topically applied Cc/Glt NM will not be deemed to be able to debride the wound either. For better therapeutic effects of the Cc/Glt NM, wound preparation is of vital importance. This is usually done with **debridement**, which is crucial for the clearance of nonviable or foreign material and reducing the bioburden to prepare the wound for healing. Although the importance of adequate debridement has been widely accepted, there is still controversy on whether the eschar, begining as a *pseudoeschar* which is a provisional matrix formed from exudated serum components at the wound, should be debrided when it accumulates[341]. Debridement is typically deemed to be surgical, but it may also be performed through the use of proper dressings and debriding agents with enzymatic, mechanical, autolytic or biologic effects. Enzymatic debridement is a highly selective method that uses naturally occurring proteolytic enzymes in an attempt to digest necrotic tissue without damaging healthy tissue, such as collagenase and papain. Collagenase specifically breaks down native collagen but is gentle on viable cells. However, papain is a nonspecific proteolytic enzyme, it breaks down fibrinous material in necrotic tissue but requires the presence of sulfhydryl groups (eg, cysteine) found in such tissue to stimulate its activity[342]. Furthermore, enzymatic agents prevent the crosslinking of exudated components and impede the forming of pseudoeschar. When it is applied together with some dressings (such as hydrocolloid dressings) that are able to rehydrate hardened scab tissue, they facilitate the autolytic debridement as pseudoschar can then be phagocytosed by wound leukocytes. Recently, another effective mechanical debridement through pressurized irrigation has been proposed, such as the VersaJet system (Smith&Nephew, Largo, FL), which has the ability to penetrate into microcrevasses in the wound bed to flush out entrapped particulate matter as

well as bacteria. It is indicated for use in wounds with concavities, necrotic wounds and deep burn wounds [343]. The term "*biodebridement*" refers to the use of medicated larvae (myiasis or maggot therapy), which can be remarkably efficacious in removing devitalized material while sparing viable, well-perfused tissue. Commercialized maggot is available due to the ability of breeding sterile flies, such as the green bottle fly, *Lucilia (Phaenicia) sericata* [344]. With this approach, larvae can be left in place for 3 days but need to be changed once the pain increases due to a change in wound pH [345]. The nanoscaled pores in the NMs have been shown to be impermeable to bacteria [346], so once the wound is debrided, the NMs will keep it clean. Thus, topically applied Cc/Glt NM is expected to aid wound healing in multiple ways.

To date, a general principal of wound treatment could be briefly described as:

- **Optimize systemic parameters**
- **Debride** nonviable tissue and reduce the wound bioburden
- **Optimize blood flow** (Warmth, Hydration, Surgical revascularization)
- **Eliminate edema** (Elevation, Compression)
- **Wound dressings** (biologic dressings selection with attention to cost-effectiveness of overall treatment) aiming to: moist wound healing, exudate removal and avoidance of additional pain or injury by dressing change
- **Pharmacologic therapy**
- **Surgical procedure** with grafts or flaps as indicated

With these in mind, it could be easier for wound practioners to judge whether or not Cc/Glt NM should be applied or when shall be an appropriate timing to apply it as non-invasive approch for wound healing in a larger context. Under such circumstance, all acute wounds should be evaluated initially to determine the mechanism before any approach for treatment is outlined, with special emphasis on identifying the cause of the wound and any complications that might influence healing, for instance, patient's medical status or mode of injury

that may lead to healing difficulties or threat of a turnover to a problem wound. These include age, ischemia, infection, malnutrition, tobacco and alcohol use, diabetes, cancer, reperfusion injury, foreign bodies, edema, pressure, irradiation, chemotherapy, to name just a few [347]. From a clinical view, **age**, **ischemia**, and bacterial **infection** are most common causative factors that will threaten the natural healing process. Thus, adequate vigilance and proper countermeasures are essential to address these risk factors so as to effectively manage most of the wounds before they become problematic. Many studies have also been engaged in an attempt to uncover the cellular and molecular basis for these risk factors. For aging, laboratory evidence indicates that molecular processes important for tissue repair in aged fibroblasts declined, which leads to decreased production of growth factors and collagen or other matrix molecules [348]. Damaged small vessels in the injury, on the other hand, induce a hypoxic wound environment, with an estimated average oxygen tensions dropping from 40 mmHg in normal tissues to 25 mmHg in the wound [349]. With this in mind, surgical and nonsurgical interventions can be undertaken to maximize oxygen delivery to tissues. "All wounds are contaminated." - Even wounds that are considered clean have a bacterial inoculum. The existence of excessive numbers of bacterial (10^5 bacteria per gram) is considered to interfere with wound healing [350], and an important mechanism of tissue hypoxia leading to wound infection is found to be the impairment of the "oxidative burst", a dramatic increase of oxygen-derived radicals to rule out bacteria from the wound. Interestingly, under constant infection or persistent inflammation, the normal defense process is prolonged and gives rise to excessive damage to normal cells by those oxygen-derived radicals [351]. Sometimes, to help evaluate the local or systemic condition of the wound patient, it is necessary to choose appropriate diagnostic tests, including useful clinical laboratory tests such as albumin, pre-albumin and transferrin levels (nutritional status); C-reactive protein and the erythrocyte sedimentation rate (markers of inflammation), complete blood count (white

blood cell numbers or if anemia is present) and in addition, laboratory tools like transcutaneous oxygen pressure (tcPO2) measurements, and so on and so forth.

Also, whether Cc/Glt NM could be applied alone or in combination with other techniques should also been considered. As our results in this study show that additionally to the current concept, the tissue response can be modulated on a cellular level through topical application of Cc/Glt NM alone, there may be room for improvement of its therapeutic ability - patients may take further advantage of combination therapy when Cc/Glt NM is in coalition with or supplementary to currently practiced surgical or non-surgical techniques for wound management. For example, **Negative-pressure wound therapy (NPWT)** or **vacuum assisted closure (VAC)**, has been a tremendous advance for wound care since its first approval by US Food and Drug Administrationthe (FDA) in 1995 [352]. It consists of a porous sponge covered by an air tight occlusive dressing and a vacuum pump to generate negative pressure. NPWT works through a series of mechanisms such as reducing edema by removing wound exudate so as to enhancing interstitial diffusion of oxygen to cells and removing deleterious enzymes (as well as bacteria derived proteases) and bacteria so as to modify the wound microenvironment toward one more conducive to healing. From clinical observation, a negative pressure of 100-125 mmHg in a continuous or intermittent manner [353] seems beneficial for most wounds. However, patients with ischemia, poorly debrided or badly infected wounds, are not indicated for the NPWT.

In some special cases, **hyperbaric oxygen (HBO)** is another option to aid wound healing by raising the oxygen saturation. It has been reported that the blood oxygen content is increased 2.5% at 2.0 ATA (absolute atmosphere), which achieves sufficient tissue oxygen tensions (10 fold higher) even when the haemoglobin-bound oxygen is absent [354]. Therefore, adjunctive HBO

therapy is a safe and effective modality to aid in healing of difficult wounds. Although the majority of the literature surrounding HBO therapy supports its use in chronic wounds without direct indication in normal wound management, it was reported to augment healing in complicated acute wounds when combined with standard wound management principles [24,25]. Further investigation is required here. Other non-surgical approaches have been advocated in wound treatment including stem cell based therapy [355], radiant heat dressing, ultrasound therapy, laser treatment, hydrotherapy, electrotherapy and electromagnetic therapy [356]. However, controlled studies and prospective clinical trials are needed to evaluate the effectiveness of these treatments before wide clinical practice.

Pharmacologic therapy is another very important approach that is usually combined with wound dressings or other measures for improved wound healing. Systemic as well as local treatment of patients with wounds can be directed at several physiological aspects of healing during the consecutive phases of tissue repair, many of which have been tested in vitro, in animal experiments, or in clinical studies. For example, studies show that Phenytoin, applied topically, promotes wound healing by inhibiting the enzyme collagenase[357]. Retinoids (derived from vitamin A) also have been shown in well documented studies to have an impact on wound healing through their effects on angiogenesis, collagen synthesis, and epithelialisation [358]. Moreover, the development of new synthetic methods allows rapid access to new pharmaceutical and medicinal compounds for wound healing. Here some most commonly used phamaceuticals are briefly discussed. **Growth factors** are naturally occurring proteins control many key cellular activities during normal tissue repair process. They can be produced either autogenously by body's platelets or macrophages exteriorly by recombinant approaches. Multiple studies have indicated that exogenous application of growth factors such as PDGF, EGF, bFGF to wound surface benefit the healing process [359].

The fact that topical wound care with growth factors appears to be effective in well-prepared wound beds may possibly be due to the fact that prolonged stay of proteases in problem wounds will rapidly degrade the peptide growth factors [360]. **Antimicrobials** are very important to control wound infection. Some antiseptics that usually are used for debridement could also be used on open wounds to kill or inhibit microorganisms with a broad antimicrobial spectrum, such as hydrogen peroxide, chlorhexidine and iodophors. Iodines have been used for more than 150 years without inducing drug resistance and its modern formulations, like the cadexomer iodine, offer sustained delivery of low levels of free iodine to the wounds [361]. Silver also has been shown efficacy against wound pathogens, such as methicillin-resistant Staphylococcus aureus (MRSA) and vancomycin-resistant enterococci (VRE) [362]. Other new agents such as recently approved super-oxidized water [363], antimicrobial peptides that are rapidly bactericidal against a broad spectrum of organisms are also proven to be effective [364]. Topical antimicrobials, on the other hand, are chemicals produced either naturally (by a microorganism) or synthetically that have traditionally been formulated as occlusive ointments or creams, which are less occlusive. For example, Neomycin (against most aerobic gram-negative rods and staphylococci), Polymixin (against some gram-negative rods) and Bacitracin (against most gram-positive organisms) are combined in a nonprescription ointment commonly used on wounds by patients and some providers [365].

It should be noted that whatever the approach, the primary objective in all these attempts is to achieve a healed wound. Certainly, more studies are in urgent need in this setting to quicken our pace to translate novel findings to modern wound therapy. Finally, with deeper understanding of wound pathophysiology, modern wound therapy is undergoing a constant change and new theories and techniques are being introduced frequently. Therefore, we must always keep abreast of advances in wound treatments that are on the

horizon.

6. GENERAL CONCLUSIONS AND PERSPECTIVES

In conclusion, we show here a simple approach to engineer a smart integrated system that can act as a mechanically competent carrier which can topically deliver bioactive curcumin to wounds and thereby improve wound healing. Curcumin was successfully formulated as amorphous nanosolid dispersion and favorably released from gelatin based biomimetic nanofibrous mats that could be easily applied topically to experimental wounds. We show synergistic signaling by the released curcumin during the healing process: (i) mobilization of wound site fibroblasts by activating the Wnt signaling pathway, partly mediated through Dkk-1; (ii) persistent inhibition of the inflammatory response through decreased expression of MCP-1 by fibroblasts. With a combination of these effects, the curcumin/gelatin blended nanofibrous mats enhanced the regenerative process in a rat model of acute wounds, opening an avenue to translate this ancient medicine for modern wound therapy. We believe that continuous research will increase the understanding of wound healing for which curcumin may be beneficial and we hope that future clinical trials will lead to the development of curcumin as a wound healing agent.

7. APPENDIX

Publications by PhD candidate 2012-2016

Awards / stipends

State Scholarship Fund (China Scholarship Council, CSC NO.201208310668), 2012

John D. Constable International Traveling Fellowship (American Ascociation of Plastic Surgeons, AAPS), 2014

Published peer reviewed papers

Xinyi Dai , Juan Liu , Huaiyuan Zheng , Johannes Wichmann , Ursula Hopfner , Stefanie Sudhop , Carina Prein , Yi Shen , Hans Machens, Arndt Schilling. Nano-formulated curcumin accelerates acute wound healing through Dkk-1 mediated fibroblast mobilization and MCP-1 mediated anti-inflammation . NPG Asia Materials. (accepted 15th Dec 2016 01:43:57)

Dai X, Nie W, Wang YC, Shen Y, Li Y, Gan SJ. Electrospun emodin polyvinylpyrrolidone blended nanofibrous membrane: a novel medicated biomaterial for drug delivery and accelerated wound healing.
J Mater Sci Mater Med. 2012 Nov;23(11):2709-16

Winkler T, **Dai X**, Mielke G, Vogt S, Buechner H, Schantz J, Harder Y, Machens H, Morlock M, Schilling AF. Three-Dimensional Quantification of Calcium Salt-Composite Resorption(CSC) In Vitro by Micro-computed Tomography (Micro-CT). JOM 04/2014; 66(4):559-565

Zheng H, Liu J, **Dai X**, Schilling AF. The Distally Based Sural Flap for the Reconstruction of the Ankle and Foot Defect in Pediatric Patients. Ann Plast Surg. 2014 Sep 3. [Epub ahead of print]

Zheng H, Liu J, **Dai X**, Schilling AF. Modified technique for one-stage treatment of proximal phalangeal enchondromas with pathologic fractures. J Hand Surg Am. 2014 Sep;39(9):1757-60. doi: 10.1016/j.jhsa.2014.06.131. Epub 2014 Aug 5

Zheng H, Liu J, **Dai X**, Schilling AF. Free conjoined or chimeric medial sural artery perforator flap for the reconstruction of multiple defects in hand. J Plast Reconstr Aesthet Surg. 2015 Apr; 68(4):565-70. doi: 10.1016/j.bjps.2014.12.031. Epub 2014 Dec 29.

Zheng H, Liu J, **Dai X**, Machens HG, Schilling AF. Free lateral great toe flap for the reconstruction of finger pulp defects. J Reconstr Microsurg. 2015 May;31(4):277-82. doi: 10.1055/s-0034-1396754. Epub 2015 Jan 28

Eberlin KR, Del Frari B, **Dai X**, Austen WG Jr. The John D. Constable International Traveling Fellowship: A Reciprocal Education in Plastic Surgery. [J] Craniofac Surg. 2015 Jun;26(4):1050-2

Liu J, Zheng H, Chen Z, **Dai X**, Schilling AF, Machens HG. Dorsal plane-shaped advancement flap for the reconstruction of web space in syndactyly without skin grafting: A preliminary report. J Plast Reconstr Aesthet Surg. 2015 Nov;68(11):e167-73. doi: 10.1016/j.bjps.2015.06.016. Epub 2015 Jun 27

Oral presentations:

19. Chirurgische Forschungstage, Würzburg, Germany. 2015 Oct 8-10
Electrospun curcumin-gelatin blended nanofibrous membrane for cell-scaffold based dermal regeneration and accelerated wound healing.

Poster presentations:

4th TERMIS World Congress, Boston, MA, USA. 2015 Sept 8-11
Electrospun curcumin/gelatin blended nanofibrous membrane: a novel medicated biomaterial for drug delivery and accelerated wound healing.

8. ACKNOWLEDGEMENTS

Nur Beharrung führt zum Ziel,

Nur die Fülle führt zur Klarheit,

Und im Abgrund wohnt die Wahrheit.

- Sprüche des Confucius,

Friedrich von Schiller

只有恒心能助你达到目的，

只有博学能使你明辨世事，

真理往往藏在事物的深底。

–孔子箴言

弗里德里希·冯·席勒

This piece of work is by far the hardest project I have ever completed, it represents not just several months of assiduous typewriting, but years of work at TUM and specifically within the Plastic Surgery Research Laboratory here at *Klinikum rechts der Isar*, where my experience has been nothing short of amazing. I still clearly remember the hazy dawn of Oct. 1st, 2012, when I first stepped onto this incredibly fascinating land of Bavaria, seeing a veil of thin, white mist hanging halfway on a line of thick pine trees just behind a vast expanse of fertile farmland - I was totally obsessed by its stunning beauty and could not help but reminiscent of my own nostalgic birthland of Suzhou, an exquisite, alluring oriental watery town said to be terrestrial paradise beneath heaven - it touches my heartstring so much!

Throughout these years my passion is to expand my limited knowledge boundary and seek interdisciplinary innovation in tissue engineering and regenerative medicine for ultimate clinical translational studies, during which time I have deeply learned that "*Truth always hides in the depth of things*". This thesis presents the lessons I learned over these years alongside the captivating river *Isar* and *Englischer Garten*, it is the result of work by dozens of people, who I wish to thank; it is alto the result of many experiences I have encountered in Germany as well as in the United States and China from dozens of remarkable organizations and individuals who I also wish to acknowledge.

First and foremost I wish to thank my advisor Prof. Dr. **Arndt F. Schilling**, research director of the Experimental Plastic Surgery Laboratory. I appreciate all his contributions of time, ideas, and advise during my study. He has been supportive not only with academic instruction, but also with emotional assists to get the most out of my stressful moment whenever I felt lost through the rough road towards my goal. I remember he used to say something like "Time is ticking" to encourage me to stay in the lab - Thanks to him that I was taught, both consciously and unconsciously, how man seeks the truth through depth of things, otherwise science could be complete Sphinx's riddle far out of my reach.

My thesis committee guided me through all these years. I could not have asked for a better mentor than Prof. Dr. med. **Hans-Günther Machens**, not only for the opportunity to let me join his great team at the very beginning, that I had several wonderful years in Munich, but also for his supervision, support and encouragement throughout my study. His expertise, understanding and patience added considerably to my study experience, his generosity and open personality make him a perfect teacher and helpful friend. My gratefulness as well to PD. Dr. **Rainer Burgkart**, not only for his supervision and assistance at all levels for the research project, but also for his especially amiable Bavarian conversation each time with me, to get rid of my uneasiness stumbling my German. I am deeply grateful for everything you Sir did for me!

Dozens of people have taught and helped me immensely at the TUM Plastic Surgery Research laboratory: **Ursula Hopfner** welcomed me in the office the first day to my work, she and **Manu Kirsch**, **Simone Schmalix**, **Debbi Tibebu**, **Mark di Frangia** have been major technical assistance and a source of friendship ever since. There are also students before me that helped in many ways: Dr. **Ziyang Zhang** helped me established contact with Professors here at TUM and prepare all necessary documents before I came to Germany, **Lili Wu**, **Elizabeth Wahl** and **Maymi Chávez** shared their personal experimental experiences with me. I also wish to acknowledge the many other students who have been working in the research laboratory with me: **Lissi Grünherz**,

Philipp Moog, **Anna Bauer**, **Cordelia Reinshagen**, **Anna Schuldt**, **Fabian Weiss** and so on. A special acknowledgment goes to my earlier office mate: Dr. **Tatjana Perisic**, she is an amazing person in too many ways.

I would like to sincerely thank all our collaborators, without whom this project would not have been possible. Dr. **Juan Liu** and Dr. **Huaiyuan Zheng**, both being excellent surgeons and very good friends of mine, have made enormous contributions to this project. A special group is not mentioned yet, because they deserve their own part: **CANTER** (Centrum für Angewandte Naturwissenschaften, Tissue Engineering und Regenerative Medizin), a joint research laboratory from Technische Universität München (TUM), Ludwig-Maximilians-Universität München (LMU) and Hochschule München. Prof. Dr. **Clausen Schaumann** has always been supportive whenever I needed to perform experiments at the CANTER lab, from the majestic castle building to the more modernized one later on; I am thankful for the enormous amount of help and teaching by Dr. **Stefanie Sudhop**, who offered me expertise and professional skill in molecular biology and the handling of polarized microscopy, **Carina Prein** had paid countless hours for hands-on guidance in using Atomic Force Microscope. Thank you as well to those who helped the progress of this project as staff and students: **Johannes Wichmann** shared his personal experience in handling macrophages; Dr. **Yi Shen** helped me establish animal facilities and all necessary documents. I also

recognize valuable advice and help from visiting scholars, Prof. **Xiaofeng Cui** (Wuhan University of Technology), Dr. **Mohit Chhaya** and Dr. **Poh Patrina** (Queensland University of Technology) and Dr. **Michelle McLuckie** (Eidgenössische Technische Hochschule Zürich) - I am very grateful for the knowledge and support I got from everyone of you.

The successful completion of this project would neither have been possible without the kind help of all individuals from different institutes, who unselfishly donate or share their professional knowledge and talent: Dr. **Qing Zhao** (LMU) and Dr. **Lisa Gfrerer** (Harvard Medical School) for cell biology and genome editing techniques; Dr. **Piul Rabbani** (New York University) for scaffold based gene delivery system; Dr. **Qiongyu Guo** (Johns Hopkins University School of Medicine) and Dr. **Wei Nie** (Donghua University) for Polymeric biomaterials and control release systems in Tissue Engineering.

I would like to acknowledge Ms. **Katrin Offe** and Ms. **Desislava Zlatanova** at the TUM's Medical Graduate Center/Faculty Graduate Center Medical Life Science and Technology, for their patience and support from the first day I was luckily enrolled into this perfect PhD program and ever since thereafter.

In regards to the organizations, I gratefully acknowledge the **Chinese Scholarship Council** (CSC), by which I have been luckily admitted in 2012, the first of its kind, as few employed personnel rather than University students

for the PhD pursuit overseas - I could not have made my PhD work possible without its financial support. I sincerely appreciate **General Konsulat der Volksrepublik China in München** and its Consul for Education, Mr. **Jiqiang Dai** and Ms.**Chongying Huang** for all their support, care and help throughout my foreign study and stay - motherland has never left me alone wherever I go. My great appreciation is yet to Dr. **Constable** and the John D. Constable Fellowship Committee of **American Association of Plastic Surgeons** (AAPS), its Associate Executive Director Ms. **Rebecca Bonsaint** and chiefs of plastic surgery divisions from three US institutions: Prof. **W.G. Austen Jr**. of Massachusetts General Hospital; Prof. **Eduardo D. Rodriguez** of NYU Langone Medical Center and Prof. **W.P. Andrew Lee** as well as Prof. **Gerald Brandacher** of Johns Hopkins Hospital, under whose kind invitation and support I could have one fulfilling and rewarding experience in the US as the 2014 Constable Fellow through TUM-GS's "Go International Program", where I met a group of amazing people, who have been an inspiration on making things perfect.

Special thanks to Prof. **Cory Sandone** from the department of art as applied to medicine, Johns Hopkins University School of Medicine, for her kind invitation to let me visit the great institute and attend the Surgical Illustration Critique, where I had a chance to know many talented medical illustrators, including Ms. **Wenjing Wu** from Memorial Sloan-Kettering Cancer Center, NewYork City,

who has helped a lot with useful advice in scientific illustration in this project.

My time at TUM was made enjoyable in large part due to these many friends and groups that became a part of my life. I am grateful for time spent with roommates and friends, for my backpacking buddies and our memorable accidental trip into *Tegernsee*, for **Nico Sollmann** and **Cem Saracel**'s hospitality, and for many other people and memories. My time at TUM was enriched by the internationalized PhD student group, **Agnieszka Pastuła**, **Giovanni Magnani**, **Liang Song**, **Zhifen Chen**, **Jiaoyu Ai**, **Christian Veltkamp**, **Shwetha Lm**, **Aayush Gupta**, **Kalliope Nina Diakopoulos**, **Anuja Sathe**... so many that I can just name a few.

None of this would have been possible without the love and patience of my family, to whom I would like to express my heart-felt gratitude, because it has been my constant source of love, concern, support and strength all these years. I would like to thank my parents who raised me with love and supported me with heart and soul in all my pursuits, especially for all burden they quietly withstood for me when my father underwent grueling chemotherapy while I was in Germany. As our Chinese saying goes, "The thread in a caring mother's hands becomes the sweater of her son outside" - Wherever the kids go, they are always accompanied by their parents' love.

I dedicate this thesis to my wife and my beloved daughter, for their

understanding, sacrificed and unconditional love and care - you are my world, I love you all dearly! My little diamond, daddy's gonna graduate from the Munich kindgarden - just like you!

„*Zu Hause in Bayern, erfolgreich in der Welt.*“ - Thank you **Technische Universität München**. I am honored to have been with you, and I'll be proud to be with you wherever I go.

9. REFERENCES

1. Shweiki E, Gallagher KE (2013) Negative pressure wound therapy in acute, contaminated wounds: documenting its safety and efficacy to support current global practice. Int Wound J 10: 13-43.
2. Demidova-Rice TN, Hamblin MR, Herman IM (2012) Acute and impaired wound healing: pathophysiology and current methods for drug delivery, part 1: normal and chronic wounds: biology, causes, and approaches to care. Adv Skin Wound Care 25: 304-314.
3. Franz MG, Steed DL, Robson MC (2007) Optimizing healing of the acute wound by minimizing complications. Curr Probl Surg 44: 691-763.
4. Talbot SG, Pribaz JJ (2010) First aid for failing flaps. J Reconstr Microsurg 26: 513-515.
5. Shimizu F, Okamoto O, Katagiri K, Fujiwara S, Wei FC (2010) Prolonged ischemia increases severity of rejection in skin flap allotransplantation in rats. Microsurgery 30: 132-137.
6. Horner BM, Eberlin KR, Ferguson KK, Hirsh EL, Randolph MA, et al. (2008) Recipient damage after musculocutaneous transplant rejection. Transplantation 86: 1104-1110.
7. Kroll SS, Schusterman MA, Reece GP, Miller MJ, Evans GR, et al. (1996) Timing of pedicle thrombosis and flap loss after free-tissue transfer. Plast Reconstr Surg 98: 1230-1233.
8. Leaper DJ, Schultz G, Carville K, Fletcher J, Swanson T, et al. (2012) Extending the TIME concept: what have we learned in the past 10 years?*. International Wound Journal 9: 1-19.
9. Millington PF, Wilkinson R (1983) Skin: Cambridge University Press.
10. Qin Y (2015) Medical Textile Materials: Elsevier Science.
11. Haj-Ahmad R, Khan H, Arshad MS, Rasekh M, Hussain A, et al. (2015) Microneedle coating techniques for transdermal drug delivery. Pharmaceutics 7: 486-502.
12. Bensouilah J, Buck P (2006) Aromadermatology: Aromatherapy in the Treatment and Care of Common Skin Conditions: Radcliffe.
13. Gawkrodger D, Ardern-Jones MR (2012) Dermatology: An Illustrated Colour Text: Elsevier Health Sciences UK.
14. McGrath J, Uitto J (2010) Anatomy and organization of human skin. Rook's Textbook of Dermatology, Eighth Edition: 1-53.
15. Brenner M, Hearing VJ (2008) The protective role of melanin against UV damage in human skin. Photochemistry and photobiology 84: 539-549.
16. Reviews C (2016) Fundamentals of Anatomy and Physiology: Biology, Anatomy: Cram101.
17. Romani N, Clausen BE, Stoitzner P (2010) Langerhans cells and more: langerin-expressing dendritic cell subsets in the skin. Immunological reviews 234: 120-141.
18. Becker Y (2012) Skin Langerhans (Dendritic) Cells in Virus Infections and AIDS: Springer US.
19. Streilein J, Bergstresser P (1984) Langerhans cells: antigen presenting cells of the epidermis. Immunobiology 168: 285-300.
20. Herring N, Wilkins R (2015) Basic Sciences for Core Medical Training and the MRCP: OUP Oxford.

21. Mishra A, Panola R, Vyas B, Marothia D, Kansara H Topical antibiotics and Semisolid Dosage Forms.
22. Dhurve R (2015) A Holistic Review on Ethosome A Promising Drug Delivery System for Topical Fungal Disease. International Journal of Pharmaceutical & Biological Archive 5.
23. Son JH (2014) Terahertz Biomedical Science and Technology: Taylor & Francis.
24. Mitchell T, Kennedy C (2006) Common Skin Disorders: Elsevier/Churchill Livingstone.
25. Albanna M, Holmes JH (2016) Skin Tissue Engineering and Regenerative Medicine: Elsevier Science.
26. Hamblin MR, Avci P, Prow T (2016) Nanoscience in Dermatology: Elsevier Science.
27. Tracy LE, Minasian RA, Caterson EJ (2016) Extracellular Matrix and Dermal Fibroblast Function in the Healing Wound. Adv Wound Care (New Rochelle) 5: 119-136.
28. Habif TP (2009) Clinical Dermatology: Elsevier Health Sciences.
29. Reviews C (2016) Human Anatomy and Physiology: Cram101.
30. Schade H, Marchionini A (1928) Zur physikalischen chemie der hautoberfläche. Archives of Dermatological Research 154: 690-716.
31. Menon GK, Norlén L (2002) Stratum Corneum Ceramides and Their Role. Skin Moisturization: 31.
32. McGrath JA, Uitto J (2008) The filaggrin story: novel insights into skin-barrier function and disease. Trends in molecular medicine 14: 20-27.
33. Madison KC (2003) Barrier function of the skin: "la raison d'etre" of the epidermis. J Invest Dermatol 121: 231-241.
34. Lee SH, Jeong SK, Ahn SK (2006) An update of the defensive barrier function of skin. Yonsei medical journal 47: 293-306.
35. Darlenski R, Kazandjieva J, Tsankov N (2011) Skin barrier function: morphological basis and regulatory mechanisms. J Clin Med 4: 36-45.
36. Hall JE, Guyton AC (2015) Guyton and Hall Textbook of Medical Physiology: Elsevier.
37. Bazett H (1930) Experiments on the mechanism of stimulation of endorgan for cold. American Journal of Physiology 93: 632.
38. Braun HA, Bligh J, Brück K, Voigt K, Heldmaier G (2012) Thermoreception and Temperature Regulation: Springer Berlin Heidelberg.
39. Arens EA, Zhang H (2006) The skin's role in human thermoregulation and comfort. Center for the Built Environment.
40. Romanovsky AA (2014) Skin temperature: its role in thermoregulation. Acta Physiol (Oxf) 210: 498-507.
41. Charkoudian N (2003) Skin blood flow in adult human thermoregulation: how it works, when it does not, and why. Mayo Clin Proc 78: 603-612.
42. Cauna N, Ross LL (1960) The fine structure of Meissner's touch corpuscles of human fingers. J Biophys Biochem Cytol 8: 467-482.
43. Biswas A, Manivannan M, Srinivasan MA (2015) Vibrotactile sensitivity threshold: nonlinear stochastic mechanotransduction model of the Pacinian Corpuscle. IEEE Trans Haptics 8: 102-113.
44. Scheibert J, Leurent S, Prevost A, Debregeas G (2009) The role of fingerprints in the coding of tactile information probed with a biomimetic sensor. Science 323:

1503-1506.
45. Skedung L, Arvidsson M, Chung JY, Stafford CM, Berglund B, et al. (2013) Feeling small: exploring the tactile perception limits. Scientific reports 3.
46. Darian-Smith I, Johnson KO, LaMotte C, Shigenaga Y, Kenins P, et al. (1979) Warm fibers innervating palmar and digital skin of the monkey: responses to thermal stimuli. J Neurophysiol 42: 1297-1315.
47. McKemy DD (2012) The molecular and cellular basis of cold sensation. ACS chemical neuroscience 4: 238-247.
48. Weston WL, Lane AT, Morelli JG (2007) Color Textbook of Pediatric Dermatology: Elsevier Health Sciences.
49. Kenins P (1981) Identification of the unmyelinated sensory nerves which evoke plasma extravasation in response to antidromic stimulation. Neuroscience letters 25: 137-141.
50. Dubin AE, Patapoutian A (2010) Nociceptors: the sensors of the pain pathway. J Clin Invest 120: 3760-3772.
51. Woolf CJ, Ma Q (2007) Nociceptors--noxious stimulus detectors. Neuron 55: 353-364.
52. Beaulieu P, Lussier D, Porreca F, Dickenson A (2015) Pharmacology of pain: Lippincott Williams & Wilkins.
53. Rost GA (1953) [Samuel Hafenreffer, author of the first textbood on dermatology in German speaking countries]. Z Haut Geschlechtskr 14: 227-230.
54. Greaves MW, Khalifa N (2004) Itch: more than skin deep. Int Arch Allergy Immunol 135: 166-172.
55. Bautista DM, Wilson SR, Hoon MA (2014) Why we scratch an itch: the molecules, cells and circuits of itch. Nat Neurosci 17: 175-182.
56. Andersen HH, Elberling J, Arendt-Nielsen L (2015) Human surrogate models of histaminergic and non-histaminergic itch. Acta Derm Venereol 95: 771-777.
57. Morita E, Matsuo H, Zhang Y (2005) Double-blind, crossover comparison of olopatadine and cetirizine versus placebo: suppressive effects on skin response to histamine iontophoresis. J Dermatol 32: 58-61.
58. Ikoma A, Steinhoff M, Stander S, Yosipovitch G, Schmelz M (2006) The neurobiology of itch. Nat Rev Neurosci 7: 535-547.
59. Zouboulis CC (2009) The skin as an endocrine organ. Dermato-endocrinology 1: 250-252.
60. Adorini L (2002) Immunomodulatory effects of vitamin D receptor ligands in autoimmune diseases. Int Immunopharmacol 2: 1017-1028.
61. Zouboulis CC (2009) Sebaceous gland receptors. Dermatoendocrinol 1: 77-80.
62. Leaper DJ, Harding KG (1998) Wounds: Biology and Management: Oxford University Press.
63. Kauvar DS, Wade CE (2005) The epidemiology and modern management of traumatic hemorrhage: US and international perspectives. Crit Care 9 Suppl 5: S1-9.
64. Alberdi F, Garcia I, Atutxa L, Zabarte M (2014) Epidemiology of severe trauma. Med Intensiva 38: 580-588.
65. Sen CK, Gordillo GM, Roy S, Kirsner R, Lambert L, et al. (2009) Human skin wounds: a major and snowballing threat to public health and the economy. Wound Repair Regen 17: 763-771.
66. (2015) Worldwide Wound Management, Forecast to 2024:

Established and Emerging Products, Technologies and Markets
in the Americas, Europe, Asia/Pacific and Rest of World. Market intelligence pp. 375.
67. Kea B, Fu R, Lowe RA, Sun BC (2016) Interpreting the National Hospital Ambulatory Medical Care Survey: United States Emergency Department Opioid Prescribing, 2006-2010. Acad Emerg Med 23: 159-165.
68. Zheng H, Liu J, Dai X, Schilling AF (2016) The Distally Based Sural Flap for the Reconstruction of Ankle and Foot Defects in Pediatric Patients. Ann Plast Surg 77: 97-101.
69. Zheng H, Liu J, Dai X, Schilling AF (2015) Free conjoined or chimeric medial sural artery perforator flap for the reconstruction of multiple defects in hand. J Plast Reconstr Aesthet Surg 68: 565-570.
70. Zheng H, Liu J, Dai X, Machens HG, Schilling AF (2015) Free lateral great toe flap for the reconstruction of finger pulp defects. J Reconstr Microsurg 31: 277-282.
71. Liu J, Zheng H, Chen Z, Dai X, Schilling AF, et al. (2015) Dorsal plane-shaped advancement flap for the reconstruction of web space in syndactyly without skin grafting: A preliminary report. J Plast Reconstr Aesthet Surg 68: e167-173.
72. Berard F, Gandon J (1964) Postoperative Wound Infections: The Influence of Ultraviolet Irradiation of the Operating Room and of Various Other Factors. Ann Surg 160: 1-192.
73. Mangram AJ, Horan TC, Pearson ML, Silver LC, Jarvis WR (1999) Guideline for Prevention of Surgical Site Infection, 1999. Centers for Disease Control and Prevention (CDC) Hospital Infection Control Practices Advisory Committee. Am J Infect Control 27: 97-132; quiz 133-134; discussion 196.
74. Zinn J, Swofford V (2014) Quality-improvement initiative: Classifying and documenting surgical wounds. Wound Care Advisor 3: 32-38.
75. Nicks BA, Ayello EA, Woo K, Nitzki-George D, Sibbald RG (2010) Acute wound management: revisiting the approach to assessment, irrigation, and closure considerations. Int J Emerg Med 3: 399-407.
76. Singer AJ, Clark RA (1999) Cutaneous wound healing. N Engl J Med 341: 738-746.
77. Enoch S, Grey JE, Harding KG (2006) Recent advances and emerging treatments. BMJ 332: 962-965.
78. Gurtner GC, Werner S, Barrandon Y, Longaker MT (2008) Wound repair and regeneration. Nature 453: 314-321.
79. Gibson DJ, Schultz GS (2013) Molecular Wound Assessments: Matrix Metalloproteinases. Adv Wound Care (New Rochelle) 2: 18-23.
80. Guo S, Dipietro LA (2010) Factors affecting wound healing. J Dent Res 89: 219-229.
81. Suzuki-Inoue K (2014) [Activation and inhibitory mechanisms of blood platelets]. Nihon Rinsho 72: 1212-1217.
82. Rodriguez ED, Neligan P, Losee JE, Warren RJ, Van Beek A (2012) Plastic Surgery: Craniofacial, Head and Neck Surgery and Pediatric Plastic Surgery: Elsevier Saunders.
83. Mirastschijski U, Jokuszies A, Vogt PM (2013) Skin wound healing: repair biology, wound, and scar treatment. Plastic surgery 3rd ed Philadelphia, PA: Elsevier Saunders: 267-296.
84. Roberts HR, Tabares AH (1995) Overview of the coagulation reactions. Molecular basis of

thrombosis and hemostasis New York: Marcel Dekker 35.
85. Marin V, Montero-Julian FA, Gres S, Boulay V, Bongrand P, et al. (2001) The IL-6-soluble IL-6Ralpha autocrine loop of endothelial activation as an intermediate between acute and chronic inflammation: an experimental model involving thrombin. J Immunol 167: 3435-3442.
86. Nathan C (2006) Neutrophils and immunity: challenges and opportunities. Nat Rev Immunol 6: 173-182.
87. Peters T, Sindrilaru A, Hinz B, Hinrichs R, Menke A, et al. (2005) Wound-healing defect of CD18(-/-) mice due to a decrease in TGF-beta1 and myofibroblast differentiation. EMBO J 24: 3400-3410.
88. Simpson DM, Ross R (1972) The neutrophilic leukocyte in wound repair a study with antineutrophil serum. J Clin Invest 51: 2009-2023.
89. Sridhar P, Liu Y, Chin LD, Borja CE, Mann M, et al. (1999) Platelet-derived growth factor-stimulated expression of the MCP-1 immediate-early gene involves an inhibitory multiprotein complex. Mol Cell Biol 19: 4219-4230.
90. Bethel-Brown C, Yao H, Hu G, Buch S (2012) Platelet-derived growth factor (PDGF)-BB-mediated induction of monocyte chemoattractant protein 1 in human astrocytes: implications for HIV-associated neuroinflammation. J Neuroinflammation 9: 262.
91. Gillitzer R, Goebeler M (2001) Chemokines in cutaneous wound healing. J Leukoc Biol 69: 513-521.
92. Weyrich AS, Elstad MR, McEver RP, McIntyre TM, Moore KL, et al. (1996) Activated platelets signal chemokine synthesis by human monocytes. J Clin Invest 97: 1525-1534.
93. Rodero MP, Khosrotehrani K (2010) Skin wound healing modulation by macrophages. Int J Clin Exp Pathol 3: 643-653.
94. Koh TJ, DiPietro LA (2011) Inflammation and wound healing: the role of the macrophage. Expert Rev Mol Med 13: e23.
95. Leibovich SJ, Ross R (1975) The role of the macrophage in wound repair. A study with hydrocortisone and antimacrophage serum. Am J Pathol 78: 71-100.
96. Eming SA, Krieg T, Davidson JM (2007) Inflammation in wound repair: molecular and cellular mechanisms. J Invest Dermatol 127: 514-525.
97. Martin P, D'Souza D, Martin J, Grose R, Cooper L, et al. (2003) Wound healing in the PU.1 null mouse--tissue repair is not dependent on inflammatory cells. Curr Biol 13: 1122-1128.
98. Martins-Green M, Petreaca M, Wang L (2013) Chemokines and Their Receptors Are Key Players in the Orchestra That Regulates Wound Healing. Adv Wound Care (New Rochelle) 2: 327-347.
99. Noli C, Miolo A (2001) The mast cell in wound healing. Vet Dermatol 12: 303-313.
100. Sternlicht MD, Werb Z (2001) How matrix metalloproteinases regulate cell behavior. Annu Rev Cell Dev Biol 17: 463-516.
101. Prunieras M, Regnier M, Fougere S, Woodley D (1983) Keratinocytes synthesize basal-lamina proteins in culture. J Invest Dermatol 81: 74s-81s.
102. Gurtner GC (2007) Wound healing: normal and abnormal. Grabb Plastic Surgery 6th Ed

Philadelphia: Wolters Kluwer-Lippincot William and Wilkins: 15-22.
103. Johnson KE, Wilgus TA (2014) Vascular endothelial growth factor and angiogenesis in the regulation of cutaneous wound repair. Advances in wound care 3: 647-661.
104. Zaja-Milatovic S, Richmond A (2008) CXC chemokines and their receptors: a case for a significant biological role in cutaneous wound healing. Histology and histopathology 23: 1399.
105. Kyriakides TR, MacLauchlan S (2009) The role of thrombospondins in wound healing, ischemia, and the foreign body reaction. Journal of cell communication and signaling 3: 215-225.
106. Martin P, Leibovich SJ (2005) Inflammatory cells during wound repair: the good, the bad and the ugly. Trends Cell Biol 15: 599-607.
107. Kalluri R, Zeisberg M (2006) Fibroblasts in cancer. Nat Rev Cancer 6: 392-401.
108. O'Toole E (2001) Extracellular matrix and keratinocyte migration. Clinical and experimental dermatology 26: 525-530.
109. Michaels Jt, Dobryansky M, Galiano RD, Bhatt KA, Ashinoff R, et al. (2005) Topical vascular endothelial growth factor reverses delayed wound healing secondary to angiogenesis inhibitor administration. Wound Repair Regen 13: 506-512.
110. Li B, Wang JH (2011) Fibroblasts and myofibroblasts in wound healing: force generation and measurement. J Tissue Viability 20: 108-120.
111. Desmouliere A, Chaponnier C, Gabbiani G (2005) Tissue repair, contraction, and the myofibroblast. Wound Repair Regen 13: 7-12.
112. Kato R, Kamiya S, Ueki M, Yajima H, Ishii T, et al. (2001) The fibronectin-derived antiadhesive peptides suppress the myofibroblastic conversion of rat hepatic stellate cells. Exp Cell Res 265: 54-63.
113. McAnulty RJ (2007) Fibroblasts and myofibroblasts: their source, function and role in disease. Int J Biochem Cell Biol 39: 666-671.
114. Inkinen K (2003) Connective Tissue Formation in Wound Healing.
115. Larjava H, Koivisto L, Häkkinen L (2000) Keratinocyte interactions with fibronectin during wound healing.
116. Stevens LJ, Page-McCaw A (2012) A secreted MMP is required for reepithelialization during wound healing. Mol Biol Cell 23: 1068-1079.
117. Mirastschijski U, Haaksma CJ, Tomasek JJ, Agren MS (2004) Matrix metalloproteinase inhibitor GM 6001 attenuates keratinocyte migration, contraction and myofibroblast formation in skin wounds. Exp Cell Res 299: 465-475.
118. Granick MS, Teot L (2012) Surgical Wound Healing and Management, Second Edition: CRC Press.
119. Falanga V (2005) Wound healing and its impairment in the diabetic foot. Lancet 366: 1736-1743.
120. Sussman C, Bates-Jensen BM (2007) Wound care: a collaborative practice manual: Lippincott Williams & Wilkins.
121. Toriseva M, Kahari VM (2009) Proteinases in cutaneous wound healing. Cell Mol Life Sci 66: 203-224.
122. Lau YK, Gobin AM, West JL (2006) Overexpression of lysyl oxidase to increase matrix crosslinking and improve tissue strength in dermal wound healing. Ann Biomed Eng

34: 1239-1246.
123. Castleman M, Hendler SS (1995) The healing herbs: The ultimate guide to the curative power of nature's medicines: Bantam.
124. Handral HK, Duggi S, Handral R, Tulsianand G, Shruthi S (2013) TURMERIC: NATURE'S PRECIOUS MEDICINE. Asian Journal of Pharmaceutical and Clinical Research 6.
125. Prasad S, Aggarwal BB (2011) Turmeric, the Golden Spice: From Traditional Medicine to Modern Medicine.
126. Araujo CC, Leon LL (2001) Biological activities of Curcuma longa L. Mem Inst Oswaldo Cruz 96: 723-728.
127. Gujral ML, Chowdhury NK, Saxena PN (1953) The effect of certain indigenous remedies on the healing of wounds and ulcers. J Indian Med Assoc 22: 273-276.
128. Kundu S, Biswas TK, Das P, Kumar S, De DK (2005) Turmeric (Curcuma longa) rhizome paste and honey show similar wound healing potential: a preclinical study in rabbits. The international journal of lower extremity wounds 4: 205-213.
129. Blumenthal M, Goldberg A, Brinckmann J (2000) Herbal Medicine. Expanded Commission E monographs: Integrative Medicine Communications.
130. Hatcher H, Planalp R, Cho J, Torti FM, Torti SV (2008) Curcumin: from ancient medicine to current clinical trials. Cell Mol Life Sci 65: 1631-1652.
131. Maheshwari RK, Singh AK, Gaddipati J, Srimal RC (2006) Multiple biological activities of curcumin: a short review. Life Sci 78: 2081-2087.
132. Sidhu GS, Singh AK, Thaloor D, Banaudha KK, Patnaik GK, et al. (1998) Enhancement of wound healing by curcumin in animals. Wound Repair and Regeneration 6: 167-177.
133. Panchatcharam M, Miriyala S, Gayathri VS, Suguna L (2006) Curcumin improves wound healing by modulating collagen and decreasing reactive oxygen species. Mol Cell Biochem 290: 87-96.
134. Ravindran PN, Babu KN, Sivaraman K (2007) Turmeric: The genus Curcuma: CRC Press.
135. Ravichandran R (2013) Pharmacokinetic study of nanoparticulate curcumin: oral formulation for enhanced bioavailability.
136. Heger M, van Golen RF, Broekgaarden M, Michel MC (2014) The molecular basis for the pharmacokinetics and pharmacodynamics of curcumin and its metabolites in relation to cancer. Pharmacological reviews 66: 222-307.
137. Priyadarsini KI (2013) Chemical and structural features influencing the biological activity of curcumin. Curr Pharm Des 19: 2093-2100.
138. Gupta SC, Prasad S, Kim JH, Patchva S, Webb LJ, et al. (2011) Multitargeting by curcumin as revealed by molecular interaction studies. Natural product reports 28: 1937-1955.
139. Nimse SB, Pal D (2015) Free radicals, natural antioxidants, and their reaction mechanisms. RSC Advances 5: 27986-28006.
140. Mishra B, Indira Priyadarsini K, Bhide M, Kadam R, Mohan H (2004) Reactions of superoxide radicals with curcumin: probable mechanisms by optical spectroscopy and EPR. Free radical research 38: 355-362.
141. Trujillo J, Chirino YI, Molina-Jijón E, Andérica-Romero AC, Tapia E, et al. (2013)

Renoprotective effect of the antioxidant curcumin: Recent findings. Redox biology 1: 448-456.
142. Priyadarsini KI (2014) The chemistry of curcumin: from extraction to therapeutic agent. Molecules 19: 20091-20112.
143. Bagchi D, Chaudhuri S, Sardar S, Choudhury S, Polley N, et al. (2015) Modulation of stability and functionality of a phyto-antioxidant by weakly interacting metal ions: curcumin in aqueous solution. RSC Advances 5: 102516-102524.
144. Mishra S, Palanivelu K (2008) The effect of curcumin (turmeric) on Alzheimer's disease: An overview. Annals of Indian Academy of Neurology 11: 13.
145. Valentini A, Conforti F, Crispini A, De Martino A, Condello R, et al. (2008) Synthesis, oxidant properties, and antitumoral effects of a heteroleptic palladium (II) complex of curcumin on human prostate cancer cells. Journal of medicinal chemistry 52: 484-491.
146. John VD, Kuttan G, Krishnankutty K (2002) Anti-tumour studies of metal chelates of synthetic curcuminoids. J Exp Clin Cancer Res 21: 219-224.
147. Gupta SC, Patchva S, Aggarwal BB (2013) Therapeutic roles of curcumin: lessons learned from clinical trials. AAPS J 15: 195-218.
148. Naksuriya O, Okonogi S, Schiffelers RM, Hennink WE (2014) Curcumin nanoformulations: a review of pharmaceutical properties and preclinical studies and clinical data related to cancer treatment. Biomaterials 35: 3365-3383.
149. Hsu CH, Cheng AL (2007) Clinical studies with curcumin. Adv Exp Med Biol 595: 471-480.
150. Prasad S, Tyagi AK, Aggarwal BB (2014) Recent developments in delivery, bioavailability, absorption and metabolism of curcumin: the golden pigment from golden spice. Cancer Research and Treatment 46: 2-18.
151. Anand P, Kunnumakkara AB, Newman RA, Aggarwal BB (2007) Bioavailability of curcumin: problems and promises. Mol Pharm 4: 807-818.
152. Wnek GE (2014) 3. Electrospun polymer fibers as a versatile delivery platform for small molecules and macromolecules: Original research article: Release of tetracycline hydrochloride from electrospun poly (ethylene-co-vinylacetate), poly (lactic acid), a blend, 2002. J Control Release 190: 34-36.
153. Li D, Xia Y (2004) Electrospinning of nanofibers: reinventing the wheel? Advanced materials 16: 1151-1170.
154. Cooley JF (1902) Apparatus for electrically dispersing fluids. Google Patents.
155. Anton F (1934) Process and apparatus for preparing artificial threads. Google Patents.
156. Taylor G. Electrically driven jets; 1969. The Royal Society. pp. 453-475.
157. Baumgarten PK (1971) Electrostatic spinning of acrylic microfibers. Journal of colloid and interface science 36: 71-79.
158. Annis D, Bornat A, Edwards R, Higham A, Loveday B, et al. (1978) An elastomeric vascular prosthesis. ASAIO Journal 24: 209-214.
159. Fisher A, De Cossart L, How T, Annis D (1984) Long term in-vivo performance of an electrostatically-spun small bore arterial prosthesis: the contribution of mechanical compliance and anti-platelet therapy. Life support systems: the journal of the European Society for Artificial Organs 3: 462-465.
160. Yarin A, Koombhongse S, Reneker DH (2001) Bending instability in electrospinning of

nanofibers. Journal of Applied physics 89: 3018-3026.
161. Reneker DH, Yarin AL, Fong H, Koombhongse S (2000) Bending instability of electrically charged liquid jets of polymer solutions in electrospinning. Journal of Applied physics 87: 4531-4547.
162. Jayakumar R, Nair S (2012) Biomedical Applications of Polymeric Nanofibers: Springer Berlin Heidelberg.
163. Zhang C, Yuan X, Wu L, Han Y, Sheng J (2005) Study on morphology of electrospun poly (vinyl alcohol) mats. European polymer journal 41: 423-432.
164. Yuan X, Zhang Y, Dong C, Sheng J (2004) Morphology of ultrafine polysulfone fibers prepared by electrospinning. Polymer International 53: 1704-1710.
165. Reneker DH, Chun I (1996) Nanometre diameter fibres of polymer, produced by electrospinning. Nanotechnology 7: 216.
166. Sill TJ, von Recum HA (2008) Electrospinning: applications in drug delivery and tissue engineering. Biomaterials 29: 1989-2006.
167. Megelski S, Stephens JS, Chase DB, Rabolt JF (2002) Micro-and nanostructured surface morphology on electrospun polymer fibers. Macromolecules 35: 8456-8466.
168. Hekmati AH, Rashidi A, Ghazisaeidi R, Drean J-Y (2013) Effect of needle length, electrospinning distance, and solution concentration on morphological properties of polyamide-6 electrospun nanowebs. Textile Research Journal: 0040517512471746.
169. Doshi J, Reneker DH. Electrospinning process and applications of electrospun fibers; 1993. IEEE. pp. 1698-1703.
170. Mit-uppatham C, Nithitanakul M, Supaphol P (2004) Ultrafine electrospun polyamide-6 fibers: effect of solution conditions on morphology and average fiber diameter. Macromolecular Chemistry and Physics 205: 2327-2338.
171. Nezarati RM, Eifert MB, Cosgriff-Hernandez E (2013) Effects of humidity and solution viscosity on electrospun fiber morphology. Tissue Eng Part C Methods 19: 810-819.
172. Beachley V, Wen X (2010) Polymer nanofibrous structures: Fabrication, biofunctionalization, and cell interactions. Prog Polym Sci 35: 868-892.
173. Zamani M, Prabhakaran MP, Ramakrishna S (2013) Advances in drug delivery via electrospun and electrosprayed nanomaterials. Int J Nanomedicine 8: 2997-3017.
174. Luo X, Xie C, Wang H, Liu C, Yan S, et al. (2012) Antitumor activities of emulsion electrospun fibers with core loading of hydroxycamptothecin via intratumoral implantation. Int J Pharm 425: 19-28.
175. Moroni L, Hendriks JA, Schotel R, de Wijn JR, van Blitterswijk CA (2007) Design of biphasic polymeric 3-dimensional fiber deposited scaffolds for cartilage tissue engineering applications. Tissue Eng 13: 361-371.
176. Yao CH, Yeh JY, Chen YS, Li MH, Huang CH (2015) Wound-healing effect of electrospun gelatin nanofibres containing Centella asiatica extract in a rat model. J Tissue Eng Regen Med.
177. Shan YH, Peng LH, Liu X, Chen X, Xiong J, et al. (2015) Silk fibroin/gelatin electrospun nanofibrous dressing functionalized with astragaloside IV induces healing and anti-scar effects on burn wound. Int J Pharm 479: 291-301.
178. Sell SA, Wolfe PS, Garg K, McCool JM, Rodriguez IA, et al. (2010) The use of natural polymers in tissue engineering: a focus on electrospun extracellular matrix analogues.

Polymers 2: 522-553.
179. Kim SE, Heo DN, Lee JB, Kim JR, Park SH, et al. (2009) Electrospun gelatin/polyurethane blended nanofibers for wound healing. Biomed Mater 4: 044106.
180. Leung V, Hartwell R, Yang H, Ghahary A, Ko F (2011) Bioactive nanofibres for wound healing applications. J Fiber Bioeng Informat 4: 1-14.
181. Dai XY, Nie W, Wang YC, Shen Y, Li Y, et al. (2012) Electrospun emodin polyvinylpyrrolidone blended nanofibrous membrane: a novel medicated biomaterial for drug delivery and accelerated wound healing. J Mater Sci Mater Med 23: 2709-2716.
182. Welz MM, Ofner CM (1992) Examination of self-crosslinked gelatin as a hydrogel for controlled release. Journal of pharmaceutical sciences 81: 85-90.
183. Dhurai B, Saraswathy N, Maheswaran R, Sethupathi P, Vanitha P, et al. (2013) Electrospinning of curcumin loaded chitosan/poly (lactic acid) nanofilm and evaluation of its medicinal characteristics. Frontiers of Materials Science 7: 350-361.
184. Sullivan SR, Underwood RA, Gibran NS, Sigle RO, Usui ML, et al. (2004) Validation of a model for the study of multiple wounds in the diabetic mouse (db/db). Plast Reconstr Surg 113: 953-960.
185. Vogel B, Siebert H, Hofmann U, Frantz S (2015) Determination of collagen content within picrosirius red stained paraffin-embedded tissue sections using fluorescence microscopy. MethodsX 2: 124-134.
186. Paetzold H, Goepfert C, Huber G, Hoenig E, Portner R, et al. (2012) The development of the collagen fibre network in tissue-engineered cartilage constructs in vivo. Engineered cartilage reorganises fibre network. Eur Cell Mater 23: 209-221.
187. Strojnik T, Kavalar R, Zajc I, Diamandis EP, Oikonomopoulou K, et al. (2009) Prognostic impact of CD68 and kallikrein 6 in human glioma. Anticancer Res 29: 3269-3279.
188. Darby IA, Laverdet B, Bonte F, Desmouliere A (2014) Fibroblasts and myofibroblasts in wound healing. Clin Cosmet Investig Dermatol 7: 301-311.
189. Bhattarai N, Edmondson D, Veiseh O, Matsen FA, Zhang M (2005) Electrospun chitosan-based nanofibers and their cellular compatibility. Biomaterials 26: 6176-6184.
190. Schiborr C, Eckert GP, Rimbach G, Frank J (2010) A validated method for the quantification of curcumin in plasma and brain tissue by fast narrow-bore high-performance liquid chromatography with fluorescence detection. Anal Bioanal Chem 397: 1917-1925.
191. Liang CC, Park AY, Guan JL (2007) In vitro scratch assay: a convenient and inexpensive method for analysis of cell migration in vitro. Nat Protoc 2: 329-333.
192. Shao S, Cai W, Sheng J, Yin L (2015) Role of SDF-1 and Wnt signaling pathway in the myocardial fibrosis of hypertensive rats. Am J Transl Res 7: 1345-1356.
193. Kabashima K, Sakabe J, Yoshiki R, Tabata Y, Kohno K, et al. (2010) Involvement of Wnt signaling in dermal fibroblasts. Am J Pathol 176: 721-732.
194. Koch S, Capaldo CT, Samarin S, Nava P, Neumaier I, et al. (2009) Dkk-1 inhibits intestinal epithelial cell migration by attenuating directional polarization of leading edge cells. Mol Biol Cell 20: 4816-4825.
195. Cruciat CM, Niehrs C (2013) Secreted and transmembrane wnt inhibitors and activators. Cold Spring Harb Perspect Biol 5: a015081.

196. Wood S, Jayaraman V, Huelsmann EJ, Bonish B, Burgad D, et al. (2014) Pro-inflammatory chemokine CCL2 (MCP-1) promotes healing in diabetic wounds by restoring the macrophage response. PLoS One 9: e91574.
197. Low QE, Drugea IA, Duffner LA, Quinn DG, Cook DN, et al. (2001) Wound healing in MIP-1alpha(-/-) and MCP-1(-/-) mice. Am J Pathol 159: 457-463.
198. Lopez-Dee Z, Pidcock K, Gutierrez LS (2011) Thrombospondin-1: multiple paths to inflammation. Mediators Inflamm 2011: 296069.
199. Akbik D, Ghadiri M, Chrzanowski W, Rohanizadeh R (2014) Curcumin as a wound healing agent. Life Sci 116: 1-7.
200. R Cundell D, Wilkinson F (2014) Curcumin: Powerful Immunomodulator from Turmeric. Current Immunology Reviews 10: 122-132.
201. MacDonald BT, Tamai K, He X (2009) Wnt/beta-catenin signaling: components, mechanisms, and diseases. Dev Cell 17: 9-26.
202. Enochson L, Stenberg J, Brittberg M, Lindahl A (2014) GDF5 reduces MMP13 expression in human chondrocytes via DKK1 mediated canonical Wnt signaling inhibition. Osteoarthritis Cartilage 22: 566-577.
203. Deshmane SL, Kremlev S, Amini S, Sawaya BE (2009) Monocyte chemoattractant protein-1 (MCP-1): an overview. J Interferon Cytokine Res 29: 313-326.
204. Schilling AF, Linhart W, Filke S, Gebauer M, Schinke T, et al. (2004) Resorbability of bone substitute biomaterials by human osteoclasts. Biomaterials 25: 3963-3972.
205. McCulloch JM, Kloth LC (2010) Wound Healing: Evidence-Based Management: F.A. Davis.
206. Lattouf R, Younes R, Lutomski D, Naaman N, Godeau G, et al. (2014) Picrosirius red staining: a useful tool to appraise collagen networks in normal and pathological tissues. J Histochem Cytochem 62: 751-758.
207. Aftab S, Tarik MM, Siddique MA, Yusuf MA (2015) Clinical and Microbiological Aspect of Wound Infection: A Review Update. Bangladesh Journal of Infectious Diseases 1: 32-37.
208. Furdell EL (2002) Publishing and Medicine in Early Modern England: University of Rochester Press.
209. Murphy D, Turner G (2007) Condottiere 1300-1500: Infamous Medieval Mercenaries: Bloomsbury USA.
210. Chak K-F, Hsiao C-Y, Chen T-Y (2013) A Study of the Effect of Shiunko, a traditional chinese herbal medicine, on fibroblasts and its implication on wound healing processes. Advances in wound care 2: 448-455.
211. Edwards H (1976) Theodoric of Cervia, a medieval antiseptic surgeon. Proceedings of the Royal Society of Medicine 69: 553.
212. Chang H, Wind S, Kerstein MD (1996) Moist wound healing. Dermatology Nursing 8: 174-178.
213. Borak T (2009) Plastic Surgery: A Timeline. The Surgical technologist 41: 507.
214. Sabale P, Bhimani B, Prajapati C, Sabalea V (2012) An overview of medicinal plants as wound healers. Journal of applied Pharmaceutical Science 2: 143-150.
215. Mukerjee A, Vishwanatha JK (2009) Formulation, characterization and evaluation of curcumin-loaded PLGA nanospheres for cancer therapy. Anticancer Res 29:

3867-3875.
216. Jagannathan R, Abraham PM, Poddar P (2012) Temperature-dependent spectroscopic evidences of curcumin in aqueous medium: A mechanistic study of its solubility and stability. The Journal of Physical Chemistry B 116: 14533-14540.
217. Khopde SM, Indira Priyadarsini K, Mukherjee T (2000) Effect of Solvent on the Excited-state Photophysical Properties of Curcumin. Photochemistry and photobiology 72: 625-631.
218. Tønnesen HH (1989) Studies on curcumin and curcuminoids. XVI. Effect of curcumin analogs on hyaluronic acid degradation in vitro. International journal of pharmaceutics 51: 259-261.
219. Tønnesen HH, Karlsen J (1985) Studies on curcumin and curcuminoids. Zeitschrift für Lebensmittel-Untersuchung und Forschung 180: 402-404.
220. Chang R, Sun L, Webster TJ (2014) Short communication: selective cytotoxicity of curcumin on osteosarcoma cells compared to healthy osteoblasts. International journal of nanomedicine 9: 461.
221. Martin D, Weise A, Niclas HJ (1967) The solvent dimethyl sulfoxide. Angewandte Chemie International Edition in English 6: 318-334.
222. Shen L, Liu C-C, An C-Y, Ji H-F (2016) How does curcumin work with poor bioavailability? Clues from experimental and theoretical studies. Scientific reports 6.
223. Tonnesen HH, Karlsen J (1985) Studies on curcumin and curcuminoids. VI. Kinetics of curcumin degradation in aqueous solution. Z Lebensm Unters Forsch 180: 402-404.
224. Lee W-H, Loo C-Y, Bebawy M, Luk F, Mason RS, et al. (2013) Curcumin and its derivatives: their application in neuropharmacology and neuroscience in the 21st century. Current neuropharmacology 11: 338-378.
225. Wang YJ, Pan MH, Cheng AL, Lin LI, Ho YS, et al. (1997) Stability of curcumin in buffer solutions and characterization of its degradation products. J Pharm Biomed Anal 15: 1867-1876.
226. Wahlstrom B, Blennow G (1978) A study on the fate of curcumin in the rat. Acta Pharmacol Toxicol (Copenh) 43: 86-92.
227. Shoba G, Joy D, Joseph T, Majeed M, Rajendran R, et al. (1998) Influence of piperine on the pharmacokinetics of curcumin in animals and human volunteers. Planta Med 64: 353-356.
228. Cheng AL, Hsu CH, Lin JK, Hsu MM, Ho YF, et al. (2001) Phase I clinical trial of curcumin, a chemopreventive agent, in patients with high-risk or pre-malignant lesions. Anticancer Res 21: 2895-2900.
229. Sharma RA, Euden SA, Platton SL, Cooke DN, Shafayat A, et al. (2004) Phase I clinical trial of oral curcumin: biomarkers of systemic activity and compliance. Clin Cancer Res 10: 6847-6854.
230. Ravindranath V, Chandrasekhara N (1980) Absorption and tissue distribution of curcumin in rats. Toxicology 16: 259-265.
231. Ravindranath V, Chandrasekhara N (1981) Metabolism of curcumin--studies with [3H]curcumin. Toxicology 22: 337-344.
232. Perkins S, Verschoyle RD, Hill K, Parveen I, Threadgill MD, et al. (2002) Chemopreventive efficacy and pharmacokinetics of curcumin in the min/+ mouse, a

model of familial adenomatous polyposis. Cancer Epidemiol Biomarkers Prev 11: 535-540.

233. Holder GM, Plummer JL, Ryan AJ (1978) The metabolism and excretion of curcumin (1,7-bis-(4-hydroxy-3-methoxyphenyl)-1,6-heptadiene-3,5-dione) in the rat. Xenobiotica 8: 761-768.

234. Pan MH, Huang TM, Lin JK (1999) Biotransformation of curcumin through reduction and glucuronidation in mice. Drug Metab Dispos 27: 486-494.

235. Vareed SK, Kakarala M, Ruffin MT, Crowell JA, Normolle DP, et al. (2008) Pharmacokinetics of curcumin conjugate metabolites in healthy human subjects. Cancer Epidemiol Biomarkers Prev 17: 1411-1417.

236. Hoehle SI, Pfeiffer E, Solyom AM, Metzler M (2006) Metabolism of curcuminoids in tissue slices and subcellular fractions from rat liver. J Agric Food Chem 54: 756-764.

237. Sharma RA, McLelland HR, Hill KA, Ireson CR, Euden SA, et al. (2001) Pharmacodynamic and pharmacokinetic study of oral Curcuma extract in patients with colorectal cancer. Clin Cancer Res 7: 1894-1900.

238. Patel BB, Majumdar AP (2009) Synergistic role of curcumin with current therapeutics in colorectal cancer: minireview. Nutr Cancer 61: 842-846.

239. Ireson CR, Jones DJ, Orr S, Coughtrie MW, Boocock DJ, et al. (2002) Metabolism of the cancer chemopreventive agent curcumin in human and rat intestine. Cancer Epidemiol Biomarkers Prev 11: 105-111.

240. Teiten MH, Eifes S, Dicato M, Diederich M (2010) Curcumin-the paradigm of a multi-target natural compound with applications in cancer prevention and treatment. Toxins (Basel) 2: 128-162.

241. Yallapu MM, Jaggi M, Chauhan SC (2010) beta-Cyclodextrin-curcumin self-assembly enhances curcumin delivery in prostate cancer cells. Colloids Surf B Biointerfaces 79: 113-125.

242. Li X, Chen T, Xu L, Zhang Z, Li L, et al. (2014) Preparation of curcumin micelles and the in vitro and in vivo evaluation for cancer therapy. J Biomed Nanotechnol 10: 1458-1468.

243. Reeves A, Vinogradov SV, Morrissey P, Chernin MC, Ahmed MM (2015) Curcumin-encapsulating Nanogels as an Effective Anticancer Formulation for Intracellular Uptake. Molecular and Cellular Pharmacology 7: 25-40.

244. Maleki M, Amani-Tehran M, Latifi M, Mathur S. A Study on Electrospun Nanofibrous Mats for Local Antibiotic Delivery; 2014. Trans Tech Publ. pp. 510-514.

245. Aboutalebi Anaraki N, Roshanfekr Rad L, Irani M, Haririan I (2015) Fabrication of PLA/PEG/MWCNT electrospun nanofibrous scaffolds for anticancer drug delivery. Journal of applied polymer science 132.

246. Puhl S, Li L, Meinel L, Germershaus O (2014) Controlled protein delivery from electrospun non-wovens: novel combination of protein crystals and a biodegradable release matrix. Molecular pharmaceutics 11: 2372-2380.

247. Lee S, Jin G, Jang J-H (2014) Electrospun nanofibers as versatile interfaces for efficient gene delivery. Journal of biological engineering 8: 1.

248. Zeng J, Yang L, Liang Q, Zhang X, Guan H, et al. (2005) Influence of the drug compatibility with polymer solution on the release kinetics of electrospun fiber formulation. J Control Release 105: 43-51.

249. Taepaiboon P, Rungsardthong U, Supaphol P (2007) Vitamin-loaded electrospun cellulose acetate nanofiber mats as transdermal and dermal therapeutic agents of vitamin A acid and vitamin E. European Journal of Pharmaceutics and Biopharmaceutics 67: 387-397.
250. Suwantong O, Opanasopit P, Ruktanonchai U, Supaphol P (2007) Electrospun cellulose acetate fiber mats containing curcumin and release characteristic of the herbal substance. Polymer 48: 7546-7557.
251. Jiang H, Fang D, Hsiao B, Chu B, Chen W (2004) Preparation and characterization of ibuprofen-loaded poly(lactide-co-glycolide)/poly(ethylene glycol)-g-chitosan electrospun membranes. J Biomater Sci Polym Ed 15: 279-296.
252. Chew SY, Wen J, Yim EK, Leong KW (2005) Sustained release of proteins from electrospun biodegradable fibers. Biomacromolecules 6: 2017-2024.
253. Tipduangta P, Belton P, Fabian L, Wang LY, Tang H, et al. (2016) Electrospun Polymer Blend Nanofibers for Tunable Drug Delivery: The Role of Transformative Phase Separation on Controlling the Release Rate. Mol Pharm 13: 25-39.
254. Wei Q (2012) Functional Nanofibers and their Applications: Elsevier Science.
255. Kim K, Luu YK, Chang C, Fang D, Hsiao BS, et al. (2004) Incorporation and controlled release of a hydrophilic antibiotic using poly (lactide-co-glycolide)-based electrospun nanofibrous scaffolds. Journal of Controlled Release 98: 47-56.
256. Lu Y, Jiang H, Tu K, Wang L (2009) Mild immobilization of diverse macromolecular bioactive agents onto multifunctional fibrous membranes prepared by coaxial electrospinning. Acta biomaterialia 5: 1562-1574.
257. Wang C, Ma C, Wu Z, Liang H, Yan P, et al. (2015) Enhanced Bioavailability and Anticancer Effect of Curcumin-Loaded Electrospun Nanofiber: In Vitro and In Vivo Study. Nanoscale research letters 10: 1-10.
258. Abrigo M, McArthur SL, Kingshott P (2014) Electrospun nanofibers as dressings for chronic wound care: advances, challenges, and future prospects. Macromolecular Bioscience 14: 772-792.
259. Merkle VM, Tran PL, Hutchinson M, Ammann KR, DeCook K, et al. (2015) Core-shell PVA/gelatin electrospun nanofibers promote human umbilical vein endothelial cell and smooth muscle cell proliferation and migration. Acta Biomater 27: 77-87.
260. Zhang Y, Lim CT, Ramakrishna S, Huang Z-M (2005) Recent development of polymer nanofibers for biomedical and biotechnological applications. Journal of Materials Science: Materials in Medicine 16: 933-946.
261. Ramakrishna S, Ramalingam M, Kumar TSS, Soboyejo WO (2016) Biomaterials: A Nano Approach: CRC Press.
262. Abrigo M, McArthur SL, Kingshott P (2014) Electrospun nanofibers as dressings for chronic wound care: advances, challenges, and future prospects. Macromol Biosci 14: 772-792.
263. Kanani AG, Bahrami SH (2010) Review on electrospun nanofibers scaffold and biomedical applications. Trends Biomater Artif Organs 24: 93-115.
264. Jayasinghe SN (2013) Cell electrospinning: a novel tool for functionalising fibres, scaffolds and membranes with living cells and other advanced materials for regenerative biology and medicine. Analyst 138: 2215-2223.

265. Sarabahi S (2012) Recent advances in topical wound care. Indian J Plast Surg 45: 379-387.
266. Supaphol P, Suwantong O, Sangsanoh P, Srinivasan S, Jayakumar R, et al. (2011) Electrospinning of biocompatible polymers and their potentials in biomedical applications. Biomedical applications of polymeric nanofibers: Springer. pp. 213-239.
267. Lee W-H, Loo C-Y, Young PM, Traini D, Mason RS, et al. (2014) Recent advances in curcumin nanoformulation for cancer therapy. Expert opinion on drug delivery 11: 1183-1201.
268. Zahedi P, Rezaeian I, Ranaei-Siadat SO, Jafari SH, Supaphol P (2010) A review on wound dressings with an emphasis on electrospun nanofibrous polymeric bandages. Polymers for Advanced Technologies 21: 77-95.
269. Mogoşanu GD, Grumezescu AM (2014) Natural and synthetic polymers for wounds and burns dressing. International journal of pharmaceutics 463: 127-136.
270. Frantz C, Stewart KM, Weaver VM (2010) The extracellular matrix at a glance. Journal of cell science 123: 4195-4200.
271. Husain M, Khan ZH (2016) Advances in Nanomaterials: Springer India.
272. Wood GC (1960) The formation of fibrils from collagen solutions. 3. Effect of chondroitin sulphate and some other naturally occurring polyanions on the rate of formation. Biochem J 75: 605-612.
273. Chandrasekaran AR, Venugopal J, Sundarrajan S, Ramakrishna S (2011) Fabrication of a nanofibrous scaffold with improved bioactivity for culture of human dermal fibroblasts for skin regeneration. Biomed Mater 6: 015001.
274. Wang T, Zhu X-K, Xue X-T, Wu D-Y (2012) Hydrogel sheets of chitosan, honey and gelatin as burn wound dressings. Carbohydrate Polymers 88: 75-83.
275. Epstein FH, Singer AJ, Clark RA (1999) Cutaneous wound healing. New England journal of medicine 341: 738-746.
276. Zaman HU, Islam JM, Khan MA, Khan RA (2011) Physico-mechanical properties of wound dressing material and its biomedical application. J Mech Behav Biomed Mater 4: 1369-1375.
277. Beumer GJ, van Blitterswijk CA, Bakker D, Ponec M (1993) A new biodegradable matrix as part of a cell seeded skin substitute for the treatment of deep skin defects: a physico-chemical characterisation. Clin Mater 14: 21-27.
278. Boateng JS, Matthews KH, Stevens HN, Eccleston GM (2008) Wound healing dressings and drug delivery systems: a review. J Pharm Sci 97: 2892-2923.
279. Lu Y, Huang J, Yu G, Cardenas R, Wei S, et al. (2016) Coaxial electrospun fibers: applications in drug delivery and tissue engineering. Wiley Interdisciplinary Reviews: Nanomedicine and Nanobiotechnology.
280. He CL, Huang ZM, Han XJ, Liu L, Zhang HS, et al. (2006) Coaxial electrospun poly (L-lactic acid) ultrafine fibers for sustained drug delivery. Journal of Macromolecular Science, Part B 45: 515-524.
281. Xu X, Chen X, Ma P, Wang X, Jing X (2008) The release behavior of doxorubicin hydrochloride from medicated fibers prepared by emulsion-electrospinning. Eur J Pharm Biopharm 70: 165-170.
282. Bolognia JL, Jorizzo JL, Schaffer JV (2012) Dermatology: Elsevier Health Sciences UK.

283. Mano J, Silva G, Azevedo HS, Malafaya P, Sousa R, et al. (2007) Natural origin biodegradable systems in tissue engineering and regenerative medicine: present status and some moving trends. Journal of the Royal Society Interface 4: 999-1030.
284. Kim SE, Heo DN, Lee JB, Kim JR, Park SH, et al. (2009) Electrospun gelatin/polyurethane blended nanofibers for wound healing. Biomedical Materials 4: 044106.
285. Ige OO, Umoru LE, Aribo S (2012) Natural products: A minefield of biomaterials. ISRN Materials Science 2012.
286. Meinel AJ, Germershaus O, Luhmann T, Merkle HP, Meinel L (2012) Electrospun matrices for localized drug delivery: current technologies and selected biomedical applications. European Journal of Pharmaceutics and Biopharmaceutics 81: 1-13.
287. Thakur R, Florek C, Kohn J, Michniak B (2008) Electrospun nanofibrous polymeric scaffold with targeted drug release profiles for potential application as wound dressing. International journal of pharmaceutics 364: 87-93.
288. Tyagi P, Singh M, Kumari H, Kumari A, Mukhopadhyay K (2015) Bactericidal activity of curcumin I is associated with damaging of bacterial membrane. PLoS One 10: e0121313.
289. Moghadamtousi SZ, Kadir HA, Hassandarvish P, Tajik H, Abubakar S, et al. (2014) A review on antibacterial, antiviral, and antifungal activity of curcumin. Biomed Res Int 2014: 186864.
290. Luo Y, Nartker S, Wiederoder M, Miller H, Hochhalter D, et al. (2012) Novel biosensor based on electrospun nanofiber and magnetic nanoparticles for the detection of E. coli O157: H7. Nanotechnology, IEEE Transactions on 11: 676-681.
291. Jia L-n, Zhang X, Xu H-y, Hua F, Hu X-g, et al. (2016) Development of a Doxycycline Hydrochloride-Loaded Electrospun Nanofibrous Membrane for GTR/GBR Applications. Journal of Nanomaterials 2016.
292. Bainbridge P (2013) Wound healing and the role of fibroblasts. J Wound Care 22: 407-408, 410-412.
293. Kingsnorth A, Bowley D (2011) Fundamentals of Surgical Practice: A Preparation Guide for the Intercollegiate MRCS Examination: Cambridge University Press.
294. Guo S, DiPietro LA (2010) Factors affecting wound healing. Journal of dental research 89: 219-229.
295. Kostandova N, Pamula A (2005) The effect of curcumin on normal human fibroblasts and human microvascular endothelial cells. California State Science Fair Project Summary.
296. Kang JY, Huang H, Zhu FQ (2009) [Effect of curcumin on growth and function of fibroblast in human hyperplastic scar]. Zhongguo Zhong Xi Yi Jie He Za Zhi 29: 1100-1103.
297. Scharstuhl A, Mutsaers HA, Pennings SW, Szarek WA, Russel FG, et al. (2009) Curcumin-induced fibroblast apoptosis and in vitro wound contraction are regulated by antioxidants and heme oxygenase: implications for scar formation. J Cell Mol Med 13: 712-725.
298. Mohanty C, Das M, Sahoo SK (2012) Sustained wound healing activity of curcumin loaded oleic acid based polymeric bandage in a rat model. Mol Pharm 9: 2801-2811.
299. Topman G, Lin FH, Gefen A (2013) The natural medications for wound healing - Curcumin,

Aloe-Vera and Ginger - do not induce a significant effect on the migration kinematics of cultured fibroblasts. J Biomech 46: 170-174.

300. Kabashima K, Sakabe J-i, Yoshiki R, Tabata Y, Kohno K, et al. (2010) Involvement of Wnt signaling in dermal fibroblasts. The American journal of pathology 176: 721-732.
301. Matucci-Cerinic M, Sacerdoti L, Perrone C, Carossino A, Cagnoni ML, et al. (1992) Pachydermoperiostosis (primary hypertrophic osteoarthropathy): in vitro evidence for abnormal fibroblast proliferation. Clin Exp Rheumatol 10 Suppl 7: 57-60.
302. Qiao L, Xu ZL, Zhao TJ, Ye LH, Zhang XD (2008) Dkk-1 secreted by mesenchymal stem cells inhibits growth of breast cancer cells via depression of Wnt signalling. Cancer Lett 269: 67-77.
303. Seifert O, Söderman J, Skarstedt M, Dienus O, Matussek A (2015) Increased expression of the Wnt signalling inhibitor Dkk-1 in non-lesional skin and peripheral blood mononuclear cells of patients with plaque psoriasis. Acta dermato-venereologica 95: 407-410.
304. Glantschnig H, Hampton RA, Lu P, Zhao JZ, Vitelli S, et al. (2010) Generation and selection of novel fully human monoclonal antibodies that neutralize Dickkopf-1 (DKK1) inhibitory function in vitro and increase bone mass in vivo. Journal of Biological Chemistry 285: 40135-40147.
305. Niida A, Hiroko T, Kasai M, Furukawa Y, Nakamura Y, et al. (2004) DKK1, a negative regulator of Wnt signaling, is a target of the β-catenin/TCF pathway. Oncogene 23: 8520-8526.
306. Shoulders MD, Raines RT (2009) Collagen structure and stability. Annu Rev Biochem 78: 929-958.
307. Aggarwal BB, Gupta SC, Sung B (2013) Curcumin: an orally bioavailable blocker of TNF and other pro-inflammatory biomarkers. Br J Pharmacol 169: 1672-1692.
308. Joe B, Vijaykumar M, Lokesh BR (2004) Biological properties of curcumin-cellular and molecular mechanisms of action. Crit Rev Food Sci Nutr 44: 97-111.
309. Singh S, Aggarwal BB (1995) Activation of transcription factor NF-kappa B is suppressed by curcumin (diferuloylmethane) [corrected]. J Biol Chem 270: 24995-25000.
310. Buhrmann C, Mobasheri A, Busch F, Aldinger C, Stahlmann R, et al. (2011) Curcumin modulates nuclear factor kappaB (NF-kappaB)-mediated inflammation in human tenocytes in vitro: role of the phosphatidylinositol 3-kinase/Akt pathway. J Biol Chem 286: 28556-28566.
311. Frey RS, Malik AB (2004) Oxidant signaling in lung cells. Am J Physiol Lung Cell Mol Physiol 286: L1-3.
312. Rosique RG, Rosique MJ, Farina Junior JA (2015) Curbing Inflammation in Skin Wound Healing: A Review. Int J Inflam 2015: 316235.
313. Chereddy KK, Coco R, Memvanga PB, Ucakar B, des Rieux A, et al. (2013) Combined effect of PLGA and curcumin on wound healing activity. Journal of Controlled Release 171: 208-215.
314. Singer AJ, McClain SA, Romanov A, Rooney J, Zimmerman T (2007) Curcumin reduces burn progression in rats. Acad Emerg Med 14: 1125-1129.
315. Kulac M, Aktas C, Tulubas F, Uygur R, Kanter M, et al. (2013) The effects of topical treatment with curcumin on burn wound healing in rats. J Mol Histol 44: 83-90.

316. Jagetia GC, Rajanikant GK (2012) Acceleration of wound repair by curcumin in the excision wound of mice exposed to different doses of fractionated gamma radiation. Int Wound J 9: 76-92.
317. Pijnenburg MW, De Jongste JC (2008) Exhaled nitric oxide in childhood asthma: a review. Clin Exp Allergy 38: 246-259.
318. Wallace JL (2005) Nitric oxide as a regulator of inflammatory processes. Memorias do Instituto Oswaldo Cruz 100: 5-9.
319. Moilanen E, Vapaatalo H (1995) Nitric oxide in inflammation and immune response. Ann Med 27: 359-367.
320. Donadelli R, Abbate M, Zanchi C, Corna D, Tomasoni S, et al. (2000) Protein traffic activates NF-kB gene signaling and promotes MCP-1-dependent interstitial inflammation. Am J Kidney Dis 36: 1226-1241.
321. Mast BA, Schultz GS (1996) Interactions of cytokines, growth factors, and proteases in acute and chronic wounds. Wound Repair Regen 4: 411-420.
322. Barchowsky A, Frleta D, Vincenti MP (2000) Integration of the NF-kappaB and mitogen-activated protein kinase/AP-1 pathways at the collagenase-1 promoter: divergence of IL-1 and TNF-dependent signal transduction in rabbit primary synovial fibroblasts. Cytokine 12: 1469-1479.
323. Trengove NJ, Stacey MC, MacAuley S, Bennett N, Gibson J, et al. (1999) Analysis of the acute and chronic wound environments: the role of proteases and their inhibitors. Wound Repair Regen 7: 442-452.
324. Yamamoto T, Eckes B, Mauch C, Hartmann K, Krieg T (2000) Monocyte chemoattractant protein-1 enhances gene expression and synthesis of matrix metalloproteinase-1 in human fibroblasts by an autocrine IL-1 alpha loop. J Immunol 164: 6174-6179.
325. Mani H, Sidhu GS, Kumari R, Gaddipati JP, Seth P, et al. (2002) Curcumin differentially regulates TGF-beta1, its receptors and nitric oxide synthase during impaired wound healing. Biofactors 16: 29-43.
326. Kant V, Gopal A, Kumar D, Pathak NN, Ram M, et al. (2015) Curcumin-induced angiogenesis hastens wound healing in diabetic rats. J Surg Res 193: 978-988.
327. Nguyen VC, Nguyen VB, Hsieh M-F (2013) Curcumin-loaded chitosan/gelatin composite sponge for wound healing application. International Journal of Polymer Science 2013.
328. Dai M, Zheng X, Xu X, Kong X, Li X, et al. (2009) Chitosan-alginate sponge: preparation and application in curcumin delivery for dermal wound healing in rat. J Biomed Biotechnol 2009: 595126.
329. Sidhu GS, Mani H, Gaddipati JP, Singh AK, Seth P, et al. (1999) Curcumin enhances wound healing in streptozotocin induced diabetic rats and genetically diabetic mice. Wound Repair Regen 7: 362-374.
330. Mehrabani D, Farjam M, Geramizadeh B, Tanideh N, Amini M, et al. (2015) The healing effect of curcumin on burn wounds in rat. World J Plast Surg 4: 29-35.
331. Lan CC, Wu CS, Huang SM, Wu IH, Chen GS (2013) High-glucose environment enhanced oxidative stress and increased interleukin-8 secretion from keratinocytes: new insights into impaired diabetic wound healing. Diabetes 62: 2530-2538.
332. McCarty SM, Percival SL (2013) Proteases and delayed wound healing. Advances in wound care 2: 438-447.

333. Kant V, Gopal A, Pathak NN, Kumar P, Tandan SK, et al. (2014) Antioxidant and anti-inflammatory potential of curcumin accelerated the cutaneous wound healing in streptozotocin-induced diabetic rats. Int Immunopharmacol 20: 322-330.
334. Zhang X, Xu R, Hu X, Luo G, Wu J, et al. (2015) A systematic and quantitative method for wound-dressing evaluation. Burns & Trauma 3: 1.
335. Matsui R, Osaki K, Konishi J, Ikegami K, Koide M (1996) Evaluation of an artificial dermis full-thickness skin defect model in the rat. Biomaterials 17: 989-994.
336. Branski LK, Mittermayr R, Herndon DN, Norbury WB, Masters OE, et al. (2008) A porcine model of full-thickness burn, excision and skin autografting. Burns 34: 1119-1127.
337. Dunn L, Prosser HC, Tan JT, Vanags LZ, Ng MK, et al. (2013) Murine model of wound healing. JoVE (Journal of Visualized Experiments): e50265-e50265.
338. Ansell DM, Holden KA, Hardman MJ (2012) Animal models of wound repair: Are they cutting it? Experimental dermatology 21: 581-585.
339. Dorsett-Martin WA (2004) Rat models of skin wound healing: a review. Wound Repair and Regeneration 12: 591-599.
340. Gunes H, Gulen D, Mutlu R, Gumus A, Tas T, et al. (2016) Antibacterial effects of curcumin: An in vitro minimum inhibitory concentration study. Toxicol Ind Health 32: 246-250.
341. Paz JC, West MP (2013) Acute Care Handbook for Physical Therapists: Elsevier Health Sciences.
342. Smith RG (2008) Enzymatic debriding agents: an evaluation of the medical literature. Ostomy Wound Manage 54: 16-34.
343. Klein MB, Hunter S, Heimbach DM, Engrav LH, Honari S, et al. (2005) The Versajet water dissector: a new tool for tangential excision. J Burn Care Rehabil 26: 483-487.
344. Mumcuoglu KY (2001) Clinical applications for maggots in wound care. American journal of clinical dermatology 2: 219-227.
345. Jones G, Wall R (2008) Maggot-therapy in veterinary medicine. Research in veterinary science 85: 394-398.
346. Ramakrishna S, Fujihara K, Teo W-E, Yong T, Ma Z, et al. (2006) Electrospun nanofibers: solving global issues. Materials today 9: 40-50.
347. Stadelmann WK, Digenis AG, Tobin GR (1998) Impediments to wound healing. The American journal of surgery 176: 39S-47S.
348. Enoch S, Price P (2004) Cellular, molecular and biochemical differences in the pathophysiology of healing between acute wounds, chronic wounds and wounds in the aged. World Wide Wounds 13.
349. Mulholland MW, Lillemoe KD, Doherty GM, Maier RV, Simeone DM, et al. (2012) Greenfield's Surgery: Scientific Principles & Practice: Wolters Kluwer Health.
350. Lawrence PF, Bell RM, Dayton MT (2012) Essentials of General Surgery: Wolters Kluwer Health.
351. Sen CK (2009) Wound healing essentials: let there be oxygen. Wound Repair and Regeneration 17: 1-18.
352. Mendez-Eastman S (1998) When wounds won't heal. Rn 61: 20-24.
353. Amarnath S, Reddy MR, Rao CH, Surath HV (2014) Timer switch to convert suction apparatus for negative pressure wound therapy application. Indian Journal of Plastic

Surgery 47: 412.
354. Staples J, Clement D (1996) Hyperbaric oxygen chambers and the treatment of sports injuries. Sports Med 22: 219-227.
355. Hu MS, Leavitt T, Malhotra S, Duscher D, Pollhammer MS, et al. (2015) Stem Cell-Based Therapeutics to Improve Wound Healing. Plastic surgery international 2015.
356. Enoch S, Grey JE, Harding KG (2006) Non-surgical and drug treatments. British Medical Journal 7546: 900.
357. Hasamnis AA, Mohanty BK, Patil S (2010) Evaluation of wound healing effect of topical phenytoin on excisional wound in albino rats. Journal of Young Pharmacists 2: 59-62.
358. Rovee DT, Maibach HI (2003) The Epidermis in Wound Healing: CRC Press.
359. Robson M, Smith P (2001) Topical use of growth factors to enhance healing. Cutaneous wound healing 2001: 379-398.
360. Cronenwett JL, Johnston KW (2010) Rutherford's Vascular Surgery, 2-Volume Set: Elsevier Health Sciences.
361. Englander L, Friedman A (2010) Nitric oxide nanoparticle technology: a novel antimicrobial agent in the context of current treatment of skin and soft tissue infection. J Clin Aesthet Dermatol 3: 45-50.
362. Thomas S (2004) MRSA and the use of silver dressings: overcoming bacterial resistance. World Wide Wounds.
363. Gunaydin M, Esen S, Karadag A, Unal N, Yanik K, et al. (2014) In vitro antimicrobial activity of Medilox® super-oxidized water. Annals of clinical microbiology and antimicrobials 13: 1.
364. Reddy K, Yedery R, Aranha C (2004) Antimicrobial peptides: premises and promises. International journal of antimicrobial agents 24: 536-547.
365. Lipsky BA, Hoey C (2009) Topical antimicrobial therapy for treating chronic wounds. Clinical infectious diseases 49: 1541-1549.